UNIVERSIDADE DA BEIRA INTERIOR
Engenharia

Multi-Objective Optimization of the Performance of an UHB Turbofan with Regeneration

Fábio Guilherme dos Santos Marques de Oliveira

Dissertação para obtenção do Grau de Mestre em
Engenharia Aeronáutica
(Ciclo de estudos integrado)

Orientador: Prof. Doutor Francisco Miguel Ribeiro Proença Brójo

Covilhã, Outubro de 2014

To my parents… for all the years of support, effort and patience in many situations.

"The art of imagination is the first step of the true engineering science"

Fábio de Oliveira

Acknowledgments

I would like to thank my parents, not only for supporting me in this academic journey where everything I needed they gave me in the quickest and the best way they could, but for all the reminders that were always made with unquestionable love. Thank you parents... I want to hear and feel your advice and support for many years to come.

To my supervisor, Professor Francisco Ribeiro Miguel Proença Brójo, whom I always be thankful for his dedication. Since his total availability from the first day that I asked him for guidance to the thesis, as all the hours he spent with me giving me advices and overcoming the difficulties of the project and even providing working conditions to his students. That is something that cannot be measured. He started as a supervisor for me, but certainly is a precious friend that I will never forget. Thank you Professor for all the dedication and good moments!

Thank you Diana Vieira for always giving me courage in difficult times, and listen my ideas throughout the project. It is and will always be something that I will be eternally grateful.

I cannot forget my friends who followed me along this journey and who always encouraged me and cared about my success: João Nogueira, Ana Luísa Azevedo, Joana Forte and Mafalda Silva.

Finally, a word of thanks to my friends and co-workers, who shared with me all the good and bad moments in all the days of work. Thank you for making my daily work something that I will miss sharing with you.

Resumo

Todos os dias o mundo enfrenta o degradar constante do seu meio ambiente. O aquecimento global, entre muitos outros problemas ambientais, apresenta-se como um gigante que silenciosamente, dia após dia, ganha maior dimensão e cujos únicos avisos são os efeitos gradualmente mais severos que o planeta apresenta. Perante um cenário cada vez mais real, preocupações públicas levantam-se sobre as condições ambientais do planeta no futuro, bem como as consequências inerentes à Humanidade. O crescimento da população humana e a sua interacção com o ambiente que a envolve, bem como uma economia global em crescente competitividade, obriga a que uma sociedade em plena evolução responda de forma mais eficaz aos desafios ambientais e económicos que se avizinham.

Sendo a indústria Aeronáutica um dos principais ramos onde as mais recentes ideias e inovações tecnológicas tomam lugar, várias iniciativas têem surgido para fazer face a estes desafios. Os problemas ambientais do planeta bem como os desafios económicos, nomeadamente a subida dos preços dos combustíveis, são cada vez mais o centro das atenções, se não mesmo os objectivos a superar nos projectos aeronáuticos da actualidade. Estes projectos visam a melhor resposta possível num mercado em expansão e de forte exigência.

Esta dissertação incide no estudo de vários parâmetros de um motor Turbofan, sendo este tipo de motor o mais utilizado na aviação comercial em todo o mundo. Neste momento, estamos perante um período de decisões críticas por parte das operadoras aéreas na renovação/actualização das suas frotas, sendo que as novas aeronaves serão equipadas com motores Turbofan que prometem melhorias a todos os níveis relativamente aos seus antecessores. Estes novos motores caracterizam-se por um Bypass superior aos motores actuais, sendo por isso denominados de UHB (Ultra High Bypass Ratio) Turbofans e possuem valores menores de SFC (Specific Fuel Consumption). Com este estudo, procura-se analisar o comportamento desses parâmetros ao longo dos novos valores Bypass, averiguando ainda se a utilização de um regenerador de calor será viável de modo a obter valores inferiores de SFC em relação a uma configuração sem regeneração. Por fim procede-se a uma optimização dos parâmetros para ambos os casos estudados, com recurso a um Algoritimo Genético de Optimização Multi-Objetivos.

Palavras-chave

Turbofan, Bypass, UHB, Regenerador de Calor, Optimização Multiobjectivos, Algoritmo Genético, Consumo Específico de Tracção (TSFC), Tracção Específica (Fs).

Abstract

Every day the world faces the constant degradation of its environment. The global warming, between many other environmental problems, presents itself as a giant that, day by day, quietly grows and which the only warnings are the gradually severe effects that the planet displays. Before an increasingly real scenario, public concerns rise about the environmental conditions of the planet in the near future, as well as the consequences for the Mankind. The growth of the human population and its interaction with the environment that contains it, as well as a global economy in an increasing competitiveness obliges that an evolving society complies in the most effective way to the environmental and economic challenges in the future ahead.

Being the aeronautical industry one of the main fields where the most recent ideas and technological innovations take place, several initiatives have been taken to cope with these challenges. The environmental problems of the planet as well as the economic challenges, namely the rise of the fuel prices, are more and more the center of attentions, if not the main objectives to overcome in current aeronautical projects. These projects aim the best possible answer in an expansion and strong demanding market.

This dissertation focus on the study of several parameters of a Turbofan engine, the type of engine most used in commercial aviation around the world. At the present moment, we are facing a period of critical decisions by the air carriers in the renewal / upgrade of their fleet, consequently the new aircrafts will be equipped with Turbofan engines that promise improvements at all levels relatively to their predecessors. These new engines are characterized by a superior Bypass regarding the current engines; they are referred as UHB (Ultra Bypass Ratio) Turbofans and possess lower values of SFC (Specific Fuel Consumption). Therefore this study is intended to analyze the behaviour of these parameters along with the new Bypass values and also evaluate if the utilization of a heat regenerator will be viable to obtain lower values of SFC relatively to a configuration without regeneration. At last, it will be carried a parameter optimization for both sets, using a Genetic Algorithm designed for Multi-Objective Optimization.

Keywords

Turbofan, Bypass, UHB, Heat Regenerator, Multi-Objective Optimization, genetic algorithm, Traction Specific Consumption (TSFC), Specific Thrust(Fs).

Contents

List of Figures

List of Tabels

Nomenclature

Variables

Fs	Specific Thrust
P	Pressure
rpc	Compressor Pressure Ratio
rpfan	Fan Pressure Ratio
TET	Turbine Entry Temperature
TSFC	Thrust Specific Fuel Consumption
V	Velocity

Acronyms

ADP	Aerodynamic Design Point
ATFI	Advanced Technology Fan Integrator
BPR	Bypass Ratio
CE	Cultural Evolution
CFD	Computational Fluid Dynamics
CO^2	Carbon dioxide
C_P	Specific Heat
CROR	Counter Rotating Open Rotor
CV	Constant Volume
DDTF	Direct Drive Turbofan
DE	Differential Evolution
DOC	Direct Operating Cost
EAs	Evolutionary Algorithms
ES	Evolutionary Strategies
EVA	Environmental Assessment
F	Thrust
FPR	Fan Pressure Ratio
GAs	Genetic Algorithms
GOR	Geared Open Rotor

GTF	Geared Turbofan
h_m	Equality Constrains
HPC	High Pressure Compressor
HPT	High Pressure Turbine
IC	Intercooler
IR	Intercooler and Regenerator
IRA	Intercooler Recuperative Aero Engine
IRC	Intercooler-Regenerative Cycle
K	Kelvin
LA	Los Angeles
LPC	Low Pressure Compressor
LPT	Low Pressure Turbine
LTO	ICAO Landing and Take-Off Cycle
$\dot{m}_a$	Mass of air intake to the engine
$\dot{m}_f$	Mass of fuel added to the combustion
$\dot{m}_h$	Mass of hot air
$\dot{m}_c$	Mass of cold air
$\dot{m}_b$	Mass flow through the core
$\dot{m_{air}}$	Mass Flow through the engine
MaTES	Matlab Turbine Engine Simulator
MO	Multiple Objective
MOGA	Multi Objective Genetic Algorithm
MOHyGO	Multi Objective Hybrid Genetic Optimizer
MOO	Multi-Optimization Objective
MOP	Multi-Objective Optimization Problem
MPL	Maximum structural payload
NO_x	Nitrogen Oxides
NPSS	Numerical Propulsion System Simulation
NPGA	Niched Pareto Genetic Algorithm
NSGA	Non Dominated Sorting Genetic Algorithm

n_x	Dimensional chromosome
OPR	Overall Pressure Ratio
Q_{net}	Average Calorific Power of the Fuel
R	Specific Gas Constant
RHE	Regenerative Heat Exchanger
SFC	Specific Fuel Consumption
SFN	Specific Thrust
SLS	Sea Level Static
SO	Single Optimization
SPEA	Strength Pareto Evolutionary Algorithm
ST	Specific Thrust
T	Temperature
TOC	Top of Climb
UHB	Ultra Bypass Ratio
VEGA	Vector Evaluated Genetic Algorithm
VITAL	Environmentally Friendly Aero-Engine
WATE	Weight Analysis of Turbine Engine
W_{cool}	Core Mass Flow
WRTC	Wave Rotor Topping Cycle

Subscripts

a	External Conditions
b	Burner
c	before combustion
f	fuel
g	after combustion
G	Gross
HPC	Polytropic High Pressure Compressor
HPT	Polytropic High Pressure Turbine
i	Admission

j	Jet speed
jb	Bypass jet
jc	Core jet
LPC	Polytropic Low Pressure Compressor
LPT	Polytropic Low Pressure Turbine
m	Mechanical
N	Net
n	Nozzle
o	Overall
p	Propulsive
reg	Regenerator
S	Specific
t	turbine
th	High thermal
01	Admission
02	Fan
03	Low Pressure Compressor
04	High Pressure Compressor
05	Combustion Chamber
06	High Pressure Turbine
07	Low Pressure Turbine
08	Hot flow leaving the regenerator
09	Exhaust gases leaving the regenerator
10	Nozzle Exit
11	Turbine Nozzle
12	Fan Nozzle

Greek Symbols

γ	adiabatic index
η	Efficiency

Π	Pressure Ratio
Ψ, Φ	Objective function
Γ	Data type of elements
δ_c	Search Space of the Objective Function

1. Introduction

1.1 Motivation

Reaching the final stage of my academic formation as an Aeronautical Engineer, it has always been my motivation to end it by studying a subject that satisfies my personal interest in my favourite area and, as well as contribute to the Aeronautical World with some future possibilities and visions.

It is my belief that for future progress of Mankind, the planet's environment cannot be forgotten anymore. The environment should not represent the final barrier in any industrial/technological areas, avoiding them to develop, but it has to be taken as the main path to bring them to the next level. For now and for the future, they must give more environmental benefits and performances than their predecessors. The propulsion area must be one of the leading areas to give the example and show proofed results of this shifting.

The Aeronautical World has its footprint in the planet's environment and being one area where propulsion is more advanced, it is imperative that changes take the first steps there. The aircrafts are major fuel consumers and for that, a contribution in global warming is due to their activity. Designing new engines where the consumption is reduced significantly and the values of its performance are not compromised, are the plans of engine makers in the present and future. In that line of action, it has always been from my deepest interest the exploration of the new engine age in the aeronautical circle. To study future possibilities that put the bets even higher, always with the intention of contributing for a more eco-friendly and powerful engines that will take the planet in consideration.

1.2 Objectives

This dissertation was made with the main goal of studding the behaviour of an UHB Turbofan regarding specific engine parameters, with the possibility of a heat regenerator application. The aim is to verify if the brand new type of engine could deliver even less fuel consumption without compromising its performance, providing a set of viable and optimized options of configuration.

1.3 Framework

The increasingly manifestations of the planet's environment are leading to a society that, more than ever, needs to pay attention to all the issues that dictate the future years of environmental stability. The aeronautical world, being one of the technological areas where innovation is imperative, must lead the example in all possible subjects. With this thesis is intended to minimize the gap between the concept of lower fuel consumption, thus

environmental friendly engines and the concept of better thrust and performance that a turbofan engine can deliver. Based on those ideas the future of aeronautical engines can reach higher levels of efficiency and performance, leaving behind the negative impact of polluting the planet, potentiating new forms of propulsion for even more ambitious projects.

1.4 Thesis Structure

The first chapter presents an introduction to this thesis, containing my motivation, the objectives for this study and the framework of the addressed theme.

The second chapter contains the state of the art. It will be made a literature review as well as relevant studies, following the conclusions.

The conceptual requirements are exposed on the third chapter. It will be presented the Turbofan Engine concept, the bypass ratio, the Brayton Cycle and the regenerated cycle. Also the new turbofan engines that will be released with the new airframes from Airbus and Boeing are presented.

The fourth chapter deals with the engine parameters. Requirements and assumptions are explained as well as the mathematical models. The first results of this thesis, the parameterization results are plotted and interpreted.

The fifth chapter opens the second phase of this thesis, where the Evolutionary Computational theory is presented to better understand the optimization concept that will be performed.

The sixth chapter emphasizes the type of algorithm that will be used in the multi-objective optimization.

The seventh chapter regards all the concepts of the multi-objective optimization. The problem setup is enunciated and the results will be calculated and plotted.

At last, the eighth and final chapter presents the thesis conclusions and reference for future possible works.

2. State of the Art

2.1 Literature Review

Many works have been developed in the last 30 years related to the possible ways to improve the performance of the Turbofan engines. Intentions of optimization of these kinds of engines have always been present after they proved in early years of service, their fantastic capabilities in commercial aviation.

The goals of reducing fuel consumption and recently cutting pollutant emissions turned the attentions once more to a successfully applied concept in ground systems for many years: regeneration.

With the recent UHB Turbofan engines for single aisle aircraft announced to be introduced in the market alongside with new the airframes in the near future, it is important to review the past and recent work investigations related with this type of engine. Different approaches of Turbofan optimization as well as the tools and technologies developed, are summarized in this section to help understand the path taken until the present days.

According to (Wulff & Hourmouziadis 1997), pollutant emissions in commercial aviation, have been a concern since the 1960s. The Meadows Report to the Club of Rome in 1972 made the industrialized countries sensitive to the issue. By the 80s, the continuous monitoring of the globe, identified global warming, the rising of the carbon dioxide in the content of the atmosphere and the depletion of the ozone layer over the Antarctic. As a result, governments and industry have responded with several research programs and the introduction of new improved products, with the major concern: the release of carbon dioxide and nitrogen oxides in the upper atmosphere and the stratosphere.

In the authors' vision, operational changes in the airline flight profiles would benefit the reduction of NO_x but would involve a major economic penalty. It is reminded that the total exhaust emissions are a result of the overall efficiency of the aircraft. This includes the thermodynamic cycle of the engine as well the aerodynamic drag of the airframe.

It was proposed that the possibility of flying in lower cruise altitudes could bring environmental benefits. A flight from Berlin to LA was rematched to avoid cruising above tropopause. However, the results showed not viable, with a dramatic effect on range reduction by 20% and increasing the CO_2 emissions by the same amount. This could only be recovered if the aircraft were optimised for the specific operational conditions, which would require a complete new fleet of airliners. Ultra high bypass ratio engines with lower specific fuel consumption and wings with laminar flow control are pointed as the right direction of development.

In the engine field, the turbofan, being the source of the aircraft exhaust, can be target of a reduction in the fuel burn and overall emissions by better cycle efficiency and lower weight by 10%. A bypass ratio of optimum SFC is pointed by several authors to be near 13; however a reduction of the specific thrust and consequently a larger and heavier engine is obtained. The possibility of variable geometry is considered with a gearbox for the low pressure shaft. By the time of the present study it was concluded that alternative recuperated thermodynamic cycles or engines with pressure rise combustion didn't appear to have any satisfactory improvements to justify the investment. Combustors are also considered, hypothesis like staged combustion, lean premixed prevaporized combustion and others are marked as potential options to the conventional method.

Due to the high emission of gases in the atmosphere in modern aviation, alternative cycles applied to the direct drive turbofan could be the answer to ensure more efficient and environmental friendly engines. The need of reducing fuel consumption is not only related to the rising costs of fuel, but also the idea of increasing the maximum payload. This is achieved by improving the global efficiency of the engine which is dependent of the propulsive and thermal propulsive efficiency. (Pasini *et al*. 2000) advance that the trend in actual propulsion systems is to use very high values for cycle maximum temperature, with an increasing discharge temperature due to operative modalities of the discharge nozzle, often working in off design conditions. This makes the heat discharged a strong influence in the system performance and heat recovery appears to be a way that needs further improvements and investigations. However there are limitations to implement this concept like the engine configuration and limitations, as weight, overall dimensions and reliability. This work studies the heat recovery in aircraft engines, evaluates the possible modalities emphasizing the regenerative process in the SFC as one of the most attractive processes for the future development.

Being the heat exchange process a direct influencer on the enthalpy drop in the exhaust nozzle, hence the velocity jet it is valid to say that the regeneration acts not only directly in the thermal efficiency, reducing the heat in the exhaust, but also in the propulsion efficiency by reducing the residual kinetic energy of the jet. These effects lead to a reduction of the specific thrust of the engine.

To evaluate if the regeneration process could bring benefits, a thermodynamic code was developed to simulate the thermal cycle and the main specific performances in different types of jet engines to evaluate the possible recoveries. It is also studied the heat exchanger configuration and the most appropriate location to apply it. "An analysis from the energetic point of view of the thermal cycle shows that a great amount of heat is wasted in the exhaust, and indicates how a recovery, total or more realistically partial, of this heat can lead to a greater efficiency of the system." This code was applied to different types of aircraft engines like in a two separate flows turbofan engine. According to (Pasini e*t al*. 2000)

the concept of regeneration in a turbofan is particularly interesting at high by-pass ratio. The majority of thrust is generated by the cold stream, while the gas generator offers the required power. Thus the enthalpy level before the exhaust nozzle of the gas generator can be lowered without losing great amount of thrust and still increase efficiency The maximum temperature was 1600K, an altitude of 10 000m, a flight Mach number of 0.8 and a fixed BPR at 7.

Results show that the recovery not only influences the process positively but also amplifies the influence of other operative parameters. The thermal efficiency when the heat recovery is present, reveals higher values of about 4% when *R*=0.5, while it rises to about 10% if *R*=0.7 as can be observed in Figure 1. These effects are sensible at low pressure ratios. In fact, for pressure ratios about 20, the value of the thermal efficiency for which R=0.5 and the conventional one practically coincide. However above a certain value of pressure ratio (nearly 30) the heat can longer be transferred, while the pressure drop in the heat exchanger remains.

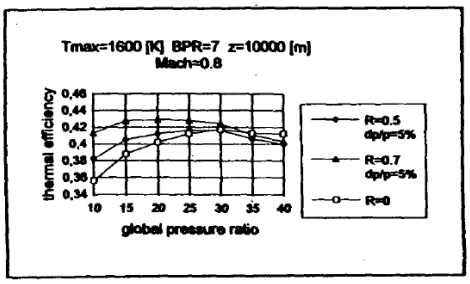

Figure 1: Thermal efficiency of a turbofan engine with regeneration (Pasini *et al.* 2000).

Regarding the heat exchange configuration, the heat can be exchanged between the two flows both in three different ways:

- First case: the conventional one (heat subtracted before expansion in the nozzle);
- Second case: heat is subtracted from gas while this is expanding in the exhaust nozzle;
- Third case: heat is extracted from gas after this is expanded in the nozzle, nearly at external pressure, before being expelled into the atmosphere;

The conventional heat transfer method revealed minimum level of fuel consumption compared to the others. However, the thermal efficiency is always better when the heat transfer is processed during the expansion (Figure 2). In the case of propulsive efficiency the results are not so clear. While at low pressure ratios, the heat subtracted during expansion seems convenient; at higher values of pressure ratio the heat exchange becomes more advantageous after the expansion. Figure 3 and Figure 4 describe the TSFC and ST in the different possibilities of expansion for R=0.4.

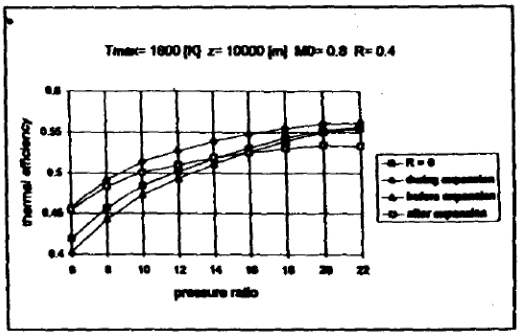

Figure 2: Thermal efficiency as function of pressure ratio, with regeneration (Pasini *et al*. 2000).

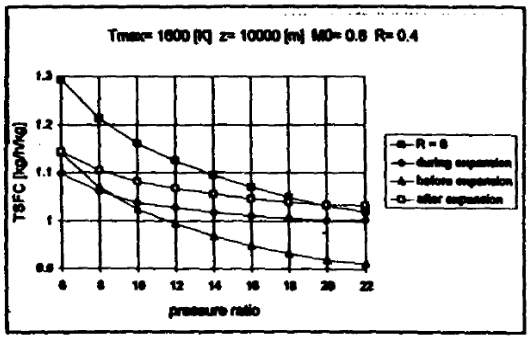

Figure 3: TSFC as function of pressure ratio, with regeneration (Pasini *et al*. 2000).

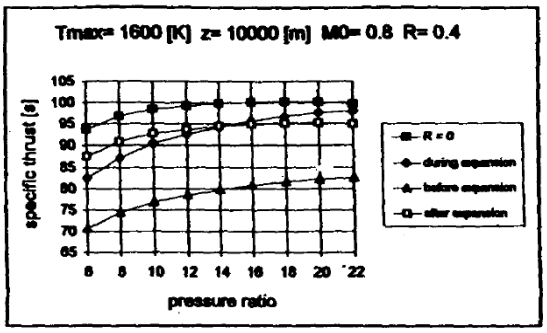

Figure 4: Specific Thrust as function of pressure ratio, with regeneration (Pasini *et al*. 2000).

As conclusions, based on results, the authors enhance the regeneration as the possibility of improving the engine characteristics (lower pressure ratio and consequently lower levels of NO_x). Problems of construction design must be further investigated to bring this next step to life: "It is possible to build a heat exchanger suitable to be mounted on aircraft power plants, both for its size and weight, and also for the amount of heat exchangeable." By the time, authors also predicted that "new engines can reach such values of BPR to be considered as a connecting bridge between turbofan and turboprop". This was a reference to the new UHB turbofans that will be on service in the near future.

Another study, following alternative thermodynamic cycles applied to high bypass ratio turbofans was made by (Andriani & Ghezzi 2006). It was driven by the technical efforts in the last years in achieving high performance levels and low specific fuel consumption. This study carries an analysis of an optimization in thermodynamic cycles under the point of view of the maximum temperature at the turbine inlet due to new materials, cooling systems and pressure ratios. The authors state that NO_x increases rapidly at combustion temperatures above 1900K meaning that OPR and TET have to be kept within acceptable limits. The concept of regeneration is applied in this study, which permits reduce the fuel consumption without increasing pressure ratio and maximum cycle temperature. Intercooled staged compression process is also studied. Previous works showed that recovery heat process can improve fuel saving, especially in turbofan and turboprop engines.

To estimate the capabilities of the regeneration, a thermodynamic code was developed to simulate different operative conditions, as flight level, flight speed Mach number, and engine characteristics, as pressure ratio, bypass ratio, turbine inlet temperature, efficiency of regeneration, etc. With this code it possible to determine the main propulsion and thermodynamic characteristics, like specific thrust, heat exchanged, thermal/propulsion and global efficiency and specific fuel consumption. The turbofan considered (Figure 5) had a BPR equal of 7, a TET of 1600K and a flight Mach number of 0.8 at 10 000m. Three cases were evaluated: the conventional engine with no regeneration (R=0), and two cases with regeneration of 50% and 70% (R=0.5 and R=0.7), both with a pressure drop of 5% on each side of the heat exchanger. The next figure shows the graphics of specific thrust and specific fuel consumption obtained with the considered configuration.

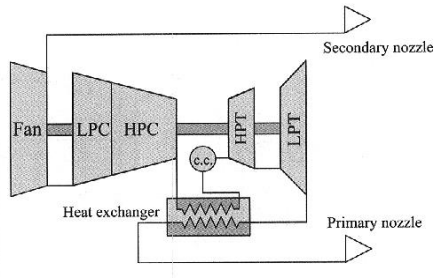

Figure 5: Turbofan Engine with regeneration (Andriani & Ghezzi 2006).

The results with regeneration, reported in Figure 6, show a higher thermal efficiency, than the conventional case of about 4% (R=0.5) and 10% (R=0.7). However, these results are valid for low pressure ratios. If the pressure ratio is increased to 20, the thermal efficiency with R=0.5 coincide with the conventional case. Above 30, the regenerative process exhibit a thermal efficiency worse than the conventional cycle. This is due to the impossibility of exchanging heat above a certain pressure ratio. The pressure drop in the heat exchanger remains, and so the configuration with exchanger is not viable. Regarding the behaviour of TSFC, it is noticed a considerably decrease in fuel consumption, especially at low values of pressure ratio. The same cannot be verified for high values of pressure ratio, where the conventional configuration, show the same values of the regenerated configuration. High values of pressure ratios are usually reached by modern turbofan to take advantage of the high TET. "It seems possible to obtain, if not lower, same levels of SFC as conventional case but at lower pressure ratio"(Figure 7). The authors suggest that this can be achieved, using a smaller, simpler and cheaper compressor. Moreover, the size of the heat exchanger should not be excessive, not larger than the fan considering that at high values of BPR, the mass flow rate of the gas generator, and consequently the flow through the heat exchanger, is much smaller than the secondary.

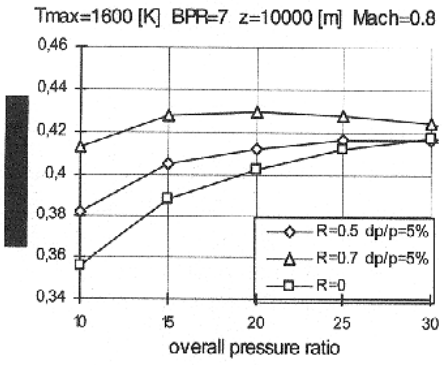

Figure 6: Thermal Efficiency in function of pressure ratio, with and without regeneration (Andriani & Ghezzi 2006).

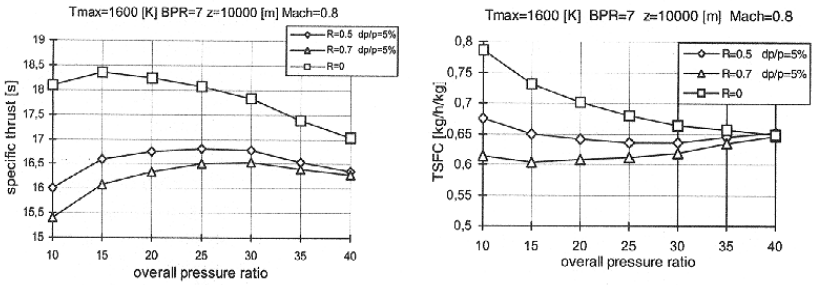

Figure 7: Specific Thrust and Specific Fuel Consumption in function of OPR, with and without regeneration (Andriani & Ghezzi 2006).

Finally, the propulsion efficiency is superior than the conventional situation (Figure 8) and once more at lower pressure ratios, due to the reduced gas kinetic energy in the exhaust, since the heat extracted has been subtracted in the heat exchanger.

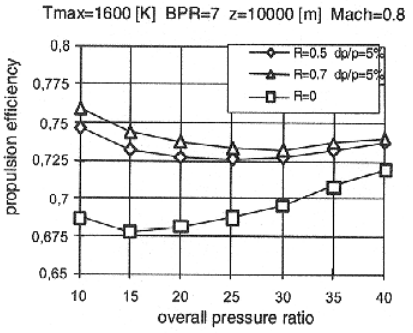

Figure 8: Propulsion Efficiency in function of OPR, with and without regeneration (Andriani & Ghezzi 2006).

The intercooling, by dividing the stages of compression, gives the possibility of cooling down the air temperature between the exit of one stage to the inlet of the following. The work necessary to improve air pressure is less, the compressor absorbs less power providing greater enthalpy drop in the nozzle for thrust. Both practice of the regeneration with intercooling is suggested as a way to obtain a greater output power and a lower specific consumption at a greater thermal efficiency. The main drawback of this configuration is the weight and size imposed by aero engines. The results cannot be compared to the regeneration because it was simulated at zero altitude and zero flight Mach number.

For conclusions, (Andriani & Ghezzi 2006), enhance the problems of size, weight and integration with the engine and the aircraft in both concepts (regeneration and intercooling). Should the problems cited above be solved, and the benefits are clear in the performances. “The introduction of regeneration in a turbofan engine has increased the thermal and propulsion efficiencies leading to a reduction of the specific fuel consumption of more than 10% at low pressure ratios. The price to pay is a reduction of the same order of the specific thrust.” The authors suggest that this loss can be counteracted by the intercooled staged compression process.

The introduction of heat exchangers for engines of two spools could be one of the solutions for better environmental engines. This possibility was studied by (Lebre & Brójo 2010). The reduction in the specific fuel consumption (SFC) and the increase of efficiency and specific thrust (ST) are compared to the penalty introduced by the extra weight. The work compares the performance parameters of a conventional engine against three alternative configurations: use of intercooler, regenerator or both. The comparison shows the influence of each parameter in specific fuel consumption, specific thrust and thermal efficiency.

This numerical analysis uses a conventional turbofan engine with 50 000lbs of thrust. Assumptions applied were a steady and one-dimensional flow; perfect gas with calorically perfect gas C_p and γ in isentropic conditions. External mechanical power is neglected; with cooling air but not bleed. The turbine entry temperature (TET) is 1500K for a specific thrust of 200 at a cruise altitude of 10 668m and Mach 0.8. The OPR is 26, the fan pressure ratio (FPR) is 1.71 and the bypass ratio (BPR) is 5.

In the engine with regenerator, the heat exchanger objective is to heat the air leaving the high pressure compressor with the heat from the exhaust gases. By introducing this component, the required fuel in the combustion is reduced. This is due to the increase of the air temperature before entering the burner, reducing temperature difference between the entry and exit of the burner. The temperature of the exhaust gases leaving the turbine is generally higher than the temperature of the air leaving the compressor. Using this, it is possible to heat the high pressurized air at the exit of the compressor by transferring heat to it from the exhaust in a counter-flow heat exchanger also known as a regenerator.

The engine with intercooler is a type of heat exchanger that is applied between the low and high pressure compressors. The air that passes through this system is cooled before entering the high compressor; consequently the work required for compression is reduced.

At last, the engine with intercooler and regenerator (IR), is characterized by a SFC lower than the conventional with higher thermal efficiency

Results show that the engine with better specific fuel consumption is the engine with regenerator. In contrary, the engine with only intercooling has the worst results, even when compared with the conventional engine (Figure 9). The authors alert that the variation of FPR has impact on ST and on the SFC. The variation of the specific thrust in function of the FPR is equal for all types of engines (Figure 10). It is also observed that the SFC is not modified by the low pressure compressor (LPC) ratio on the conventional and regenerated engines as would expected. By raising the OPR in the conventional engine, it is observed that has the same values of SFC as in the engine with intercooler (Figure 11).

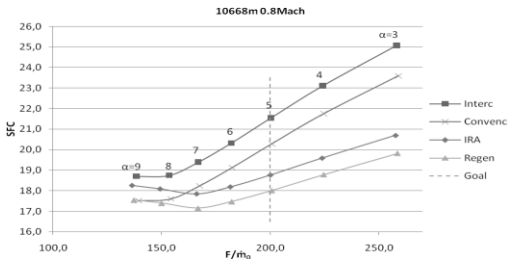

Figure 9: SFC in function of ST (Lebre & Brójo 2010).

Increasing OPR provokes a decrease in SFC. Engines with regeneration or IR cycles the opposite is observed, “An increase in the overall pressure ratio leads to an increase in specific fuel consumption”. This can be observed in Figure 12 along with the correspondent ST.

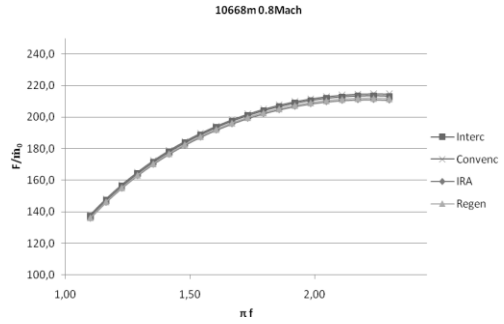

Figure 10: ST in function of FPR (Lebre & Brójo 2010).

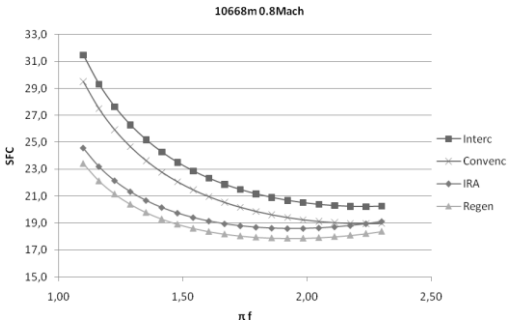

Figure 11: SFC in function of FPR (Lebre & Brójo 2010).

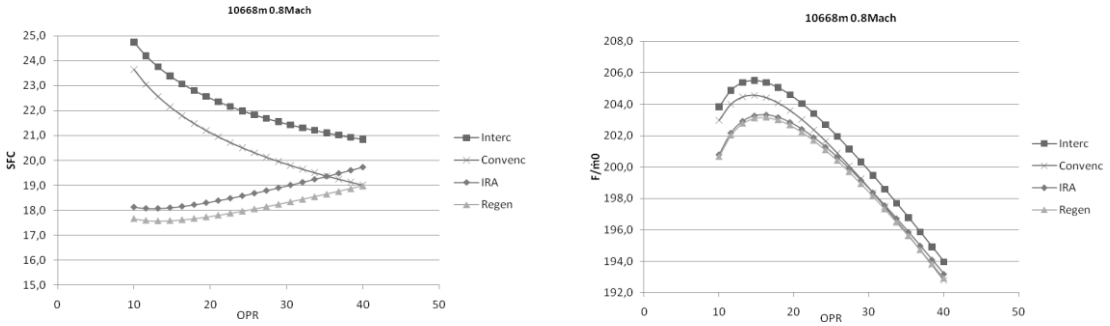

Figure 12: SFC and ST in function of OPR (Lebre & Brójo 2010).

The thermal efficiency is a parameter that increases with the use of the regenerator. From the engines studied, results show that engines with regeneration have higher efficiencies than the engines without it (Figure 13). The FPR is a parameter that influences thermal efficiency which can be increased for low values of FPR. Thermal efficiency does not suffer variation with LPC in the case of the absence of the regenerator. Although an increase in the LPC ratio leads to an increase in SFC and a decrease in thermal efficiency. Another important parameter observed was in the case of a regenerator being present; the increase of OPR has a negative influence on thermal efficiency, while without it the opposite occurs.

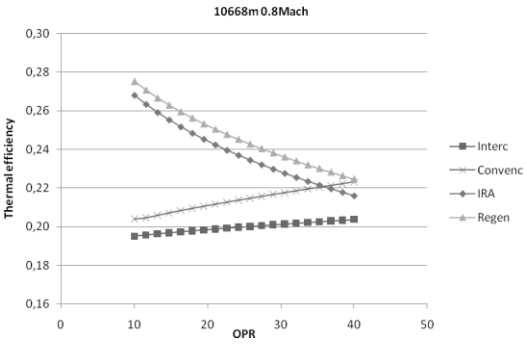

Figure 13: Thermal Efficiency in function of OPR (Lebre & Brójo 2010).

The conclusions of this work revealed that the engine only with intercooler has the worst SFC results and lower thermal efficiency. The engine with intercooler and regenerator has better SFC and thermal efficiency compared to the conventional engine used in this study. “But it is not the one with better values of specific fuel consumption and thermal efficiency. The engine with only regeneration has the lowest values of specific fuel consumption and the highest for thermal efficiency.” The IR also has lower values of performance compared to the

engine with only regenerator. “With this behaviour can be deduced that the influence of the regenerator is larger than the intercooler for the range of parameters considered.” The engine with regenerator is pointed to be the best in SFC and thermal efficiency.

(Humhauser 2005) points that in the near future, the idea of aiming better thermal/propulsive efficiency with more fuel, noise and efficient components, will have to take into account the possibility of increasing the bypass ratio and reduce the fan tip speeds as well as the jet velocities. These measures will help the enhancement of propulsive efficiency and noise reduction.

Regarding the thermal efficiency, (Humhauser 2005), suggests that increasing the overall pressure ratio (OPR) and the turbine entry temperature (TET) is necessary to achieve the desired goals. The research in improved cores may counteract the weight penalties from enlarging BPR and fan diameters. Expectations of values for OPR and TET, for long range applications are 50 and 2000K-2100K respectively.

The geared turbofan concept (Figure 14) is the answer suggested by the author for aiming those kinds of bypass ratios and OPRs. “Since more than 15 years, Pratt and Whitney America (P&WA), Pratt & Whitney Canada (P&WC), Fiat Avio and MTU are jointly working on the development of geared turbofan engine technologies for small and large thrust class applications.”

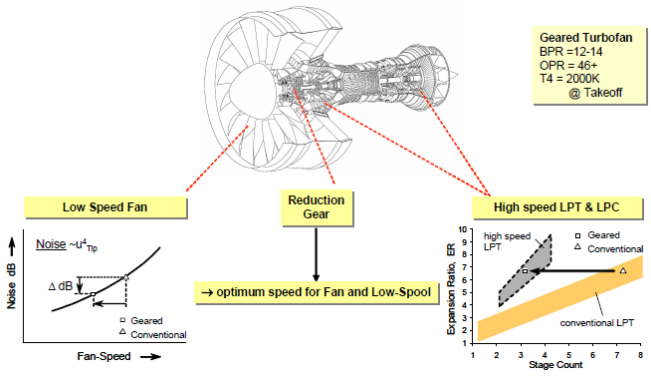

Figure 14: The Geared Turbofan Concept (Humhauser 2005).

(Riegler & Bichlmaier 2007) make an analysis of the concept and the development status of the geared turbofan. The concept of applying a speed reduction gear on the low spool of a two-shaft engine between the slow spinning side (Fan) and the fast spinning side (LPC and the LPT) have been investigated for two decades. It provides the possibility of an additional degree of freedom which benefits the optimization of the turbo machines independently, keeping high work extraction on a low number of stages. The aerodynamic losses can be

lowered and putting efficiencies in higher values. By de-coupling the Fan speed from the rest of the low spool machinery, this principle intention is to further increase the bypass ratio in order to improve propulsive efficiency. As a consequence, TSFC decreases as well as noise and weight. It can be applied to long range missions and wide body aircrafts, but mid-range single aisle aircrafts and regional jets are also considered.

The maintenance costs benefits due to reduced stage and airfoil count are most valued by the operators as well as the 70% reduction weight of the LPT which counteracts new or heavier components of the engine.

This concept represents the next step in performance, emissions (due to low fuel burn), noise and does not impose unreasonable risk to the customer (Figure 15), as a more revolutionary step like the counter-rotating turbo machinery concept. However the open rotor concepts can provide higher TSFC and fuel burn benefits, they are struggling with achieving noise requirements and the technology improvement is still one decade away. There is a need of dramatic changes of engine/airframe integration.

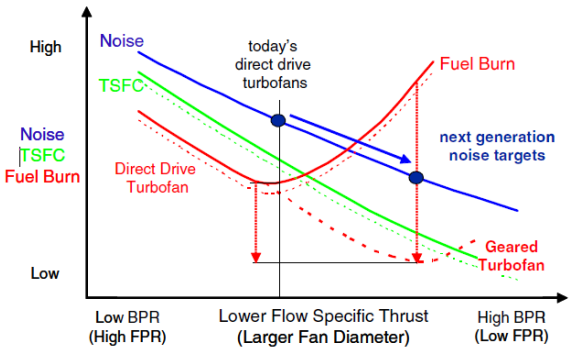

Figure 15: Predicted Parameters of the Geared Turbofan Technology (Riegler & Bichlmaier 2007).

Therefore, according to (Riegler & Bichlmaier 2007), the GTF "is the only turbofan engine concept which allows significant reduction in fuel burn, maintenance cost and noise at the same time, and which will be technology ready near-term to support EIS dates the aircraft manufacturers and airline customers are envisioning.". From the author's view it is stated that "the GTF engine is THE best concept for the demands of the market".

An optimization study of the GTF engine is performed by (Breu *et al.* 2011). In this work the targets are: minimize the emissions, and compare the results against a direct drive turbofan for a given mission. Mechanical design analysis is also performed so it can be possible to predict the effects of the weight engine and the nacelle drag.

This analysis includes a preliminary design and evaluation of the aircraft generated in the house code GISMO, which will provide performance and nacelle drag results. Regarding the engine, the performance is evaluated by GESTPAN (generic tool for gas turbine design and analysis). Weight and dimensions are performed by the design tool WEICO. The optimization of the engine was assessed by the optimization software ISIGHT. The parameters chosen to apply in the optimization software were: BPR, fan pressure ratio and the overall pressure ratio.

In the design point of the engine it is noted that an increase of BPR will origin a bigger fan diameter, which will influence drag and weight in a negative way. Despite of the reduction in fuel consumption while the BPR increases, the author's alert for the fact that for some values of BPR more stages in the LPT are added, thus weight will be added to the engine. These effects will be more incisive in the direct drive turbofan, in such a way that it is stated: "it is worth considering going to a slightly lower BPR than the optimum if the part count can be reduced". The fuel burn will decrease with the increasing of the OPR, although this was kept constant for both engines (40) as well as the TET (1850K).

Results indicate that 3% lower fuel consumption for the mission is achieved for the GTF. In terms of bypass ratio it does not differ too much for both engines (12.5 for the DDTF and 13.5 for the GTF), however the number of stages of the HPC in the DDTF will be significantly higher adding extra weight. The total engine weights are 3100kg for the DDTF and 2880kg for GTF, giving a 220kg of weight saving on the geared configuration (Table 1).

Table 1: Weight and Dimensions of a DDTF and a GTF configurations (Breu *et al.* 2011).

	DDTF	GTF
Total engine weight [kg]	3100	2880
Fan weight [kg]	888	906
Booster/IPC weight [kg]	66	55
HPC weight [kg]	87	48
HPT weight [kg]	66	78
LPT weight [kg]	555	221
Gearbox weight [kg]	–	170
LP-shaft weight [kg]	44	18
Fan diameter [m]	1.84	1.87
Nacelle length [m]	3.8	3.4
Blade height last stage HPC [mm]	12.3	13.5

Therefore it can be concluded that all characteristics combined with other structural innovations can potentially deliver fuel benefits for GTF engine. The weight reduction and the lower stage loading with higher component efficiencies prove to be the next step of the turbofan market.

The two future engine concepts (Geared Turbofan and Open Rotor) are often compared in similar conditions. While the first is the next step in ducted turbofans, the other brings a more revolutionary arquitecture design. Benefits and drawbacks meet these two kinds of engine and are exposed by (Becker *et al.* 2013). This investigation considered a 150 passenger short range airliner, where the GTF is a standard two shaft engine while the Open Rotor is a counter rotating aft mounted three shaft pusher. Both concepts are numerically optimized for a set of discrete operating points, where the component efficiencies and cooling technology of the core engines are aligned in the same technology level. It is intended to analyse fuel efficiency of overall aircraft as well as weight/drag estimations. The engines are submitted to a flight mission, where cruise condition was selected as the master design point since it is the most important flight condition regarding consumption.

The optimizer modified a set of independent variables such as LPC, HPC pressure ratios, TET and BPR in order to find the optimal solution in cruise fuel efficiency (Table 2). In the GTF the fan pressure ratio was automatically iterated to achieve optimal velocity ratio between the core and bypass nozzle.

Table 2: Independent variables used in the optimization process (Becker *et al.* 2013).

Concept	Parameter	Unit	Min	Max
GTF	LPC PR	[-]	2.0	5.0
	HPC PR	[-]	5.0	15.0
	TET	[K]	1500	1600
	BPR	[-]	10	16
CROR	LPC PR	[-]	5.0	10
	HPC PR	[-]	5.0	10
	TET	[K]	1550	1650

The results feature a GTF with a bypass ratio of 12.2, with an ideal fan pressure ratio of 1.38. The estimated weight of this propulsion system is approximately 3201kg with a smaller core and a lighter nacelle configuration, while the CROR engine exhibits a predicted mass of 4097kg. The authors suggest that an increase in weight reduction is possible by applying composite materials in the fan to overcome the penalty of its increased size. The superior weight of the open rotor has a consequence in the reduction of the maximum structural payload (MPL) by 1390kg, whereas a minor increase of the MPL can be verified in the GTF. The BPR of the CROR is seven times larger than the GTF resulting in a propulsive advantage. That advantage is seen in a SFC improvement relative to the baseline model by 36% against 20% from the GTF (Figure 16). The OPR and TET were kept constant at 46.9 and 1509K.

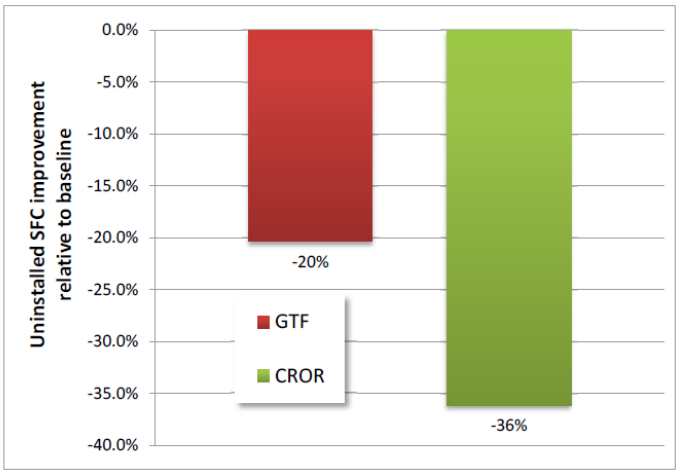

Figure 16: Uninstalled cruise SFC of the GTF and CROR (Becker *et al.* 2013).

The flight mission executed by these engines was over 4465Km. The GTF was capable of reducing 19.4% relative to the baseline model and the CROR achieved the 30.2% fuel cut. The results from the GTF are superior to the claimed by Airbus and Pratt & Whitney for the A320Neo equipped with the PW1100G.

As conclusions from this work, (Becker *et al*. 2013) state that despite the weight penalty of 28% of the CROR compared to the GTF, its propulsive efficiency outweighed the issue with a 12-13% fuel burn cut over the GTF. However engine installation effects of the study need to be more developed to assure the described benefits, which sustains (Riegler & Bichlmaier 2007) conclusion on this topic. Nevertheless, the authors point the open rotor as the next answer over the near term new engines (PW1000G and LEAP-X) with the potential to offer even more benefits for the 2025 engine generation.

Regarding the GTF, this kind of engine suffers a penalty in drag and weight if conventional nacelles are used. New composite materials and engine-airframe integration like embedded engines are pointed to help circumvent these drawbacks. The increase in BPR may lead to a small core size, in contrast with the cruise and top of climb temperatures that will be superior to the conventional values. Technology developments are required to improve the specific power of the core.

Another similar study was performed by (Larsson *et al*. 2011), in which a geared open rotor and an ultra-high bypass ratio geared turbofan engine are compared and assessed. The priorities were minimizing the block fuel through the specific thrust level and the resulting engine emissions from a flight mission with a 2020 predicted technology. This multidisciplinary analysis contains computational models that capture the engine performance, aircraft design/performance as well as the direct operating costs and emissions, using the EVA[1] code. The mechanical and aerodynamic design, engine component weight and dimensions were worked by the design tool WEICO. Both of this programs were integrated together to work with a commercial integration and optimization environment.

The GTF of this study is a two shaft configuration with a conventional reduction gearbox. On the other side, the open rotor is a geared contra-rotating pusher configuration with a core of a two spool turbojet; the propulsor consists in a power turbine that drives two contra rotating propellers with swept blades. A planetary gearbox is between the propellers and the power turbine. OPR and TET were kept constant with the purpose to provide mid-cruise conditions as well as optimal BPR for SFC. The studies relatively to a direct turbofan for the year 2020 showed that reducing the specific thrust can improve the propulsive efficiency but worsens the transmission efficiency, introducing a constraint in the search for the optimal engine design. At FPR of 1.2 there's no thermodynamic benefit from further reducing the specific thrust. Similar results were obtained in the fan and LPT polytropic efficiencies (Figure 17).

[1] A code developed in (Kyprianidis *et al*. 2008) for environmental assessment of novel propulsion engines.

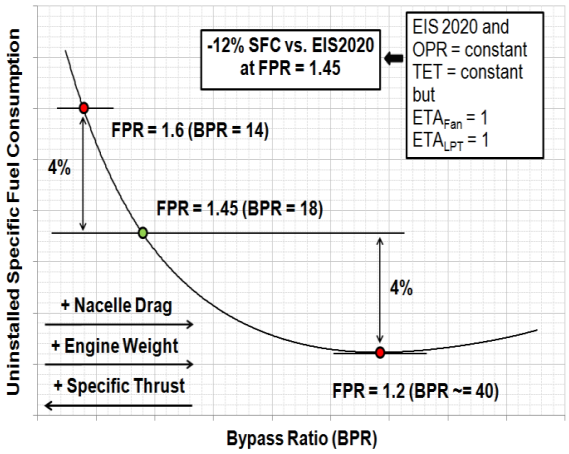

Figure 17: Estimated 2020 uninstallled SFC benefits from reducing ST in a conventional turbofan engine with optimal LP and core (Larsson *et al.* 2011).

Considerations were made:

- Raising the efficiency of the fan and LPT directly improves SFC as well as the optimal BPR value at a constant specific thrust.
- Limited SFC benefits may be acquired by reducing specific thrust beyond a fan pressure ratio of 1.45.

Predictions from the authors for the year 2020, reveal that by reducing the specific thrust in a direct drive fan conventional core engine for long haul applications, the block fuel benefits have a consequence of 10 % increase in fan diameter and 4% reduction in FPR (translating in a 14% reduction in specific thrust) and resulting in a 2% improvement uninstalled SFC at mid-cruise. The engine weight would increase by 17% along with the higher nacelle drag and the resultant block fuel benefit would only be of 0.85% (Figure 18). "It can therefore be concluded that the commercial competitiveness of reduced specific thrust turbofan designs will largely depend on how the aviation market evolves in the years to come until 2020." According to (Larsson et al. 2011), the block fuel benefits are highly dependent on the engine thrust to weight ratio. Therefore, the engine design for minimum block of fuel represents a trade-off between improving thermal and propulsive efficiency and reducing engine weight and nacelle drag, knowing that depends primarily on specific fuel consumption, engine installed weight and nacelle drag.

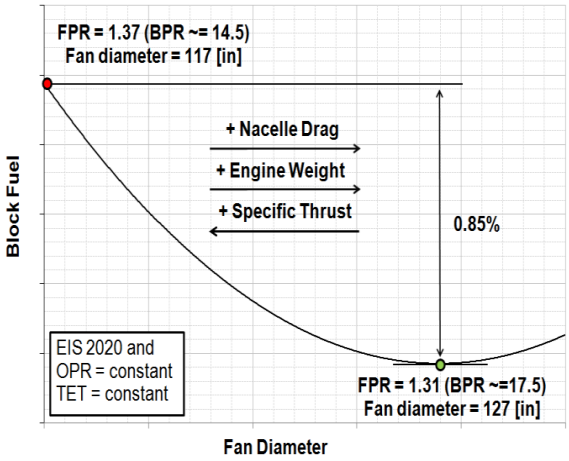

Figure 18: Estimated 2020 block fuel benefits from reducing ST in a conventional turbofan engine for long range applications (Larsson et al. 2011).

Regarding the engine temperatures, the authors also show the trends for engines designed for long haul applications. These new engines will have new temperatures for maximum combustor outlet and turbine blade metal. Following is the Figure 19 that predicts the evolution of the turbine entry temperatures until 2020 and the respective technology of the blade material.

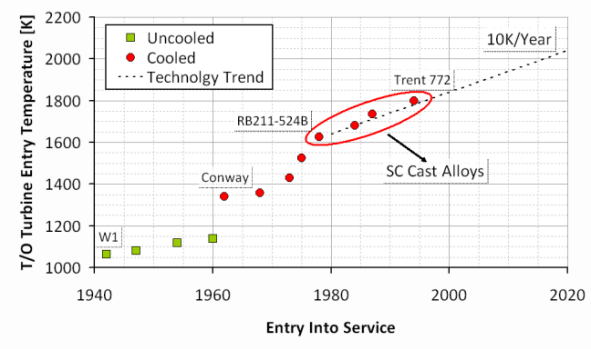

Figure 19: Turbine blade material technology chronology and maximum TET (Larsson *et al.* 2011).

Results show that the open rotor concept provides substantial fuel saving potential compared to the ducted fans, it gives 14% lower SFC than the GTF. Although heavier in weight, the reduced SFC and nacelle drag can compensate the drawbacks. The variation of the open rotor bypass is bigger than the GTF in different operating points. In mid-cruise conditions, the GTF can deliver the lowest SFC as possible; the same cannot be achieved in the open rotor. This is verified in off-design conditions, where the propeller efficiency is reduced as the engine is throttled down (Figure 20 and Figure 21).

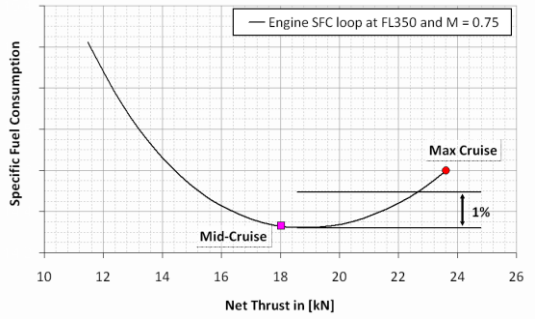

Figure 20: SFC in function of Net Thrust for fuel optimal GTF (Larsson *et al.* 2011).

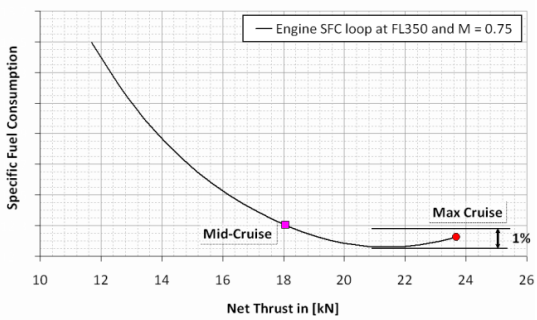

Figure 21: SFC in function of Net Thrust for fuel optimal GOR (Larsson *et al.* 2011).

In terms of weight for both engines, the large fan of the GTF is a major player to the total weight, whereas the open rotor, the major part of its weight results from the propellers, associated structural components and a heavier gearbox. It can be observed that the open rotor engine core is roughly 50 kg heavier, due to the intermediate pressure turbine that is not present in the geared engine (Table 3 and Table 4).

Table 3: GTF weight distribution (Larsson *et al.* 2011).

Fan (including cold structures)	770 kg
Engine core	180 kg
Low pressure turbine including turbine exhaust frame and low pressure shaft	420 kg
Gearbox	215 kg
Nacelle including thrust reverser	800 kg
Accessories, nozzles, bypass duct, bearings	270 kg
Total weight	2655 kg

Table 4: Open Rotor weight distribution (Larsson *et al.* 2011).

Engine core	230 kg
Low pressure turbine and turbine exhaust frame	510 kg
Gearbox	505 kg
Propeller weights and rear structures	1335 kg
Nacelle	95 kg
Accessories, nozzles, bypass duct, bearings	275 kg
Total weight	2950 kg

A sensivity study was made to evaluate the block fuel impact in component efficiency/technology. Results show that the sensitivities from the changes in components efficiency are superior in the GOR than for the GTF. Varying component efficiencies, the core velocity varies and the velocity ratio moves away from the optimal point. Since the jet velocities for the open rotor are lower, the sensivity figure is higher for the propellers than for the fan regarding that a larger part of the thrust is produced by the propellers compared to the fan.

”With CO_2 emissions being directly and linearly correlated with fuel flow and hence block fuel, it can easily be concluded that the GOR concept offers a reduction of up to 15% in CO_2”.

As conclusions, despite the heavier engine of the open rotor, the reduced SFC and nacelle drag makes up for this. However, the mid cruise operating point is not at the bottom of the SFC loop. A precise trade-off is necessary regarding the size of the engine and the design point for the propellers, since for short haul aircraft, the major part of the flight is spent in climbing to cruise, rather than cruising. It is also stated that 6% lower in DOC can be expected from the geared open rotor concept than from the GTF at current fuel prices. Although the exposed benefits of the GOR, the authors remind that introducing a new concept in the market has large risks, such as: delayed introduction of the product to the market, increased development costs and late design changes. So they leave the question for future investigations: “Can the potential reduction in DOC outweigh the technological risks involved in introducing an open rotor configuration into the market.”

A study performed by (Guynn *et al.* 2009) enhance the clear benefits of increasing the bypass ratio in terms of SFC, however these benefits may not translate into aircraft system level benefits due to integration penalties. With that idea in mind, the primary objective of this study was to determine if the TSFC and noise improvements of high values of BPR could really translate into overall aircraft system benefits. This study addresses the design trade space for advanced turbofan engines applied to the single-aisle transport (737/A320) replacement entering service in the 2015-2020 time frames. It is possible that the engines for the 737/A320 replacement will continue the trend of raising the BPR, leading to ultra-high bypass ratio (UHB) engines. The benefits of higher bypass associated technologies such geared fan drive, can bring improved propulsive efficiency. However bypass ratios at which fuel consumption is minimized may not require geared technology, however a geared fan drive

enables higher bypass ratio designs which result in lower noise, all of these pros and cons are considered in this study. “The 737/A320 class considered in this study represent a significant portion of the global airline fleet. Sixty-five percent of the new aircraft produced over the next 20 years are projected to be in this class. Advances made to reduce the noise and emissions of these aircraft could provide a considerable positive contribution to the goal of minimizing the future environmental impact of aviation.”

The approach consisted in the development of a series of analytical engine models, apply them to an airframe and assess the overall performance and noise characteristics. The main parameter of interest to the study was the fan pressure ratio (FPR), knowing that the BPR is inversely proportional to fan pressure ratio. As fan pressure ratio is reduced, to maintain thrust fan mass flow must increase, which results in higher bypass ratio. The projected engine models for the 2015 time frame were developed by a design team with a common design approach and set of technologies assumptions to enable this consistency. The baseline model was a two spool separate turbofan. Variations like fan drive approach (geared vs direct); FPR, the low spool-high spool compression work split, the type of fan nozzle (fixed or variable geometry), OPR and Mach number were considered. All the engines were developed with the same Aerodynamic Design Point (ADP), which is Mach number, altitude and thrust, as well as equal OPR with two variants: “low work” and “high work”. The “low work” engines have a lower pressure rise across the low pressure compressor (consequently higher pressure rise across the high pressure compressor), the inverse situation is the “high work” The ADP selected was a nominal top-of-climb (TOC) for the airframe. To meeting a thrust target at TOC conditions, a SLS thrust target of 23 000lb (hot day, ISA+27°F) was implemented. The low fan pressure ratio engines inherently have a greater loss of thrust with airspeed, than high fan pressure ratio engines. To assure the required thrust for ADP, the low FPR engines are operated at higher temperatures. However, high temperatures on the low FPR engines could lead to a reduced hot section life and greater maintenance than high fan pressure ratio engines. The engine life and maintenance influences were not studied.

The numerical tools used for this evaluation were the Numerical Propulsion System Simulation (NPSS) for the cycle analysis of the engines and the Weight Analysis of Turbine Engines (WATE) for the aeromechanical characteristics of the engine weight; emissions were obtained from a correlation developed by NASA combustor technologists during the latter stages of NASA’s Ultra–Efficient Engine Technology Program.

This investigation resulted in three different sets of engines having different design rules and assumptions. Each set contains 16 different configurations for a total of 48 engine/airframe combinations. The primary differences between the three sets were OPR at ADP and ADP/cruise Mach number. In the first set all of the engines were designed with an OPR of 32 at TOC similar to of the CFM56 engine. Higher OPRs can lead to smaller compressor blades, although there are limits to how small compressor blades can be manufactured and how

efficient they are. The second set of engines was made to obtain an OPR increase to 42, changes were made in LPC and HPC pressure ratios. The two first sets were designed with a Mach number of 0.80. (Guynn *et al*. 2009) say that in order to increase fuel efficiency, some suggest that the replacement of the 737/A320 families can be designed to fly significantly slower. Due to environmental and economic pressure, the airliners may be willing to lose some productivity (speed) for reduced fuel consumption. Following the same idea, the last set of engines was developed with a reduced Mach number to 0.72 to evaluate the performances.

The results of the ramp weight show that there is a clear preference for high work geared designs at fan pressure ratios up to 1.5 and for low work direct drive engines at higher fan pressure ratios. The weight penalty associated with the low FPR is consistently in the three sets. All the three sets reduce the ramp weight with a higher FPR. Regarding the block fuel, it is observed that the worse values are for engines with very low FPR. The minimum block fuel consumption occurs in the 1.55 to 1.6 FPR range. Geared engines are preferred bellow a fan pressure ratio of 1.5, the same as for the ramp weight (Figure 22). In the three sets the fuel consumption is reduced by high OPR and lower cruise Mach number.

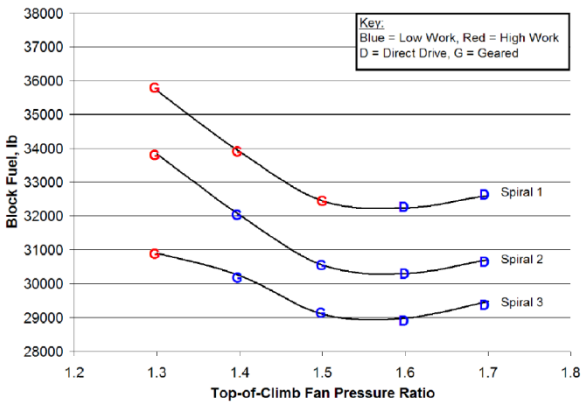

Figure 22: Block fuel in function of FPR (Guynn *et al*. 2009).

Like the ramp weight, the emissions of NO_x decrease with the increasing fan pressure ratio, being the geared configuration beneficial up to FPR of 1.6 (Figure 23). All the variations of the parameters are well observed in the results, but the noise with the FPR variation is superior comparing the variation in the weight, fuel consumption or emissions.

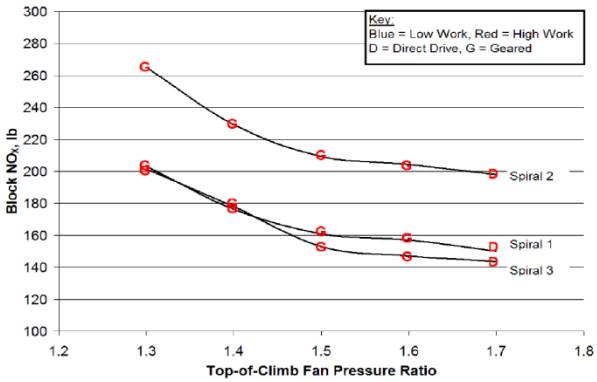

Figure 23: Block NO_x in function of FPR (Guynn *et al*. 2009).

The results lead to a low FPR UHB engines that can offer the possibility of a lower aircraft noise, but at the expense of slightly higher fuel consumption and total NO_x. In an isolated engine, a low FPR (higher bypass ratio) is beneficial for both reducing fuel consumption and noise. However, when applied in the airframe, the desire for lowering theses values may not lead to the same optimum fan pressure ratio. Reduced indicators of noise and LTO NO_x are achieved by driving the fan pressure ratio as low as possible, whereas good values for vehicle weight, block fuel, and block NO_x are achieved with higher values of FPR. This leads to the conclusion that are series of design trade-offs that must be established (Table 5). For example: a low FPR may benefit the noise reduction, however incurs an increase in fuel consumption compared to what could be achieved with a higher fan pressure ratio setup.

Table 5: Second Setup Trade-Offs (Guynn *et al*. 2009).

	Ramp Weight	Block Fuel	Block NO_x	LTO NO_x	Cum. EPNdB
Low, Geared, FPR=1.4	+8.6%	+5.7%	+21.6%	+4.8%	+0.2
High, Geared, FPR=1.4	**+7.3%**	**+5.9%**	**+15.8%**	**+2.3%**	**Minimum**
Low, Geared, FPR=1.5	+3.1%	+0.8%	+11.9%	+1.3%	+5.2
High, Geared, FPR=1.5	**+2.3%**	**+1.6%**	**+5.8%**	**Minimum**	**+5.3**
Low, Direct, FPR=1.5	+4.3%	+1.1%	+12.8%	+0.8%	+5.4
High, Direct, FPR=1.5	+7.8%	+6.2%	+11.2%	+2.8%	+5.8
Low, Geared, FPR=1.6	+2.8%	+2.5%	+10.7%	+7.9%	+12.5
High, Geared, FPR=1.6	+1.3%	+2.7%	+3.1%	+6.1%	+12.4
Low, Direct, FPR=1.6	**+1.0%**	**Minimum**	**+8.1%**	**+5.1%**	**+11.9**
High, Direct, FPR=1.6	+3.1%	+3.7%	+4.7%	+5.9%	+12.5
Low, Direct, FPR=1.7	**Minimum**	**+1.3%**	**+1.2%**	**+14.3%**	**+16.7**
High, Direct, FPR=1.7	**+1.6%**	**+4.4%**	**Minimum**	**+13.4%**	**+17.1**

The low work, geared and direct drive cases and the high work geared cases, have a relatively good weight, fuel efficiency, noise, and emissions results. (High work, direct drive, FPR =1.5 case has inferior performance to the other FPR=1.5 cases). The bypass ratios obtained were between 12.5 and 14.5. It is believed that the general characteristics of the engines studied are similar to what is offered by Pratt and Whitney geared engine to the Bombardier CSeries aircraft. The thrust level target of the CSeries is 23 000lb, the same used in this study at SLS condition. The fan diameter for the CSeries is expected to be 73 inches, the same used in the

two first setups with a FPR of 1.5. Bypass is predicted to be 12, similar to the FPR 1.5 engines studied.

The first setup offered 15% reduction in ramp weight, up to a 24% in block fuel consumption, up to 73% reduction in block NO_x and up to a 58% reduction in NO_x emissions per landing-take-off cycle. However these results occur in different engine designs. The second setup offers greater potential then the first one. Potential fuel consumption benefit is up to 29% as well as the ramp weight that could be up to 16% less. However they have less NO_x reduction potential due to the higher emissions associated with higher OPR: 64% in block of NO_x and 54% reduction in NO_x per LTO cycle. Regarding the third setup, the fuel consumption benefit was nearly the same as the second setup. However, lower emission indices associated with the lower cruise Mach lead to a large reduction in block NO_x than the second setup (69%).

As conclusions of the analysis, large diameter associated with UHB engines can be accommodated for a 737/A320-class vehicle, with simple modifications such as increased landing gear length or changes to wing dihedral. The best FPR is dependent on the metric of interest and ground rules, arquitectures and assumptions. Empty and ramp weight are minimized with high fan pressure ratio; block fuel consumption is minimized with a fan pressure ratio of ~1.6; block NO_x emissions are minimized with high FPR; and LTO NO_x and certification noise are minimized with FPR as low as possible. The FPR is always constant with OPR and design Mach number. The geared configuration enables propulsion systems at lower fan pressure ratios that were not possible with a direct drive fan. It is desired for FPR (top of climb) below 1.5 (roughly BPR>13). At a FPR of 1.5, a low work LPC, direct drive engine can provide results similar to a geared engine. However, with a FPR above 1.5, a low work direct drive engine provides better overall aircraft system in the metrics studied than the geared engines.

(Guynn *et al*. 2009) conclude that if the design goal is to minimize ramp weight, block fuel, or block NO_x, geared fan engine technology is not necessary, if the minimums for the metrics occur at a FPR greater than 1.5. However if the design objective is to minimize airport area environmental impacts, a geared system is the way to follow because it enables a practical low FPR engine design. The best balanced designs are the 1.5 FPR designs. In the metrics of interest (ramp weight, fuel consumption, emissions and noise), either the high work LPC with a geared fan, or the low work LPC with geared or direct drive fan are well balanced options.

The new GTF engine will be the next turbofan step in commercial aircraft for the next years. This technological step will represent the best answer in current technology to cut down pollutant emissions; however, the application of alternative cycles creates the question if the goals can be pushed further. These cycles were previously studied in the direct drive turbofans and now are starting to be explored in this next engine generation.

This can be verified in the study objectives performed by (Boggia & Rüd 2004). The work focuses on the exploration of the thermodynamic cycle of an intercooler and a MTU-designed exhaust gas recuperator applied to a 3-shaft geared turbofan configuration. The cycle optimization of two variant of engines is made with different fan diameters and BPR values for long range applications at cruise conditions, although other design points of the flight are considered. The fuel consumptions and emissions are calculated as well as the weight of the heat exchanger. The goal is to optimize them to improve the overall aircraft economic balance Parameters like BPR, OPR, temperature levels and component characteristics were analysed.

This investigation is carried out by MTU in a novel concept aero engine dubbed IRA: Intercooled Recuperative Aero Engine. The purpose of the heat exchanger in the hot exhaust is to bring back thermal energy from engine exit to the combustion chamber. This allows a fuel saving because part of the burner temperature is supplied by the exhaust. Although, it is imperative that exists a sufficient temperature difference between compressor exit and turbine exit. For a high exchange level in the recuperator there must be a high temperature in the LPT outlet so lower SFC values can be reached. A variable geometry of the turbine system provides high turbine exit temperature. The low exit temperature of the compressor is assured by the intercooler.

The thermodynamic cycle of IRA concept, offer higher efficiencies with lower OPR values, which is crucial to a high heat exchange level and also offers lower NO_x emission level as well as a weight reduction in the core turbomachinery. One of the challenges of this program is the development of the layout of the recuperator modules and the piping system due to the limited space in the exhaust section. An OPR of 30 and a TET limit of 1800K have been chosen for both engine versions.

All the benefits of the geared turbofan are once more exposed in this study: the fan and low pressure system are capable of running at their optimum speeds, offering a stage reduction. There is a weight reduction in the core and in the low pressure system which can also influence the production costs. The noise is also reduced by the fan (high BPR) and the LPT, revealing a tonal noise being shifted into higher frequencies.

The results (Table 6) show an OPR of 30 and a TET limit of 1800K for both engine versions with engine thrust kept constant. Low OPR enables low core mass flow which drives the BPR beyond 25 even though the fan diameters are within a usual range. “The two selected cycles are a compromise between design goals (lowest possible SFC and core size) and design constraints (over maximal temperature and maximum fan diameter).” It is also observed higher burner temperature can provide better SFC values, which can be justified with higher heat exchange registered when the temperature difference mentioned before is increase. “However, gains get smaller with increasing temperatures”. A significant result is that an

increase toward higher OPR does not benefit the SFC results. Figure 24 and Figure 25 provide the variations of SFC according to the OPR and BPR.

Table 6: Results for both engines of the IRA cycle (Boggia & Rüd 2004).

D_{FAN}	92 in	109.9 in
F_N @ T/O	45 klb	45 klb
F_N @ M.Cl.	9.5 klb	9.5 klb
F_N @ Avg.Cr.	7.1 klb	7.1 klb
BPR @ Avg.Cr.	17.1	26.5
Core Size @ M.Cl.	3.20 kg	2.99 kg
Gear Ratio	3.1	4.3
OPR @ M.Cl.	30.0	30.0
T4 @ M.Cl.	1943K	1944K
T4 @ Cruise	1899K	1899K
T41 @ M.Cl.	1800 K	1800 K
SFC@ Avg.Cr. [lb/h/lb]	0.509	0.493
ΔSFC vs. reference @ Avg.Cr.	-16.0 %	-18.7 %

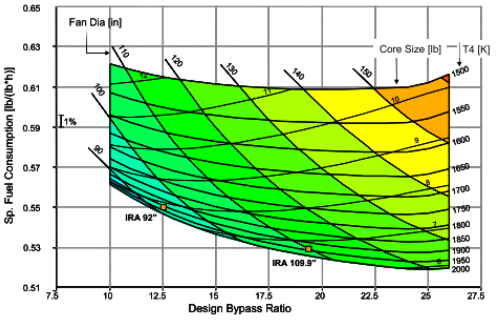

Figure 24: SFC in function of the BPR of IRA cycle at Max. Climb (Boggia & Rüd 2004).

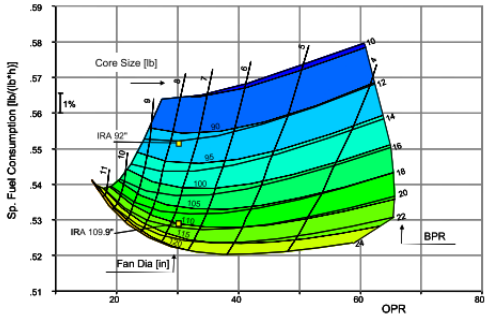

Figure 25: SFC in function of the OPR of IRA cycle at Max. Climb (Boggia & Rüd 2004).

As conclusion the IRA showed a SFC reduction of 18.7% relative a 1995 technology turbofan and NO_x emissions would be 60% lower than the corresponding ICAO-96 limit. In comparison with a GTF from 2015 technology, the prediction is 8% improvement for SFC. The geared configuration may double the improvements concerning fuel burn and noise thanks to BPR beyond 12 and 13. The drawbacks of this concept are pointed as the complexity of the engine construction, additional expensive components as well as the reliability/life issues of the same due to higher temperatures loads and heat exchanger modules. These penalties, according to (Boggia & Rüd 2004), must be balanced with better operating costs and the development of constructive solutions to reduce the overall engine weight, resulting in lower fuel consumption. Investigations and technology programs to develop this technology must continue to provide the necessary know-how.

Another interesting study about innovative cycles for the future aircraft propulsion is made by (Corchero *et al.* 2008). The work developed is part of the EnVIronmenTALly aero-engine program and consists in the application of three new thermodynamic cycles to aircraft propulsion. This focus study is looking for benefits on fuel consumption, carbon dioxide, nitrogen oxides emissions and noise. The analysed cycles were: intercooler-regenerative, the

wave rotor topping and the constant volume combustor engines. The work started from a baseline model, a next-generation UHB turbofan short-range aero engine with a BPR above 12 and two possible design conditions were considered (SLS and cruise at 10 668m with M_0=0.8). The required technological level and emissions are analysed and represented by the turbine entry temperature (TET). Therefore the influence of these new cycles is exposed as well as the design changes to the baseline model.

The authors alert that the previous growth in aircraft industry was focused on minimum fuel consumption and manufacturing/maintenance costs. Today, with a 5% growth in air travel per year, not only these points are important but a new line of interest has emerged that drives the technology in the aero engines: the pollutants. Emissions from NO_x gases, mainly the CO_2 emissions are measured by the specific fuel consumption (SFC); and at last the noise. Therefore it is pointed that engines with higher thermal and propulsive efficiencies are the solution to reduce the SFC at a given flight velocity decreasing the CO_2 production. The specific thrust (ST) also influences the fuel burnt and noise emission and being another crucial engine variable to pay attention. It represents the amount of thrust per unit of airflow mass coming into the engine. Therefore it can translate the engine size, weight and drag. Higher ST lowers the engine size. To attend the efficiencies, (Corchero *et al*. 2008) suggest that the maximum temperature and the OPR of the cycle have to be pushed up resulting in a lower SFC. Many European programmes are committed to achieve these goals.

The purpose of the VITAL program in a short-term is the application of an optimized LPT, which drives a fan with an UHB and a booster in the engine core from a previous fixed modern gas generator. Arquitectures like direct and geared drives as well as counter-rotating fans are included in the program. Propulsive efficiency improvement goals and also weight reduction of the LPT spool are present. In a long term, this program is devoted to innovative cycles to improve engine efficiencies and emissions.

The present work considered that the LPT spool and the bypass stream were optimized to get a maximum feasible propulsive efficiency. Bypass data (bypass ratio, outer fan pressure ratio, outer fan efficiency and mass flow), booster data (pressure and efficiency) and inner fan data (inner fan pressure ratio and inner fan efficiency) are assumed constant. The same is also for the bled air for turbine cooling system, represented by the TET value. Enthalpy and entropy were considered as well as transport coefficients along with the temperature change. Fuel air ratio, specific heat ratio and other variations with temperature are enabled.

Regarding the IRC cycle, IC cools the whole core mass flow, W_{cool}. It represents the ratio between the bypass heated mass and the total bypass flow. While the RHE transfers the energy from the LPT exit to the combustor entry, considering stagnation pressure losses on both streams, cool and hot. The regenerative thermal ratio or regenerative efficiency range varies from 0.6 to 0.9. In the both design points studied, two representative designs were

considered: constant TET and the other at constant ST (constant values equal to the baseline engine).

The results were scaled by reference to the baseline engine model values at respective flight conditions SLS+15 or cruise. For IRC cycle, at SLS, stagnation losses are equal to 3 per cent and will increase if highly compact heat exchangers are used. A target of 0.9 for regenerative efficiency, which benefits the SFC at maximum, represents the target to achieve for aero-engines and it is possible in terrestrial applications.

Different cooling bleed configurations were also analysed for constant ST designs. The benefits vary from practically nil for $\eta_R = 0.6$ to above 15 per cent with $\eta_R = 0.9$, and low OPR when cooling air is bled at the exit of the RHE. This cooling configuration provides benefits because the cooling air is bled at higher temperature than when it is bled at the RHE entry (Figure 26 and Figure 27).

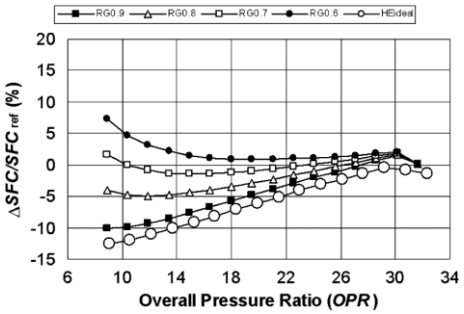

Figure 26: ΔSFC in function of OPR, for constant ST, with regeneration and cooling air bled before the RHE (Corchero *et al*. 2008).

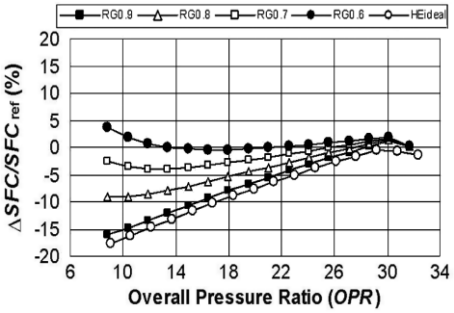

Figure 27: ΔSFC in function of OPR, for constant ST, with regeneration and cooling air bled after the RHE (Corchero *et al*. 2008).

However bleeding the cooling air before the RHE entry, shows a SFC benefit due to the decrease of cooling air mass flow. By putting the cooling the air at the exit of the RHE it registered a clear loss of cooling ability for high RHE efficiencies and low OPR when the higher benefits can be reached. Results also reveal an OPR reduction compared to the baseline which leads to a smaller HPC on low SFC designs. Benefits TET values and NO_x emissions are practically the same in both cooling configurations (before and after). For the best SFC setups the TETs and NO_x are similar to the baseline (Figure 28 and Figure 29).

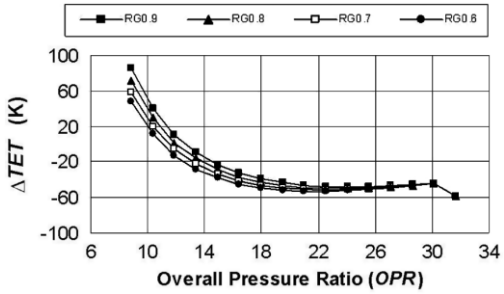

Figure 28: ΔTET in function of OPR for constant ST, with regeneration and cooling air bled before the RHE (Corchero *et al*. 2008).

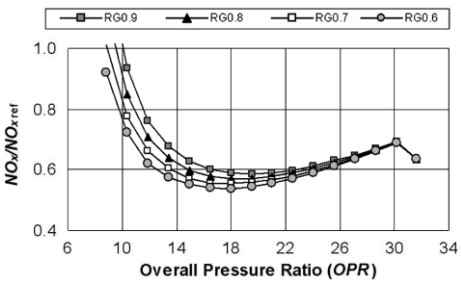

Figure 29: NO_x in function of OPR for constant ST, with regeneration and cooling air bled before the RHE (Corchero *et al*. 2008).

Although in higher OPRs where clear benefits are for SFC and emissions, there are also benefits for TET and an increase of engines life: a reduction of 20°will double turbine's life, decreasing manufacturing and maintenance costs. On constant TET studies the results were practically the same mentioned before with a SFC benefit for ST, but also an increase of TET when compared with results for constant ST designs (Figure 30 and Figure 31).

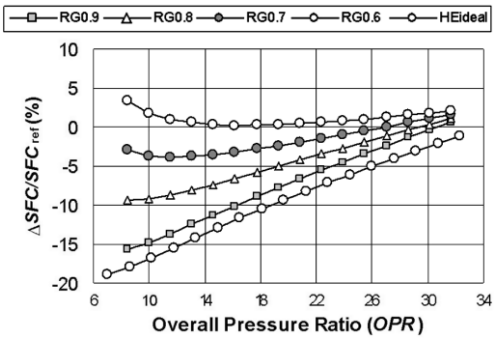

Figure 30: ΔSFC in function of OPR for constant TET, with cooling air bled after the RHE (Corchero *et al*. 2008).

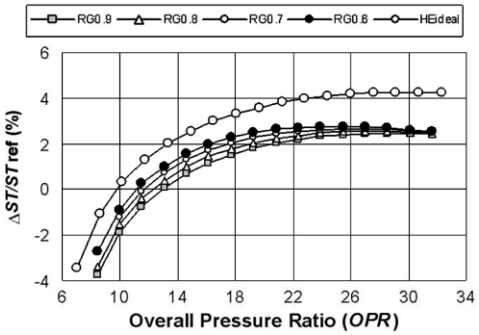

Figure 31: ΔST in function of OPR for constant TET, with cooling air bled after the RHE (Corchero et al. 2008)

On cruise conditions constant TET and ST (same at applied and studied. Both cases showed benefits on SFC, emissions and noise. It is known that at this flight point, the flow capacity of the heat exchangers will be lower; consequently lower pressure losses are also expected. At higher OPRs the SFC benefits on IRC cycle are zero because the RHE cannot work due to the temperature at the exit of the LPT. It is lower than the temperature exit of the HPC. Similar results of the SLS study were obtained and the authors stat that "the TET and the overall pressure ratio of the baseline engine really provide the possibilities of using some new components in the case of the IRC". The OPR of the baseline cruise condition is higher than at SLS, the opposite is with TET; this compromises the use of RHE like explained before. In the Figure 32, the SFC primarily decreases and then increases with OPR until a limit is reached. This limit represents the values that a RHE can be installed. After this limit, the SFC decreases as a consequence of the continuous increase of OPR, since it influences the standard Brayton cycle. Therefore, this leads to the necessity of evaluation where and when a RHE can be applied.

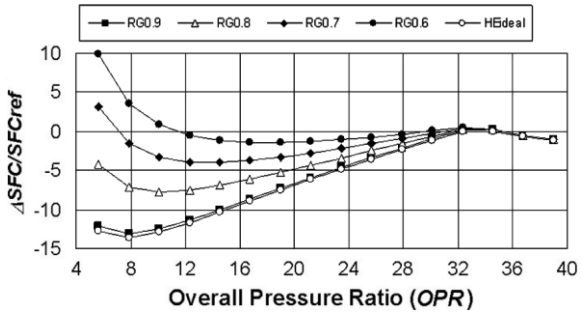

Figure 32: SFC in function of OPR for constant ST in cruise conditions, with regeneration and cooling air bled before the RHE (Corchero *et al*. 2008)

The benefits in this study for the SFC go from 3 to 15 per cent. The best values are from the IRC cycle and the worse are to the wave rotor. These values are worsened when the design pressure ratio increases. On the point of view of NO_x emissions, the IRC and CV have similar results, while the wave rotor drastically increases emissions; "this is an important handicap of the WRTC". Regarding lowering the TETs designs (Corchero *et al*. 2008) say that are no benefits of this approach for the IRC cycle and designs for a minimum SFC. It is more imperative a good regenerative efficiency, highly dependent on the level of the heat exchanger technology, and its size (drag and weight values). High values of these points can mitigate the benefits provided by this cycle. However even with a $\eta_R = 0.8$, which represents an appropriated value on current technology; major benefits can be obtained despite the increased weight and size.

Summarizing all the three cycles analysed the authors give some additional considerations:

- The IRC cycle is the most promising development with the current technology, however small heat exchangers with high efficiencies are needed to obtain the all shown benefits. The reliability and life of the heat exchanger is crucial, a failure could be critical in aircraft propulsion;

- The wave rotor needs in-depth aerodynamic developments to improve its efficiency and achievable pressure ratio;

- The CV, promises high benefits but there are also matters of great concern. The unsteadiness which leads to a performance loss as well as into unsteady working conditions for the turbine; the cooling process and the combustion system;

The authors conclude that a significant decrease of the SFC can be achieved (up to 15%), depending on cycle considered. At the current technology level the IRC is located above the CV due to the technology level on terrestrial applications in sea and terrestrial power generation and appears to be the most achievable. The benefits of SFC can also be translated into benefits for NO_x emissions except in the wave rotor due to the increase of cycle pressure and temperature. The constant ST can lead to a lower engine TETs which will benefit engine's life cycle especially in the CV model.

2.2 Relevant Studies

This section contemplates some works which the objectives, procedures and conclusions contribute as guidelines for the intended study. It will be also shown a brief market study that will help comprehend the trend of the aero engines for short haul flights in the next years.

Being this study a multi-objective optimization performed by genetic algorithms, the purpose of the following work is to give a general formulation of MO optimization. Pareto optimality

concepts and solution approaches with examples of MO problems in the power systems field are given. This investigation was performed by (Ngatchou *et al*. 2005) which enhance that "Optimization is an essential process in many business, management, and engineering applications. In these fields, multiple and often conflicting objectives need to be satisfied." To solve these problems, traditionally, converting all objectives into a single objective function (SO) is the procedure. The main objective is to find the solution that minimizes or maximizes this single function with all the necessary constraints. In the end the solution acquired represents a compromise between all the objectives.

The conversion into a SO function from a MO function is usually done by merging all the objectives in a weighted function, or simply transforming all but one of the objectives into constraints. However this has several limitations:

- It requires a foreknowledge about the relative importance of the objectives, as well as the limits on the objectives that are converted into constraints;
- The merged function leads to only one solution;
- Trade-offs between objectives cannot be easily evaluated;
- The solution may not be attainable unless the search space is convex;

This procedure leads to the conclusion that a simple optimization process is no longer viable for systems with multiple and often conflicting objectives. The best for engineers is to know all possible optimization solutions of all objectives simultaneously. Multi-Objective optimizations are often applied to power systems, in environmental/economic load dispatch, minimizing costs, fossil fuel emissions and minimizing system losses. This kind of problems are harder to solve because there is no unique solution like in the SO problems, instead, the MO problems provide a set of acceptable trade-off optimal solutions named Pareto front. The optimization is considered the analytical phase of the multi criteria decision making process which determines all the solutions of the problem that are optimal in the Pareto sense. The chosen solution will be the most desirable to the designer. The Pareto set allows the designer to make a decision by seeing a wide range of options since it contains the solutions that are optimum from an "overall" standpoint; unlike the SO process that ignores the trade-off viewpoint. This advantage can provide better understanding of the global system where a decision has its impact on the objectives that can be explored. The formulation of a MO may be:

$$\text{Minimize } \vec{y} = \vec{F}(\vec{x}) = [f_1(\vec{x}), f_2(\vec{x}), \dots, f_N(\vec{x})]^T,$$

$$\text{Subject to } g_j(\vec{x}) \leq 0, j = 1,2, \dots, M \qquad (1)$$

Where $\vec{x} = [x_1, x_2, \dots, x_P]^T \in \Omega$

$\vec{y}$ is the objective vector, g_j's are the constraints and $\vec{x}$ is a *P*-dimensional vector representing the decision variables within the parameter Ω. The space created by the objective vectors is called the objective space. Consequently, the subspace of the objective vectors that satisfies the constraints is called the feasible space. There are possible uncountable solutions, the so-called non-dominated solutions, which an objective cannot be improved without degrading at least another one; this situation demonstrates compromises or trade-offs between the objectives.

To evaluate solutions the concepts of Pareto dominance and Pareto optimality are frequently used. "A solution belongs to the Pareto set if there is no other solution that can improve at least one of the objectives without degradation of any other objective." So, Pareto dominance is used to compare rank decision vectors. For example, if $\vec{u}$ dominates $\vec{v}$, in Pareto sense means that $\vec{F}(\vec{u})$ is better than $\vec{F}(\vec{v})$ considering the objectives, and there is at least one objective function where $\vec{F}(\vec{u})$ is strictly better than $\vec{F}(\vec{v})$. A solution $\vec{a}$ will be Pareto optimal if it cannot be improved on one of the objectives without damaging at least one other objective. Thus, the objective vector will be $\vec{F}(\vec{a})$ and is called Pareto dominant vector, or non-inferior or non-dominated vector. All Pareto optimal solutions form the Pareto optimal set, and the corresponding objective vectors are on the Pareto front (Figure 33).

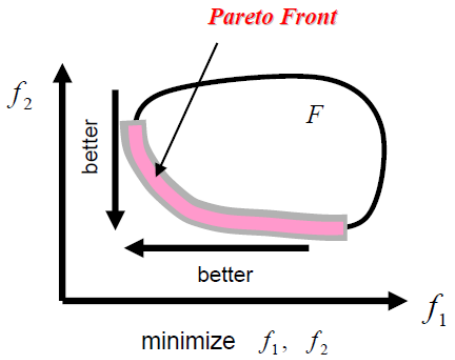

Figure 33: Example of a Pareto Front (Ngatchou *et al.* 2005).

To solve MO problems, there several ways of solution approaches. The classical approaches that were already mentioned, consisted in converting the MO into a SO for further scalar optimization application techniques. These approaches always require a good knowledge from the designer in ranking the objectives and the target values. Approaches of this kind are best fitted to find a unique solution, which satisfies all the criteria and preferences. Such techniques try to approximate the Pareto front by essentially repeating the solution process after changing the aggregation parameters (weights or target levels). If a local front is non-dominated the global front is not necessarily non-dominated. While it is relatively simple to

implement these techniques, in MO problems they are mostly inefficient and sensitive to the shape of the Pareto front. Following some technique examples:

- Weighted Aggregation;
- Goal Programming;
- ε – Constraint;

On the other hand, the second set of approaches is recent due to the advance in computational capabilities and the development of metaheuristic algorithms in the present days. This scenario enables the determination of the Pareto frontier by optimizing simultaneously all the objectives separately and in some cases the application of Pareto ranking processes. "These techniques are advantageous for real-life problems, particularly those appearing in the context of power systems since they present to the DM all possible, or at least a wide range of trade-offs between objectives." These population-based algorithms have the advantage of evaluating multiple potential solutions in a single iteration. They reveal extreme flexibility when previous information about targets to match is unknown, unlike the SO problem. The method of these techniques is to search through the Pareto-optimal set while the diversity in population is assured to prevent an early convergence.

All of this process is made by evolutionary computing that emulates the biological evolution process. The concept is based on a population of individuals which represent different solutions and will evolve to find the optimal solutions. The fittest individuals are chosen, mutation and crossover operations are applied to form the next generation. The methods include genetic algorithms (GAs), evolutionary algorithms (EAs) and evolutionary strategies (ES). They are very similar, except in the criteria of application of the fitness selection, mutation and crossover operations. However "confusion should be avoided between there hybrid evolutionary algorithm-based techniques, and the ones geared toward determining the Pareto efficient solutions". For the second set techniques the authors called them "Intelligent Techniques" and are composed of:

- Non-Pareto-Based Approach: Vector Evaluated Genetic Algorithm (VEGA);
- Pareto-Based Approaches;

The objective of the last mentioned technique consists in finding the set of non-dominated individuals in certain population. These individuals earn the highest rank in the analysis and are eliminated from the contention measures. The process will be repeated and similar treatment is applied to a new set of individuals until the entire population have an assigned fitness score. A mechanism named Sharing is applied to prevent the algorithm to converge to a single region of the Pareto front by regulating the density of solutions in the hyperspace

spanned by the objective vector or the decision vector. Mutation and crossover applications are then performed to acquire the next generation of individuals. However, the main drawback is the loss of performance as the number of objectives decrease due to computational efficiency. To minimize this issue, methods like sharing and manual setup adjusts in the optimization preferences are needed (example: number of Pareto samples). Following are some examples of Pareto-Based Approaches that are commonly used:

- The Multi Objective Genetic Algorithm (MOGA). In this algorithm, the fitness value of an individual is proportional to the number of other individuals it dominates. Evolutionary techniques can be applied in the objective space or in the decision space;

- The Non-dominated Sorting Genetic Algorithm (NSGA) uses a layered classification technique. The individuals which are non-dominated are classified with the same fitness value and the sharing technique is applied in the variable space. The process is repeated to the next individuals with lower fitness values;

- The Niched Pareto Genetic algorithm (NPGA);

- Strength Pareto Evolutionary Algorithm (SPEA);

With this work, the authors exposed different solution approaches for MO problems. They concluded that the classical methods cannot stand to the requirements of many real-life optimization problems, where the recent intelligent techniques assessed by computational power reveal up to the challenge. Some of the techniques and algorithms are indicated as the most efficient and applied in several areas, especially in thermal and energy fields.

The study performed by (Borguet *et al.* 2007), consisted in a multi-objective optimization performed in a turbofan, which the objectives were to minimize the specific fuel consumption at cruise conditions, as well as to maximize the specific thrust during the take-off phase. The variables were: the BPR, the FPR, and the HPC ratio. The optimization was executed by a genetic algorithm and a modular gas turbine simulation tool (Matlab Turbine Engine Simulator – MaTES), which performs a thermodynamic analysis.

The genetic algorithms (GAs) are the most recognized and practiced form of Evolutionary Algorithms. They make a stochastic optimization technique that mimics the Darwin's principles of natural selection and survival of the fittests. This kind of algorithms is indicated particularly for multi-objective optimization problems due to the minimization of the risk to converging to a local optimum. This capability is achieved because of the simultaneous processing of the whole candidate solutions, representing a huge benefit in real design problems.

Regarding the engine, the separated flows turbofan was selected, because "has revealed to be the optimum configuration for high subsonic commercial aircraft". The modelling is composed by equations of mass, momentum and energy balances and empirical information derived from rig tests or advanced CFD, regarding each component of the engine. The fluids applied are considered perfect gases with constant specific heats with the corresponding values before and after the combustor.

Before executing the program, it is possible to assign specific design parameters like: corrected inlet mass flow, BPR, FPR and HPC and combustor exit temperature. The conservations laws are applied; example: the power required by the fan dictates the enthalpy drop in the LPT, which is a direct and non-iterative calculation of the engine cycle and performances. However, the engine cycle and performances are dependent of the operating point (altitude, flight Mach number,ΔT_{ISA}) and the value of control variables like the fuel flow. For this part, the conservation laws result in a set of compatibility equations that have to be verified. Therefore there are three performance parameters that are considered:

- Net Thrust (FN), which is the available force to propel the aircraft. It consists in the sum of the gross thrust of the core and bypass nozzles minus the momentum drag;
- The Specific Thrust (SFN), being the amount of thrust per unit mass flow. It can be useful to compare engines of different sizes, as well as engines of the same type but with different sizes;
- The Specific Fuel Consumption (SFC) is the ratio of the fuel flow and the net thrust and it is inversely proportional to the global efficiency of the engine;

This code is evaluated by a test-case to assess its capabilities (Table 7). This evaluation is made by a commercial software dedicated to gas turbine modelling, GasTurb. The results carried out by MaTES are similar to the GasTurb leading to the conclusion that the developed code provides satisfactory results for preliminary studies. Its modular structure allows various type of engines to be simulated, as well as introducing new specific modules (turbine cooling or blow-off valves) without the need of rewriting the entire engine model.

Table 7: Validation Test Main Specifications
(Borguet *et al.* 2007)
DESIGN-POINT MAIN SPECIFICATIONS

$\mathrm{h} = 0$ m	$M_{fl} = 0.0$
$\Delta T_{ISA} = 0$ K	$\pi_d = 0.99$
$\mathrm{WR}_{fan} = 300$ kg/s	$BPR = 5.50$
$\pi_{fan} = 1.70$	$\eta_{p,fan} = 0.91$
$\pi_{hpc} = 8.00$	$\eta_{p,hpc} = 0.90$
$\pi_b = 0.97$	$\eta_b = 0.99$
$\mathrm{TIT} = 1400$ K	$\eta_{p,hpt} = 0.91$
$\eta_{p,hpt} = 0.91$	$\pi_n = 0.99$

Regarding the optimization loop, the GAs use artificial populations of individuals that represent possible solutions. Several GAs are used in real optimization problems, however the majority are based on the same iterative procedure. The individuals are characterized by genes, which result from the coding of the parameters of the optimization problem. Each individual is analysed regarding the objectives and the limitations of the optimization problem. In the individuals analysis, it is used the process of selection, which calculates the probability that each individual is part of the next generation. The new individuals (children) are generated by using the best features of the previous generation (parents) and sometimes, innovating ones. "The evolution of those individuals, through the genetic operators, tend to improve the quality of the population and to converge to a global optimum." In a Multi-Objective Optimization Problem (MOP) can be interpreted as $\min f(x)$, and it has not a unique solution, instead, a set of compromised solutions that can be classified, by the Pareto dominance concept, into dominated and non-dominated ones. The last ones represent the best compromise and are distributed on the Pareto front. In this kind of problems the GAs are able to provide as many Pareto-optimal solutions as possible in a single run; they are less susceptible to the shape or continuity of the Pareto front. It means they can approximate concave or non-continuous Pareto fronts that an aggregating approach could not solve. These capabilities are convenient to solve unconstrained MOPs and Pareto based approaches (MOGA, NSGA, NPGA, etc.). The GA used in this study, the MOHyGO (Multi-Objective Hybrid Genetic Optimizer), is based on the MOGA algorithm with the addition of extra features. The selection of individuals consists on a "penalized tournament" that randomly chooses and compares individuals (generally two):

- If they are all feasible, the best ranked element according to MOGA wins;
- If they are all infeasible, the one having the lower penalty factor value wins;
- If one is feasible and the others are infeasible, the feasible individual wins;

The test case applied to the engine simulation tool and the GA has three design variables: FPR, HPC and BPR (Table 8).

Table 8: Design Variables for the Optimization (Borguet *et al.* 2007).

DESIGN VARIABLES

Variable	min	max
π_{fan}	1.5	1.8
π_{hpc}	3	12
BPR	2	8

The optimization considered two objectives: specific fuel consumption (SFC) at cruise conditions, and the second one the specific thrust (ST) at take-off rating. The cruise regime is defined as the design point which makes the take-off rating be treated as an off-design point

(Table 9). For the calculation, the GA calls the engine model and the SFC at cruise is primarily obtained. Then the SFN in take-off conditions is calculated for the off-design calculation.

Table 9: Design Point Parameters (cruise) (Borguet *et al.* 2007).

DESIGN-POINT PARAMETERS

$h = 10668$ m	$M_{fl} = 0.85$
$\Delta T_{ISA} = 0$ K	$\pi_d = 1.00$
$\eta_{p,fan} = 0.90$	$\eta_{p,hpc} = 0.89$
$\pi_b = 0.99$	$\eta_b = 0.99$
TIT $= 1300$ K	$\eta_{p,hpt} = 0.91$
$\eta_{p,hpt} = 0.91$	$\pi_n = 0.99$

The results show that the GA has been run with a population of 200 individuals during 50 generations, which is equal to 10 000 calls of the engine simulation tool. The optimization process resulted in 76 Pareto-optimal solutions (Figure 34). Due to the variety of results, the final choice of parameters will be determined by a smart compromise between the different objectives, based on engineering criteria like in all multi-objective evolutionary optimizations. The engine size being upper-bounded for practical reasons, coupled with the required take-off thrust, translates to a lower bound on the SFN. The FPR and the HPC are near their maximum values: respectively 1.8 as 12 as shown in Table 10. "With the current technology the SFN is nearly constant with respect to the overall pressure ratio (OPR) while the SFC is and inverse function of the OPR. Increasing FPR leads to an increase in the SFN and a decrease in the SFC." As a consequence, the best solutions have different BPR. Middle BPR values provide high SFN and SFC because it enhances the contribution of the core stream and its high exhaust speed, while greater BPR lowers the SFN and the SFC due to the slower bypass stream.

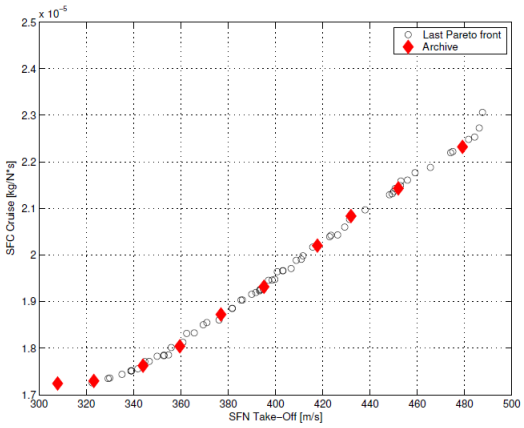

Figure 34: Optimization Results (maximization of the SFN and the minimization of the SFC) (Borguet *et al.* 2007).

Table 10: Optimal Solutions from the Pareto Front (Borguet *et al.* 2007).

$SFN(\times 10^{-2})$	$SFC(\times 10^{5})$	BPR	π_{fan}	π_{hpc}
3.231	1.729	6.620	1.732	11.799
4.319	2.083	2.933	1.775	11.857
3.769	1.872	4.414	1.784	11.572
4.177	2.020	3.267	1.791	11.743
3.595	1.804	5.011	1.793	11.838
3.951	1.931	3.855	1.793	11.751
3.439	1.762	5.623	1.780	11.959
4.520	2.143	2.564	1.795	11.846
3.078	1.724	7.514	1.603	11.582
4.792	2.232	2.131	1.795	11.996

As conclusions the authors highlight the contributions of the GAs providing the best solutions to this particular problem. (Borguet *et al.* 2007) suggest that additional effects such as noise, or pollutant emissions should be introduced in the model to define new variables to be evaluated. For a more realistic optimization, aerodynamic, mechanic and thermal simulations on engine components are needed in future studies.

Following is some data from a report, (Analytics 2013), that translates the trend of aero engines market in the year of 2012 and predicts the behaviour of the market for the next years. This report considers short and long haul flight engine categories, however considering the context of this thesis, it will only be emphasized the short haul category. This study helps to understand how the aero engine market and decisions by the manufacturers will influence the future years.

The delivered powerplants to the majority of the airliners are from the CFM International and Pratt & Whitney. It is up to these manufacturers to supply next generation of narrowbodies in order to enable a step-change in operating economics.

With the new A320neo and 737 Max arrivals in a few months choosing the right engine never have been more important or harder. “The choice between the CFM Leap-1A and P&W PurePower1100G is no longer a soft bet on a secondary supplier to an already chosen airframe.”

With a more attention to the Airbus 320neo, the airframe has some minor changes except the engine that will power it. The commitment and strategies of the engine makers to achieve the 15% rise in fuel efficiency imposed by Airbus, translates this is not a simple race to see who provides the engine but can be the choosing side from the airliners for the technology that dictates the future of gas turbine technologies. From one side, the debate of the reliance on new and exotic materials by the Leap-1A and on the other side the introduction of a reduction gear inside the PW1100G.

From a global point view, CFM International and its US shareholder General Electric are the lead producers in their markets. Together, 70% of the 2416 engines delivered in 2012 came from these manufacturers (Figure 35). While in the widebody sector began a more levelled up

activity as the Boeing 787 deliveries got fully under way, the single-aisle and regional jets markets also began to shift as P&W progressively grows the geared turbofan's market share.

ENGINE MANUFACTURER RANKING

Rank	Manufacturer	2012 deliveries Engines	2012 deliveries Share	Backlog* Engines	Backlog* Share
1	CFM International	1,278	53%	8,742	47%
2	International Aero Engines	422	17%	1,568	8%
3	General Electric	388	16%	1,812	10%
4	Rolls-Royce	238	10%	2,214	12%
5	Engine Alliance	56	2%	356	2%
6	Pratt & Whitney	34	1%	1,228	7%
	Undecided	-	-	2,560	14%
TOTAL		2,416		18,480	

NOTES: *At 31 December 2012. Data for installed engines based on Airbus/Boeing types. Excludes corporate and military operators. SOURCE: Flightglobal Insight analysis using Ascend Online Fleets

Figure 35: Engine Manufacturer Ranking (Analytics 2013).

CFM is a leader in engines installed on commercial Airbus and Boeing in 2012. It also secured 47% of the order backlog with 8742 engines, while Rolls-Royce was second with 12% share (2214 engines). Rolls Royce holds a strong position in the A330 order backlog and is the only engine manufacturer for the A350XWB with the Trent XWB. The active commercial fleet from Airbus and Boeing at 31 December 2012 was a total of 17034 aircraft, where 6931 is from Airbus and 10103 from Boeing. The lead engine manufacturer from these aircrafts was CFM International with 51% market share: 8752 aircraft (3153 with Airbus and 5599 with Boeing) (Figure 36).

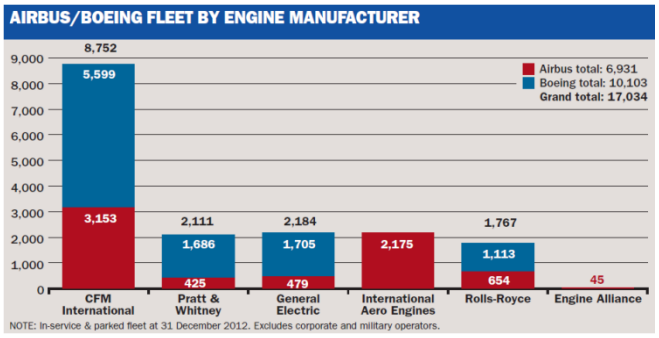

Figure 36: Airbus/Boeing fleet by engine manufacturer (Analytics 2013).

In the short haul flights, the CFM56 is the primary engine for the Boeing 737NG, but also an option for the A320 family. In the near future, CFM will equip the 737Max with the Leap engine, although it can be an option for the A320neo. However the second option for the new A320 is the Pratt & Whitney PW1000G geared turbofan. The share for the A320 in 2012 shows a dominant CFM with 53% against 47% from IAE. With the introduction of the geared turbofan from P&W, a true race with different participants with different technologies is ongoing. The order backlog at the end of 2012 showed a 37% share for CFM, 21% for IAE and 16% for Pratt & Whitney. However the 26% undecided can change everything for the next years (Figure 37).

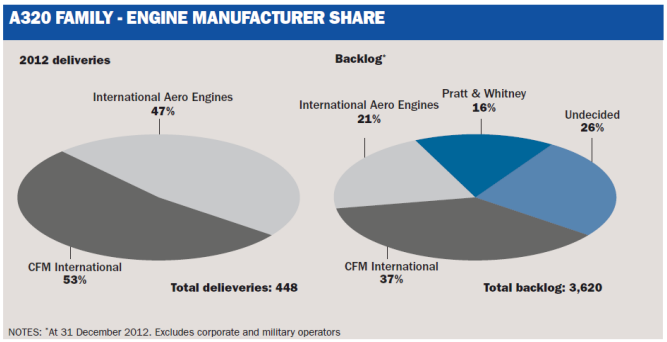

Figure 37: A320 market share in 2012 (Analytics 2013).

In the regional section, General Electric scored a 54% market share for deliveries followed by Pratt & Whitney and Powerjet (43% and 4% respectively). The backlog reveals a loss of terrain from General Electric to its adversaries. With a total of 1172 engines, the P&W detains 50% of the market followed by GE with 36% and Powerjet 14% (Figure 38).

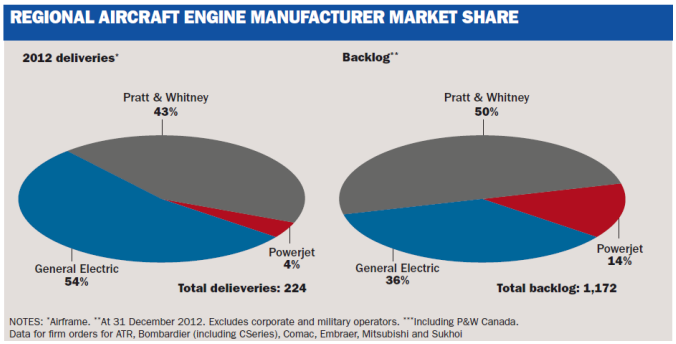

Figure 38: Regional Engine Market Share (Analytics 2013).

The main leader of the regional aircraft market for many years has been Embraer, delivering more than 940 E-Jets in the last decade and holding a backlog for some 220 more. However its dominance is in risk by the Canadian and Japanese manufacturers. These manufacturers embraced the GTF technology from Pratt & Whitney and the new Bombardier CSeries and the Mitsubishi MRJ regional jets showed significant efficiency gains making Embraer losing orders.

Facing this scenario, Embraer decided re-engining path. It will replace the E-Jet's General Electric CF34s with the same GTF technology that its rivals have apart new improvements. These changes are made by Embraer in order to regain market leadership from the other competitors.

Naturally, the Japanese manufacturer states that the advantage of the MRJ is not only from the GTF technology but it sets apart from other competitors using last engineering technology and aerodynamic designs.

Apart from other models the Bombardier 130-160 seat CS300 is able to compete with smaller variants of the Airbus and Boeing's A320 and 737 families. In that way, Bombardier has a product that straddles the regional and mainline aircraft markets.

In this report, it is also possible to observe all commercial aircrafts and engines in active. This includes narrow/wide bodied aircraft, regional and Russian jets in passenger, freighter and quick change roles (Figure 39 and Figure 40).

WORLD COMMERCIAL AIRCRAFT		
MANUFACTURER	AIRCRAFT	ENGINES
CFM International	8,369	17,108
General Electric	4,405	9,610
Rolls-Royce	2,598	5,741
Pratt & Whitney	2,250	5,160
International Aero Engines	2,234	4,468
Other	750	2,520
TOTAL	20,606	44,607

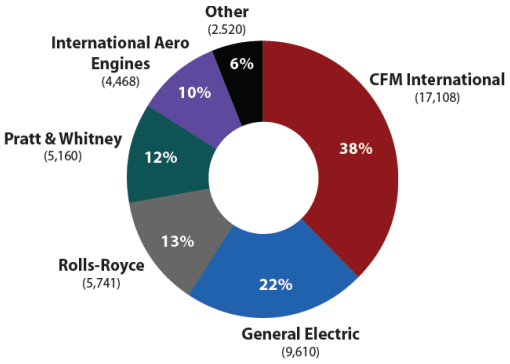

Figure 39: World Commercial Aircraft Engine Share (Analytics 2013).

COMMERCIAL NARROWBODY AIRCRAFT		
MANUFACTURER	AIRCRAFT	ENGINES
CFM International	8,185	16,372
International Aero Engines	2,234	4,468
Pratt & Whitney	1,257	2,665
Rolls-Royce	644	1,288
TOTAL	12,320	24,793

COMMERCIAL WIDEBODY AIRCRAFT		
MANUFACTURER	AIRCRAFT	ENGINES
General Electric	2,188	5,176
Rolls-Royce	1,018	2,581
Pratt & Whitney	993	2,495
CFM International	184	736
Engine Alliance	47	188
TOTAL	4,430	11,176

COMMERCIAL REGIONAL JETS		
MANUFACTURER	AIRCRAFT	ENGINES
General Electric	2,217	4,434
Rolls-Royce	935	1,870
Lycoming	97	388
Honeywell	83	332
Pratt & Whitney Canada	18	36
Powerjet	13	26
TOTAL	3,363	7,086

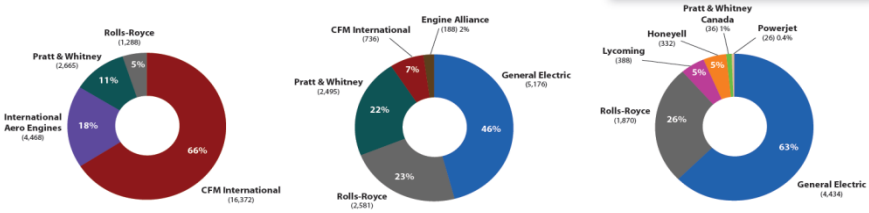

Figure 40: Engine market share by market group (Analytics 2013).

From report can be concluded that exists the possibility in the future for a shifting in the aero engine market leaders. All will be due to the new powerplants and consequently the airliners options to equip their fleet, specially the A320neo: “How to power the A320neo is far from a straightforward decision for airlines, but their choices will help define the future of gas turbine engine technology”.

3. Conceptual Requirements

3.1 The Turbofan Engines

First termed by Rolls-Royce as bypass turbojet, these types of engines are the most reliable engines ever developed. The turbofan engines were developed as a compromise between the turboprop and turbojet engines Characterized by being fuel efficient and quiet turbine engines, they feature continuous combustion and smooth rotation. Similar to the turbojet engines, the gas generator has three sections:

- Fan and compressor section;
- Combustion chamber;
- Turbine section;

The fan provides a large amount of the air mass to the interior of the engine, creating two streams of air flow through the engine. The primary stream is pressurized by the compressors and travels through all the components. The second stream, the majority of the inlet air, goes around the engine core through a nozzle-shaped chamber, identified as cold nozzle, leaving the rest (the primary stream) through the engine core where it mixes with fuel and ignites. The result of the combustion expands in a hot temperature through the turbine section, spinning the turbine as it exits the engine. At the exit of the engine, the streams may mix and both are expelled from a single nozzle. This spinning from the turbine generates motion to the engine shaft. Consequently, the rotation from the shaft spins the fan of the front of the engine making possible the compression of more air, keeping the continuity of the cycle.

Until 1946 several types of ducted-fan engines were built but none attracted much attention. However, Rolls Royce in 1956 introduced them to the market with a BPR of three and more. General Electric followed the same steps in 1965 with the TF39 (BPR of 8) and still leads with the GE90 with a BPR close to 9.

This configuration of engines reveals big advantages compared to the turboprop and the turbojet engines. For example: the fan is not large as a propeller, reducing the increase of speeds along the blade, making possible higher speeds before the generation of vibrations. The fan can take in air at a greater rate than a propeller allowing the engine to produce greater thrust. The aerodynamics is privileged due the insertion of the fan in a duct raising efficiency. Consequently, at higher speeds the flow is less separated and fewer shocking development. It is possible for a turbofan to suck more air than a turbojet, more fuel efficient and equal some high performance velocities. It can power a civil transport at

transonic speeds up to Mach 0.9. For geared turbofan engines, the gearbox which connects the compressor/fan and turbine is small as the fan is smaller, reducing the weight and drag present in a turboprop design (El-Sayed 2008).

Following (Figure 41), are several types of turbofan engines:

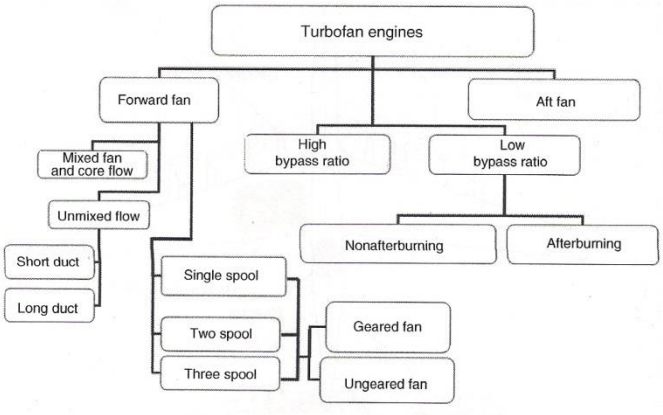

Figure 41: Turbofan engine types (El-Sayed 2008)

Turbofans can be classified according the positon of the fan (forward or aft) as well as the bypass ratio (low or high). The high BPR turbofans are usual in large commercial airliners. The current levels of bypass are 5 or higher. Due to the mentioned characteristics, this type of turbofans is optimal for commercial aircrafts. On the other hand the low BPR are applied in military operations. Regarding the forward fan, two configurations are possible: mixed or unmixed. The two streams that were previously described can be ejected separately (unmixed type-Figure 42) or the cold stream leaving the fan mixes with the hot stream leaving the last turbine before leaving the engine from one nozzle (Figure 43). Still, the unmixed turbofan can have short or long ducts.

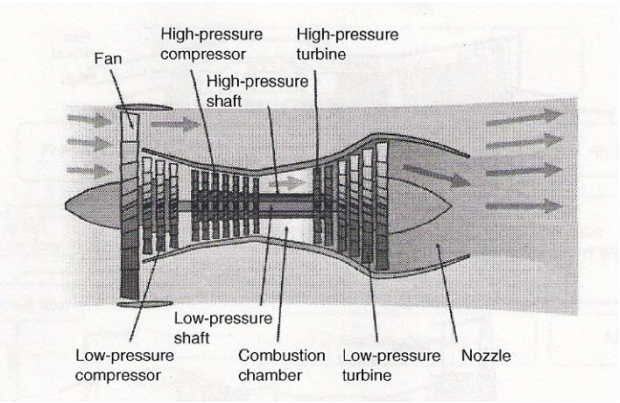

Figure 42: Unmixed Turbofan (El-Sayed 2008).

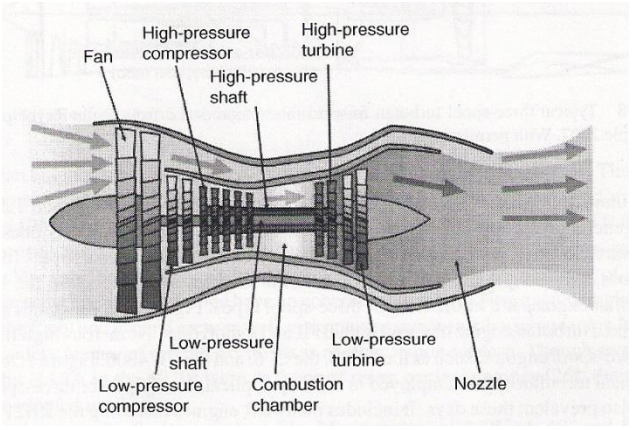

Figure 43: Mixed Turbofan (El-Sayed 2008).

The forward fan can be also classified according to the number of spools. In the present days, the single-spool turbofan is very uncommon, leaving the majority of the turbofans for two or three spools. The geared configuration or direct drive, are two types of configurations that will play a major role in the number of spools.

The low BPR turbofans may also be classified as afterburning or nonafterburning engines. The former resemble all recent military airplanes. Being mostly mixed type and due to the high fuel consumption, the afterburning is not used during extended periods of time. This option is enabled when it is necessary to have much thrust as possible (takeoffs in short runways and in combat scenarios (El-Sayed 2008).

3.2 The BPR

The bypass ratio or BPR is defined as the mass flow of air moving outside the core divided by the mass flow through the core:

$$bpr = \frac{\dot{m}_b}{\dot{m}_c} \tag{2}$$

The BPR is the main influencer on the efficiency, because for a given core the bypass ratio determines the jet velocity. Also, it dictates the appearance, size and weight of the engine. In the past, bypass ratios that exceed 10 were a scenario not very much attractive. However, in the present days it is becoming a strong reality as the technology progresses. For this, it is necessary to install a gearbox between the LP turbine and the fan, to allow the turbine to run faster.

Low fuel consumption is one of the major concerns in commercial aircrafts. Such a requirement needs a high overall efficiency. The overall efficiency is the product of propulsive and thermal efficiency, which are the values that help to choose the better bypass ratio:

$$\eta_0 = \eta_p \eta_{th} \tag{3}$$

For a high thermal efficiency η_{th} it is recommended a high inlet turbine inlet temperature and a high pressure ratio. This would lead to a high jet velocity if all the available power were used to accelerate the core flow as it is the turbojet engine. However, it is known that very high jet velocities give low propulsive efficiency η_p. For a very good propulsive efficiency, the engine will have to generate its thrust by accelerating a large mass flow of air by only a small amount of jet velocity, like the turbofan engine (Figure 44). It was to improve the propulsive effiency of the turbojet, that the bypass turbofan was developed. With the BPR only part of the air taken is fully compressed and passed through the combustion chambers and turbines. The rest of the air is slightly compressed and moves round the combustion chambers and then is exhausted at a relatively low speed, producing thrust at a fairly high propulsive efficiency. On the contrary, the air that was exposed to the combustion is ejected at a high speed, producing thrust at a comparatively low efficiency. The total propulsive efficiency is thus slightly greater than a simple turbojet engine with the same thrust, due to the major contribution of the bypassed air at a low speed (Houghton & Carpenter 2003). Following is the propulsive efficiency equation, as known as the Froude's equation, where V is the flight speed and V_j the total jet velocity speed.

$$\eta_p = \frac{2V}{V + V_j} \tag{4}$$

The limitations and advantages of the propulsive and thermal efficiencies opened the way for the high bypass engine for subsonic propulsion exploration.

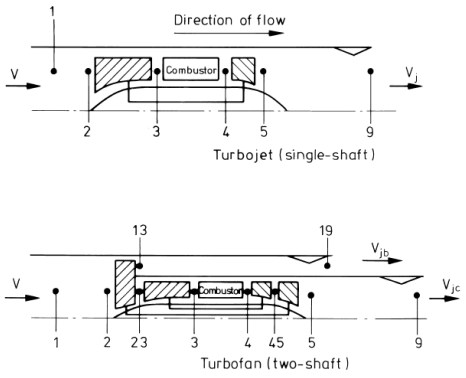

Figure 44: Representative schematics of a Turbojet and a Turbofan (Cumpsty 2003).

For a given overall pressure ratio and turbine inlet temperature it is possible to determine the available power per unit mass flow rate through the core. From that it is necessary to decide how much of the pressure shall be expanded in the LP turbine and in the nozzle of the core stream. In other words, it is the quantity of power which will be extracted in the LP turbine for the bypass stream and how much kinetic energy will be supplied to the core jet stream.

As mentioned before, the velocity of the core jet V_{jc} is larger than the velocity of the bypass jet V_{jb}, due the LPT and the fan being to some extent irreversible, contrary to the core nozzle

which is virtually loss free. Larger thrust is obtained if $\frac{V_{jb}}{V_{jc}}$ is approximately equal to the product $\eta_t \eta_f$ of the LPT and fan isentropic efficiencies. Therefore, the indicated way to optimize the BPR on SFC and thrust is to select values of BPR and then calculate the jet velocities values from which thrust and SFC are acceptable. The following example exhibits that if we increase the BPR it will increase the thrust which is the gross thrust F_G and the net thrust F_N. Considering an increase of BPR from 6 to 10, the gross thrust increases by 39% and the net thrust 6%(Cumpsty 2003).

In cruise conditions the net thrust is the most relevant, while in the take-off, where the drag is small, the net thrust is nearly equal to the gross thrust. If we fixate the core, a greater BPR gives a much larger take-off thrust. The same situation is verified at cruise flying point, where a higher BPR give a much greater thrust at take-off or on the test bed.

The following graphics (Figure 45) are obtained from cruising at Mach 0.85 at 31000 ft, OPR for core = 40, TET = 1450K, FPR 1.6 where the core and bypass jet velocities are equal (Cumpsty 2003).

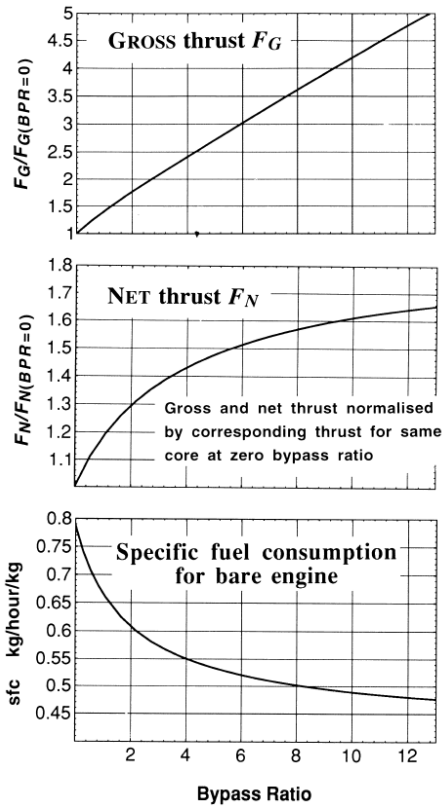

Figure 45: Estimated variation in thrust and SFC with BPR for a constant core (Cumpsty 2003).

These graphics reveal that if the BPR increases it can be possible lowering the SFC due to an improvement in propulsive efficiency. However, the amount of improvement is reduced as

the BPR increases and V_j decreases, since propulsive efficiency must tend to a limit of 1.0 as the jet velocity tends to the flight speed (eq.4).

Although the increase of BPR shows benefits, it also has drawbacks that must be overtaken in the future. For a bigger BPR, for a given size of core, the engine becomes larger and heavier. A larger nacelle raises the drag, which affects negatively the net thrust and increases the SFC. Further developments have to consider aerodynamic designs in order to reduce the drag, keeping in mind that the overall percentage will rise in inexorably as the bypass ratio goes up. With new materials and concepts a smaller and more powerful core can be developed, therefore the bypass ratio can be higher for the same size of fan and the same nacelle drag.

It is also important to keep in mind that the SFC is different for a 'bare' engine and an installed one as shown in the Figure 46. One of the main problems of a higher bypass is the increased weight of the engine and the nacelle. Like mentioned before, those increases are a penalty to be considered in cruise drag and reduced payload as well as reduced flight range. As the weight of the engine increases the wings are able to lift less payload, so the revenue of the airline declines. Therefore, in very high values of BPR, with a very large engine, the aircraft itself begins to be affected; the wings have to be higher off the ground and their aerodynamic performance is impaired by the engines.

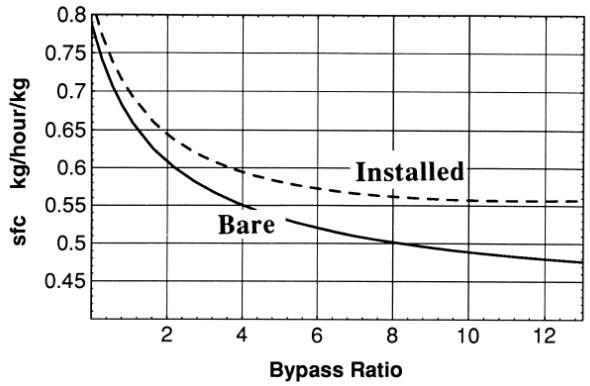

Figure 46: Estimated variation of SFC in function of the BPR for bare and installed engine (same conditions as Figure 45) (Cumpsty 2003).

Regarding the noise emissions, a higher BPR results in a smaller fan pressure ratio, consequently a larger fan with reduced tip speed is permitted and gives a lower jet velocity. This situation generates lower noise from the engine. Although of being heavier, this point is where the GE90 engine has been most successful, with a BPR of 9 against the engines from Pratt & Whitney and Rolls Royce (BPRs of 6). "To minimise the noise the makers sought to minimise the jet velocity and the fan speed, requiring the largest possible bypass ratio and fan diameter". With the development of the technology, the power output from a given size of core (same mass flow though the core) will increase. "In other words the optimum bypass ratio for lowest fuel consumption is likely to increase with time." (Cumpsty 2003)

However, in terms of propulsive efficiency or noise is not totally wrong to say that the BPR is not the better descriptor for an engine. Despite the advance in technology (higher FPR and TET), which will permit a more efficient core for the same amount mass flow through it, this can lead to a situation where the BPR can be held constant while the jet velocity of the bypass stream would rise. On the contrary, if the jet velocities are to be kept constant or reduced for reasons mentioned before, the bypass ratio would be increased.

Therefore, the specific thrust is another parameter that can help to define the engine's performance in what matters for propulsive efficiency and noise. It is defined by the net thrust per unit mass flow through the engine, and it is equal to the difference between the average jet velocity and the flight velocity, expressed in m/s.

$$ST = \frac{F_N}{\dot{m}_{air}} \tag{5}$$

Therefore, the engine can be defined by its size, pressure ratio, BPR and specific thrust. (Cumpsty 2003)

3.3 The Brayton Cycle

The Brayton cycle was developed by George Brayton in an oil-burning engine that he developed nearly 1870. In the present days, this cycle is applied in gas turbines when the compression and expansion processes exist in rotating machinery. By introducing the air from the surrounding ambient of the engine, the compressor actuates raising the temperature and pressure of the inlet mass of air. The pressurized air is conducted to the combustion chamber, where with the addition of fuel, the mass of air is burned at constant pressure. The combustion results in high temperature gases that enter in the turbine, being expanded to the atmospheric pressure generating power. Since the exhaust gases are expelled to the exterior without being recirculated, this cycle can be classified as open cycle (Figure 47).

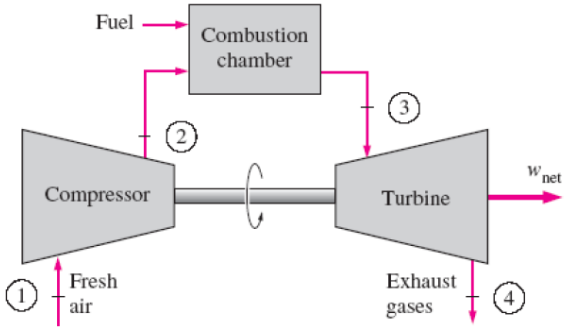

Figure 47: Open Cycle gas turbine engine (A. Çengel & A. Boles 2006).

This cycle consists in four internally reversible processes:

- 1-2 Isentropic Compression (performed on a compressor);
- 2-3 Constant Pressure heat addition
- 3-4 Isentropic Expansion (performed on a turbine)
- 4-1 Constant Pressure heat rejection

Following are the T-s and P-v diagrams of this ideal cycle (Figure 48):

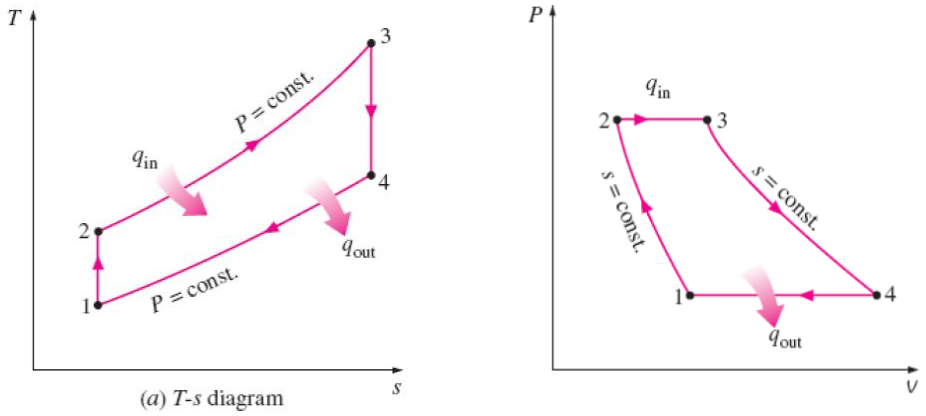

Figure 48: T-s and P-v diagrams of the ideal Brayton Cycle (A. Çengel & A. Boles 2006).

In the end of the state 3 it is registered the highest temperature, constrained to a value accordingly to the maximum material temperature that the turbine blades can embrace. This constraint dictates the maximum pressure ratios that can be used in the all cycle. Therefore it is imperative that the tradeoffs between the pressure ratios and the network output be considered. With a less work output per cycle, a larger mass flow rate is needed to maintain the same power output (A. Çengel & A. Boles 2006).

The intake air in the gas turbines supplies the necessary oxidant for the combustion of the fuel and it is used for cooling to keep the temperature of the components within safe limits. This is possible due to the fact that the drawn air is more than what is needed for the complete combustion of the fuel. Also, the mass flow rate through the turbine is greater than that through the compressor; the difference is justified by the mass flow rate of fuel injected. Therefore it can be said that cycle has conservative results for open-loop gas turbine engines assuming constant mass flow. This principle is not only applied to the aircraft propulsion but in electric power generation as stand-alone units or in conjunction with steam power plants on the high temperature side (A. Çengel & A. Boles 2006).

The development of the gas turbines has largely growth since 1930s. The first gas turbine built had an efficiency of only about 17% due to the low efficiency of the compressor and

turbine, low turbine inlet temperatures do to material limitations. The efforts to improve the cycle efficiency concentrated in three areas:

- Increasing the turbine inlet temperatures: taken as the primary approach to improve the efficiency of a gas turbine, the inlet temperatures have increased steadily from about 540ºC in 1940s to 1425ºC of even higher in the present days. New materials and cooling techniques of the components allowed this advance. A high turbine inlet temperature with an air cooling technique requires combustion temperature to be higher to compensate the cooling effect. The use of steam enabled an increase of the TET, without increasing the combustion temperature and it is a much more effective heat transfer medium than air.

- Increasing efficiencies of turbomachinery components: More effective techniques for computer-aided design turn possible the creation of these components aerodynamically with minimal losses.

- Modifications to the basic cycle: By applying intercooling, regeneration and reheating to the simple cycle, the efficiencies of early gas turbines were practically doubled. However these improvements, cannot be justified unless the decrease in fuel costs offsets the increase in operation costs.

3.4 Regeneration Cycle

As mentioned earlier, in the State of the Art chapter, the temperature of the exhaust gas leaving the turbine is often considerably higher than the temperature of the air leaving the compressor. This situation creates the possibility of the high pressurized air leaving the compressor be heated by transferring heat to it from the exhaust gases, which are at a superior temperature. A counter-flow heat exchanger can be applied to this end usually called regenerator or recuperator (Figure 49).

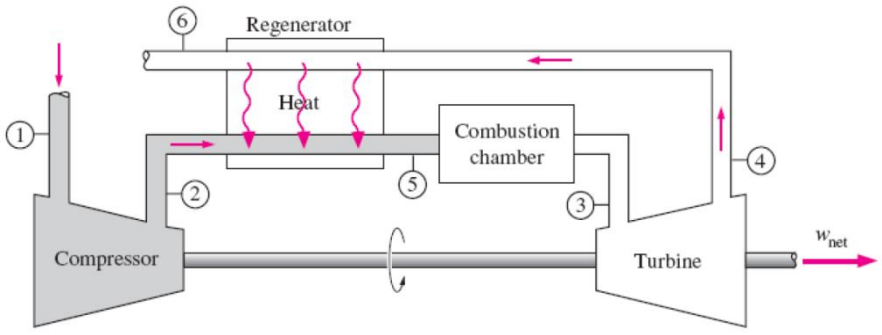

Figure 49: Gas Turbine with regenerator (A. Çengel & A. Boles 2006).

As a result of the regeneration, the thermal efficiency of the Brayton cycle is increased due to the part of energy of the exhaust gases used to preheat the air entering the combustion

and that is normally rejected to the atmosphere. This portion of introduced heat decreases the heat input requirements (fewer fuel applied) for the same network output. However, it is crucial to keep in mind that when the turbine exhaust temperature is lower than the compressor exit temperature the use of a regenerator is not viable. Still, if a regenerator was incorporated in the described cycle, the heat will flow in the reverse direction, decreasing efficiency and raising the fuel consumption.

Regarding the regenerator, the highest temperature is in *T*4, when the exhaust gases leave the turbine and enter in it. At the exit of the regenerator *T*5 the temperature is inferior compared to *T*4. In an ideal situation the air would leave the regenerator at the same temperature of *T*4. Following is the *T*-*s* diagram of the regenerated cycle (Figure 50).

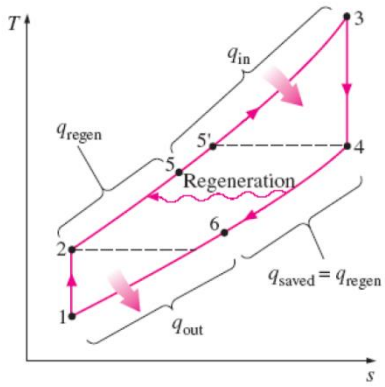

Figure 50: *T*-*s* diagram of a Brayton regenerated cycle (A. Çengel & A. Boles 2006).

3.5 The New Engines: PW1000G and CFM Leap

In this section it will be briefly presented the new turbofan engines that will be applied into the reworked airframes of the A320 and Boeing 737, and also in some smaller aircrafts of the regional market. The choice of the airlines between these two engines will dictate the trends of the turbofan technology and the market engine in the next years, (Analytics 2013).

Due to the fact that these engines are not yet officially in service and are still subject to technical modifications, the following information is not totally assured by the sources and in some cases it is possible that some data will be speculative. Nevertheless, for reasons previously explained and pointed by several authors, the trend for the BPR as technology develops, is to rise, which is one of the objects in study in this thesis and verified in these two new engines.

3.5.1 Pratt & Whitney PW1000G

The PW1000G (Figure 51) is the designation for the P&W's new high-bypass geared turbofan, previously known as the Advanced Technology Fan Integrator (ATFI). One of the main objectives of this model is to improve considerably the propulsive efficiency comparatively to

other engines from the same segment and characteristics Thrust values are expected to be similar to the GE-36 and the CFM56-7B24.

Figure 51: PW1000G (Banda 2014).

The new GTF components use ceramic matrix composites, which can provide higher engine operating temperatures also raising the thermal efficiency. The lower density of the composite materials results in a 50% reduction in the engine weight and a 15% decrease in fuel burn. From P&W, statements claim that the PW1000G shows a 12% improvement in fuel burn reduction over the 0.37 *lb/lbf-h* from the CFM56-7B turbofan. Besides the fuel burn decrease, the CO_2 emissions are expected to reduce 15% and NO_x emissions 50%. Noise is also taken into account and a reduction of around 20% compared to other engines is also claimed. These numbers can be very attractive to the airlines due to the emission taxes and airport landing fees (Aiken *et al.* 2009).

The advanced gear system (Figure 52), allows the engine's fan to operate at a different speed from the low-pressure compressor turbine, giving the possibility to extract higher efficiencies from each one of the components of the engine. This geared system applied to the shaft, decouples the rotation speed of the high-pressure turbine and the inlet fan, allowing the latter to spin at one-third the speed of the former achieving optimal speed for each component. The load of the LPT is also reduced (S. Arvai 2011).

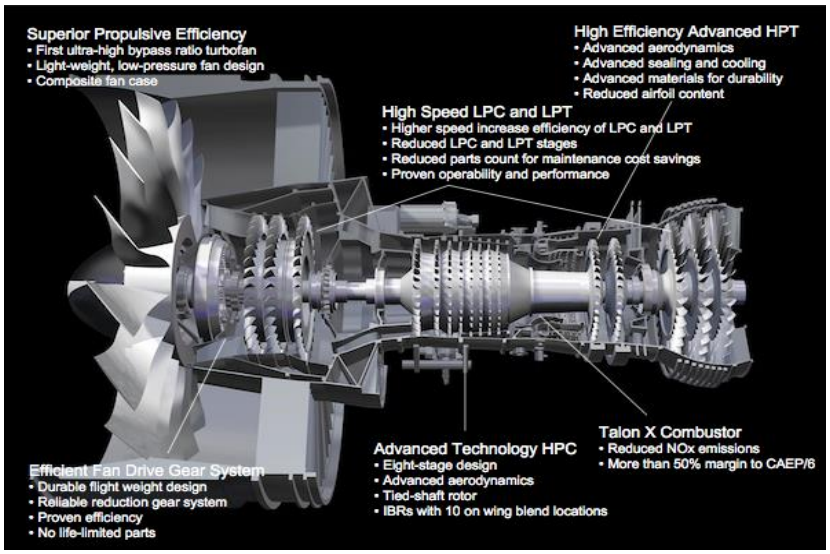

Figure 52: PW1000G technical configurations (S. Arvai 2011).

All of these configuration characteristics generate a bypass ratio for the PW1100G of 12:1, twice the 6:1 ratio of the V2500. The inlet fan is 10 cm wider than the LEAP-1A but it only uses three stages in the LPT. On the contrary the CFM opponent requires seven stages in the low pressure turbine. This can translate in an advantage regarding the final weight of the engine like mentioned in the State of the Art chapter. MTU is responsible for supplying the three-stage low-pressure turbine and half of the engine's eight-stage high-pressure compressor (S. Arvai 2011).

For the PurePower PW1100G aimed for the A320neo family, already in test phase, P&W decided to remove a variable area fan nozzle, which was initially in the design project. This was justified with the objective "to make the engine lighter and less complex" (Analytics 2013).

The engine was tested on the P&W owned 747SP, and the second phase of flight testing was conducted on an A340-600. The engine flew for the first time from Toulouse in October 2008 (Analytics 2013).

From the market point of view, although the geared turbofan concept not being new, it has never been introduced into service, leaving the airlines to rely on test results for key assumptions, including lifecycle maintenance cost. This engine will option for the A320neo after P&W failed to reach an agreement with Rolls-Royce to offer the engine jointly through the IAE venture, which also includes JAEC and MTU Aero Engines (Analytics 2013).

In March 2011, the Indian low-cost carrier IndiGo selected the PW1000G to power up to 150 updated A320s. The operator signed an agreement with Airbus to be the launch customer for the new variant of turbofan engine, which is due for entry into service in October 2015 (Analytics 2013).

The regional jets and small narrowbodies market will be affected as well by the Pure Power engine, since it has already dominated the sales for the new generation of airframes. Selected for the Mitsubishi MRJ regional jet (PW1200G), Bombardier CSeries airline (PW1500G) and is offered as an option on the United Aircraft (UAC) Irkut MS-21 (PW1400G) (Analytics 2013).

The first flight test of the PW1217G for the MRJ on P&W's 747SP was in 30 April 2012 beginning the year-long flight test for engine certification. The first delivery of the 78-92 passenger aircraft will be in the summer of 2015 (Analytics 2013).

While in January of 2013, Embraer announced that it had selected the Pure Power family to power exclusively the new second generation of E-Jet aircraft family. The entry to service is scheduled for 2018 with the PW 1700G and PW1900G engines (Analytics 2013).

Bombardier initialized the system tests and simulations of the engine with its 100-150 passenger CSeries aircraft in 2012. By the time, the intentions were to perform the test flight in the end of 2012 and bring the aircrafts into service in late 2013 (Analytics 2013).

In the date of 2013, the PW1000G family order backlog stood at 590, 165, 145 and 128 for the A320neo, MRJ, CSeries and MS-21 aircraft respectively. There we also 835 A320neo family aircraft on order, which the decision regarding the engine selection had yet to be taken (Analytics 2013).

Following (Table 11), is the estimated specifications table of PW1000G family:

Table 11: Estimated Specifications for the PW1000G (Canada 2014).

Engine	Fan Diameter (m)	BPR	Static Thrust	SFC	Noise (St.4)	CO_2(t/ac/yr)	NO_x (margin to CAEP 6)	Aircraft	Estimated Service Entry
PW1124G PW1127G PW1133G	2.1	12:1	24,000-33,000 lbf (110-150 kN)	-15%	-20 dB	-3.600	-55%	A320neo	October 2015
PW1215G PW1217G	1.4	9:1	15,000-17,000 lbf (67-76 kN)	−12%	−15 dB	-2,700	−50%	Mitsubishi Regional Jet	2017
PW1428G PW1431G	2.1	12:1	28,000-31,000 lbf (120-140 kN)	-15%	-20 dB	-3.600	-55%	Irkut MS-21	2016
PW1519G PW1521G PW1524G	1.9	12:1	19,000-24,000 lbf (85-107 kN)	−14%	−20 dB	-3,000	−55%	CSeries	2015
PW1700G	1.4	9:1	15,000-22,000 lbf (67-98 kN)	-12%	-15 dB	-2.700	−50%	E-Jets E2	2018
PW1900G	1.9	12:1	15,000-22,000 lbf (67-98 kN)	-15%	-20 dB	-3.000	−55%	E-Jets E2	2018

3.5.2 CFM Leap

The Leap turbofan engine is pointed to be the successor of the CFM56 line when was launched at the 2005 Paris air show and it has been in development since 1999. The Leap (Leading Edge Aviation Propulsion) technology brings features made in previous years by GE and Snecma with engines such as the GE90 and GEnx.

Getting in some details of the Leap's arquitecture can provide a better perspective of the effort that was put in the engine from a technology point of view (Figure 53). All Leap fans will have 18 blades, which are significantly less than the CFM56-B's 36 titanium blades and the CFM56-7B's 24 blades. With a new lighter containment structure, the total weight saving will be 455kg per aircraft compared with a same-sized fan using metal blades and case (S. Arvai 2011).

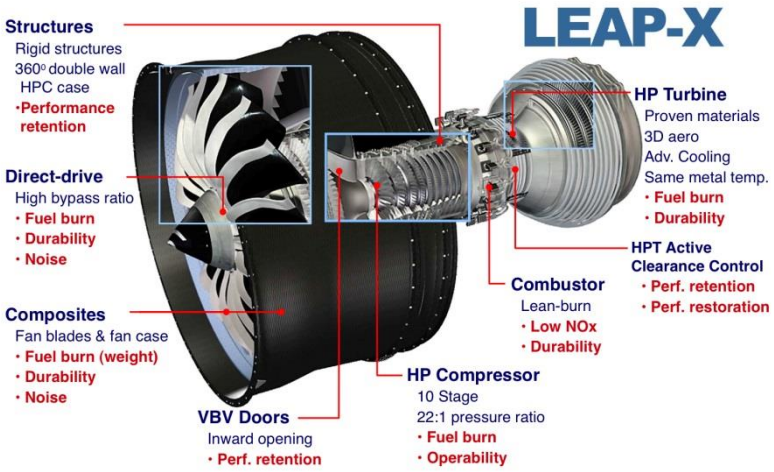

Figure 53: Features of the CFM Leap-x (S. Arvai 2011).

Here the new exotic materials perform a crucial role aiding to push harder the numbers. Ceramic matrix composites are applied in the shroud encasing of the first stage of the high-pressure turbine. CFM initially attempted to apply the single-stage architecture on this new family, but in the end the decision was to switch to a two-stage HPT. As a consequence, an erosion in maintenance cost advantage is predicted, similarly the CFM56 (single-stage) versus the V2500 (two-stage). Despite this situation, CFM is confident that can offset the higher maintenance cost of the turbines by using materials that have to be replaced less frequently (Analytics 2013).

One of the features that CFM brings from the GEnx is the combined blade and disc, or blisk, in the first of the 10 stage HPC. This compressor section will more advanced than in any previous GE aircraft engine. However in the CFM engine the blisks will be present in the first five stages of the 10 stage compressors. In addition to the blisks, new materials and the two stage high pressure turbine will largely improve the thermal efficiency of the engine, leading CFM to claim a double digit improvement in fuel efficiency with a conventional architecture (Analytics 2013).

Being a conventional arquitecture present in the Leap, the low-pressure turbine and inlet fan rotate at the same speed. The inlet fan and booster stages require seven stages in the low pressure turbine. Like in all conventional arquitectures, as the inlet fan diameter widens, the tips of the blades spin faster than the speed of sound, reducing efficiency and causing noise and vibration problems.

The first Leap-1A was scheduled to be assembled in August 2013 and be ready for testing by the end of September. It will be one of the two engine options for the Airbus A320neo, scheduled for 2015. In December 2010, Virgin America was the first airline to order 30 re-engined A320neo aircraft. Since its launch, the A320neo has received more than 2000 orders, putting it in the place of the fastest selling commercial aircraft in history (Analytics 2013).

New entrants in the regional market like COMAC and Irkut were also split over the engine decision between the Leap 1-C and the PW1400G.

The Leap-1B will be exclusive for the Boeing 737 Max. In December 2011, Southwest Airlines became the launch customer for the re-engined narrowbody, placing a firm order for the 150 737 Max aircraft. The Dallas-based airline, which was also the launch customer for both the Boeing 737 Classic and 737 Next Generation series, will take delivery of its first 737 Max in 2017. Air Asia stood as the leading customer as of May 2013 with an order backlog of 264 aircraft followed by Lion Air with 201. Other significant customers of the 737 Max are American Airlines, Norwegian and United Airlines. By May of 2013 Boeing's backlog for the 737 Max stood at 1285 units.

Regarding the Leap-1C has been chosen by Comac as the exclusive powerplant for its C919, a 168-190 passenger single-aisle twinjet. It will be the largest commercial airliner ever to be designed and built in China.

In April 2013, CFM International started building the first parts for the common Leap-1A and 1C engines for the A320neo and C919 families. By the time, the design of the Leap-1B was frozen indicating that all three versions of the single-aisle powerplant have formally entered the assembly stage. Multiple engines will perform ground-test runs before flight testing starts in 2014.

Following is the Table 12 with some predicted values for the Leap family:

Table 12: Estimated Specifications for the Leap Engine (CFM 2013; S. Arvai 2011).

Engine	LEAP-1A	LEAP-1B	LEAP-1C
Fan Diameter (m)	2.0	1.74	1.9
BPR	~10:1	~8.5:1	~9.2:1
Static Thrust	24,500–32,900 lbf (109–146 kN)	23,000–28,000 lbf (100–120 kN)	27,980–30,000 lbf (124.5–133.4 kN)
Fuel Burn (vs. CFM56-7BE)	~ -15%	~ -15%	~ -15%
Number of Stages	1-3-10-2-7	1-3-10-2-5	1-3-10-2-7
Aircraft	Airbus A320neo	Boeing 737 MAX	COMAC C919
Estimated Service Entry	2016	2017	2016

4. Engine Parameters

4.1 Requirements

The intentions of this study are based in the new trends of the aircraft and engine market for the next coming years. The new airframes from Airbus and Boeing (the A320neo and the Boeing 737Max), will be equipped with a new generation of engines that will have a BPR superior to its predecessors. Although these aircraft manufacturers bring new airframes to the market, the propulsion requirements of theses airframes are similar to the old ones.

For the purpose of this study, some engine characteristics will be imposed based in the propulsion requirements of the old airframes and engines. However, at the same time, it will be changed and explored the already known characteristics from the engines makers (Pratt & Whitney and CFM), like a higher BPR, higher TET, new fan and compressor ratios and an increase in efficiency of the components. These characteristics were mentioned previously by several authors in the "State of the Art" and in the "The New Engines: PW1000G and CFM Leap" chapters.

Therefore the engine in study will be based on a two shaft engine with a high bypass ratio destined to power the new narrowbodies from Airbus and Boeing (A320neo and 737Max respectively). Since the new engines will have BPRs superior or equal to 10, we can assume that they are designated as ultra-high bypass turbofans. The aim is to evaluate the engine performance, regarding the specific thrust and the consumption.

This project creates several setups of engines by taking into account some specific imposed requirements which will be tried to match each analysis. The flight point in study will be the cruise phase. Table 13 shows the fixed characteristics of the engine as well as the flight phase.

Also, the introduction of a regenerative cycle will permit to assess the behaviour and the viability of the engine with these new types of propulsive and thermal characteristics.

Table 13: Fixed Engine and Flight Characteristics (S. Arvai 2011; CFM 2013; Airbus 2012).

Cruise Altitude: 36 000 [ft.]
Cruise Temperature: 216.8 [K]
Cruise Pressure: 22 700 [Pa]
Cruise Speed: 230 [m/s]
Cruise Thrust: 32 785.839 [N]

4.2 Assumptions

To obtain the engine values and perform further calculations, it is necessary to define some conditions and assumptions that will influence the calculation process. Therefore the assumptions are:

- One dimensional flow;
- Steady flow;
- The fluid detains a perfect gas behaviour at a constant molecular weight;
- Bleed air is not considered;
- The compression and expansion processes are polytropic;
- Before the combustion phase, the values of C_p and ϒ for the air are: $C_{pc} = 1005 \frac{J}{Kg}.K$ and $\gamma_c = 1.4$;
- After the combustion phase, the values of C_p and ϒ for the air are: $C_{pg} = 1148 \frac{J}{Kg}.K$ and $\gamma_g = 1.333$;
- The specific gas constant is $R = 287 \frac{J}{Kg} K$;
- The temperature at the exit of the LPT must always be superior than at the exit of the HPC in order to assure the integrity of the cycle;
- The average calorific power of the fuel is $Q_{net} = 43.1\ MJ/Kg$;

The next Table 14 will present the component efficiencies that were assumed and kept constant during all the calculation process:

Table 14: Assumed Component Efficiencies (Mattingly 2002).

Component	Symbol	Value
Admission Efficiency	η_i	0.98
Fan Efficiency	η_{fan}	0.90
LPC Polytropic Efficiency	η_{LPC}	0.90
HPC Polytropic Efficiency	η_{LPC}	0.90
Burner Efficiency	η_b	0.995

Burner Pressure Ratio	Π_b	0.96
LPT Polytropic Efficiency	η_{LPT}	0.89
HPT Polytropic Efficiency	η_{HPT}	0.91
Regenerator Efficiency	η_{reg}	0.80
Regenerator Pressure Ratio	Π_{reg}	0.95
Nozzle Efficiency	η_n	0.90
Mechanical Efficiency	η_m	0.995

4.3 Mathematical Model

The following mathematical model presents the main equations for a forward fan unmixed two-spool engines. These equations are based according (El-Sayed 2008) and are adapted for this study. As a final result, the parameters obtained are the specific thrust and specific fuel consumption. These parameters will be used to compare several setups of engines in function the BPR.

4.3.1 Conventional Model

To aid in the formulation of the equations, the schematic engine layout is represented in Figure 54:

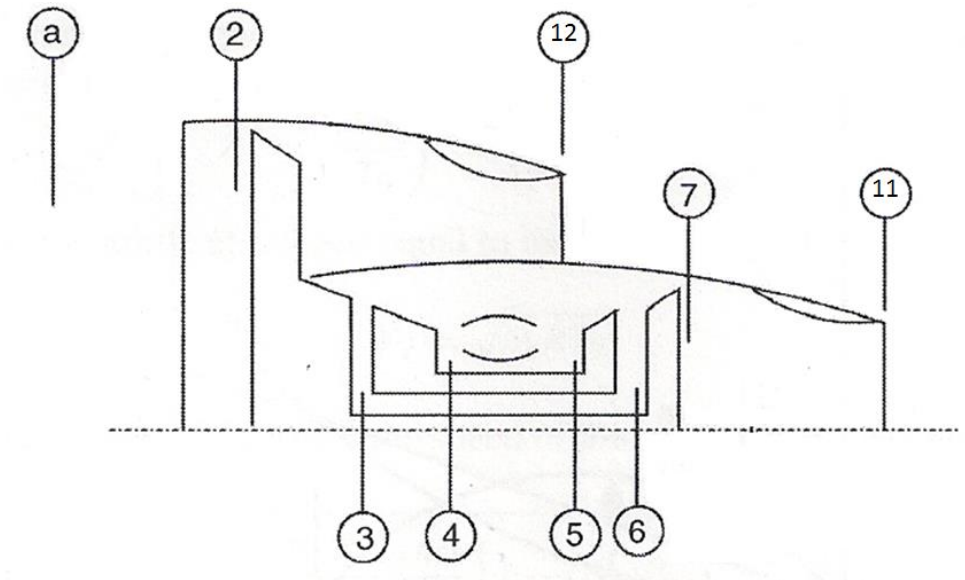

Figure 54: Layout of a two-spool turbofan engine (Adapted from (El-Sayed 2008)).

- Admission:

The relation of temperatures will be:

$$T_{01} = T_a + \frac{C_a^2}{2c_p} \tag{6}$$

Where C_a is the flight speed and T_a.the external temperature.

The relation between pressures:

$$p_{01} = p_a\left[1 + \eta_i \frac{C_a^2}{2c_p T_a}\right]^{\frac{\gamma}{\gamma-1}} \tag{7}$$

Where p_a is the ambient pressure.

- Fan:

$$p_{02} = (p_{01})(\Pi_{fan}) \tag{8}$$

Here is applied the relation between temperatures in a polytropic compression:

$$\frac{T_{02}}{T_{01}} = \left(\frac{p_{02}}{p_{01}}\right)^{\frac{n-1}{n}} \tag{9}$$

Where $\frac{n-1}{n} = \frac{\gamma-1}{\gamma\eta_{\infty c}}$, $\eta_{\infty c}$ is the efficiency of the respective component.

- Low Pressure Compressor:

$$p_{03} = \frac{p_{04}}{\sqrt{\Pi_c}} \tag{10}$$

Here is applied the relation between temperatures in a polytropic compression:

$$\frac{T_{03}}{T_{02}} = \left(\frac{p_{03}}{p_{02}}\right)^{\frac{n-1}{n}} \tag{11}$$

Where $\frac{p_{04}}{p_{02}} = \Pi_c$

- High Pressure Compressor:

$$p_{04} = \Pi_c \times p_{02} \tag{12}$$

Here is applied the relation between temperatures in a polytropic compression:

$$\frac{T_{04}}{T_{03}} = \left(\frac{p_{04}}{p_{03}}\right)^{\frac{n-1}{n}} \tag{13}$$

- Combustion Chamber:

$$p_{05} = \Pi_b \times p_{04} \tag{14}$$

$$f = \frac{C_{pa}.T_{04} - C_{pg}.TET}{C_{pg}.TET - Q_{net}.\eta_b} \tag{15}$$

f represents the fuel air ratio.

- High Pressure Turbine:

To calculate the temperature at the outlet of the HPT, an energy balance between the HPC and the HPT is expressed by the relation:

$$(1+f)C_{pg}(TET - T_{06}) = \frac{C_{pa}(T_{04} - T_{03})}{\eta_m} \tag{16}$$

For the pressure calculation, it is applied the relation between temperatures in a polytropic expansion:

$$\frac{TET}{T_{06}} = \left(\frac{p_{05}}{p_{06}}\right)^{\frac{n-1}{n}} \tag{17}$$

- Low Pressure Turbine:

An energy balance between the fan and the LPC from one side and the LPR on the other side is expressed by the relation:

$$(1+f)C_{pg}(T_{06} - T_{07}) = \frac{C_{pa}(T_{03} - T_{02}) + (1+B)C_{pa}(T_{02} - T_{01})}{\eta_m} \tag{18}$$

For the pressure calculation, it is applied the relation between temperatures in a polytropic expansion:

$$\frac{T_{06}}{T_{07}} = \left(\frac{p_{06}}{p_{07}}\right)^{\frac{n-1}{n}} \tag{19}$$

- Turbine Nozzle:

It is assumed that there are no changes in the total pressure and total temperature in the jet pipe between the turbine and the nozzle. Next, a check for nozzle choking is performed. The critical pressure is calculated from relation:

$$\frac{P_{07}}{P_c} = \frac{1}{\left[1 - \frac{\left(\frac{1}{\eta_n}\right)(\gamma_g - 1)}{\gamma_g + 1}\right]^{\frac{\gamma_g}{\gamma_g - 1}}} \tag{20}$$

If $P_c \geq P_a$ then the nozzle is choked. The temperature of the gases leaving the nozzle is obtained from the relation:

$$\frac{T_{07}}{T_{11}} = \frac{\gamma_g + 1}{2} \tag{21}$$

Therefore the gases leave the nozzle at a speed equal to the sonic speed or

$$V_{11} = \sqrt{\gamma_g R T_{11}} \tag{22}$$

Otherwise, if the nozzle is unchoked $(P_{11} = P_a)$, then the speed of the gases leaving the nozzle is now given by

$$V_{11} = \sqrt{2C_{pg}(T_{07} - T_{11})} \tag{23}$$

- Fan Nozzle:

Here, the fan nozzle is also checked to de determine if it is whether choked or unchoked. The critical pressure is calculated from relation:

$$\frac{P_{02}}{P_c} = \frac{1}{\left[1 - \frac{\left(\frac{1}{\eta_{fan}}\right)(\gamma_c - 1)}{\gamma_c + 1}\right]^{\frac{\gamma_c}{\gamma_c - 1}}} \tag{24}$$

If $P_c \geq P_a$ then the nozzle is choked. The temperature of the gases leaving the nozzle is obtained from the relation:

$$\frac{T_{02}}{T_{12}} = \frac{\gamma_c + 1}{2} \tag{25}$$

Therefore the gases leave the nozzle at a speed equal to the sonic speed or

$$V_{12} = \sqrt{\gamma_c R T_{12}} \tag{26}$$

Otherwise, if the nozzle is unchoked $(P_{12} = P_a)$, then the speed of the gases leaving the nozzle is now given by

$$V_{12} = \sqrt{2C_{pa}(T_{02} - T_{12})} \tag{27}$$

Finally, after some calculations the specific thrust and thrust-specific fuel consumption are obtained for a respective BPR:

The specific thrust will be:

$$F_s = \frac{F}{\dot{m}_a} \tag{28}$$

Where $\dot{m}_a$ is the total mass of air intake to the engine.

And the thrust-specific fuel consumption is given by:

$$TSFC = \frac{3600 \cdot \dot{m}_f}{F} \tag{29}$$

Where $\dot{m}_f$ is the mass of fuel added to the combustion.

4.3.2 Regenerator Model

Following are presented the equations of the regenerative cycle. The regenerator is adapted at the exit of the LPT proceeding to a heat exchange with the pressurized gases leaving the HPC, before entering in the combustion chamber. The equations are adapted to the already exposed ones for the conventional cycle. The layout of the engine configuration can be observed in the Figure 55.

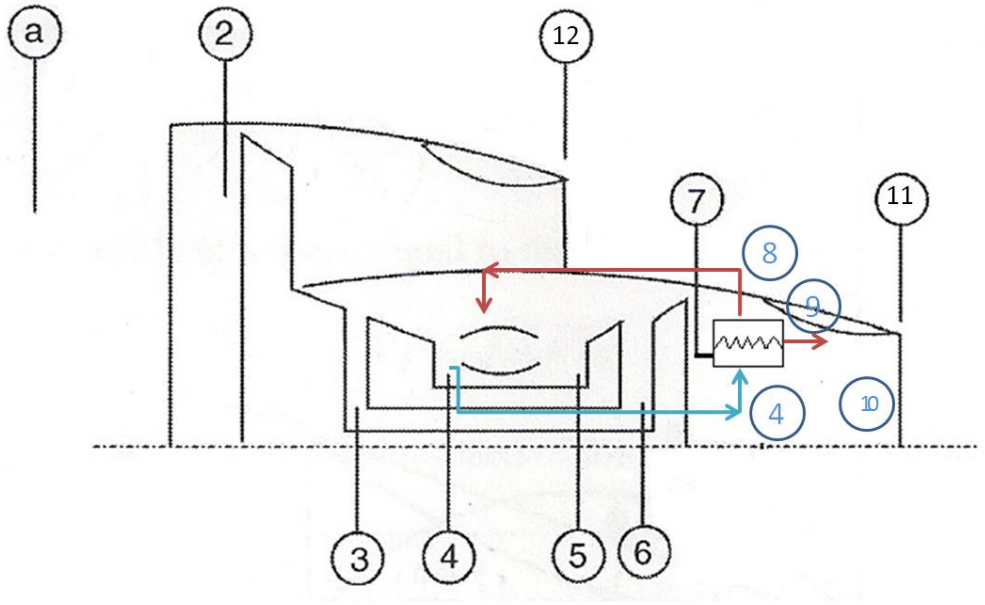

Figure 55: Layout of a two-spool turbofan engine with regenerator (Adapted from (El-Sayed 2008)).

An energy balance and the efficiency equation are applied to the regenerator in order to obtain the temperatures T_{08} and T_{09}.

$$(\dot{m}_h + \dot{m}_f)C_{pg}(T_{07} - T_{09}) = \dot{m}_h C_{pa}(T_{08} - T_{04}) \tag{30}$$

$$\eta_{reg} = \frac{C_{pa}(T_{08} - T_{04})}{C_{pg}(T_{07} - T_{09})} \tag{31}$$

The pressures, P_{08} and P_{04} are calculated considering the regenerator pressure ratio.

$$P_{08} = P_{04} \cdot \Pi_{reg} \tag{32}$$

$$P_{09} = P_{07} \cdot \Pi_{reg} \tag{33}$$

Since there is a pressure drop in the regenerator, it is necessary to calculate a new fuel air ratio for the combustion ($f'reg$) and new temperatures and pressures for the HPT and LPT.

$$f'reg = \frac{C_{pa}.T_{08} - C_{pg}.TET}{C_{pg}.TET - Q_{net}.\eta_b} \tag{34}$$

The next Figure 56 shows the regenerator station numbering, used in the energy balance on equation 30:

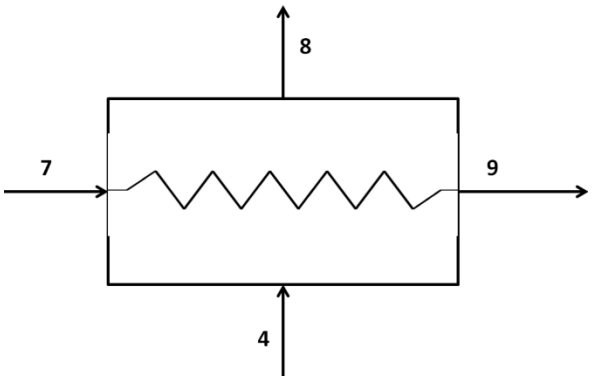

Figure 56: Regenerator Station Numbering

- Number 7: hot gases from the LPT;
- Number 4: cold flow from the HPC;
- Number 8: hot flow destined to enter in the combustion chamber;
- Number 9: Exhaust gases;

4.4 Calculation Strategy

After the engine type has been selected, the flight point of the mission was also defined.

To perform an analysis, assumptions and constrains were defined according to the mathematical model used. It is expected that the results do not reveal exact values due to some parameters that are assumed as constant. Instead, an approximation is obtained; however, the credibility of the results is assured.

The mathematical model is applied to the conventional cycle and it is adapted to the alternative cycle with the introduction of the regenerator.

For the parameterization, independent variables were selected and tweaked in order to evaluate all the possible setups, so an initial performance map of the engine can be obtained. The independent variables in this study will be: the BPR and the TET (already mentioned in the Requirements subsection), the fan pressure ratio (*rpfan*) and the compressor pressure ratio (*rpc*). These engine variables were parameterized with the following values:

- BPR: from 10 to 20;
- TET: 1500K/1800K and 2100K;

- Compressor Pressure Ratio: 10/15 and 20;
- Fan Pressure Ratio: 1.2/1.5 and 1.8;

To execute the parameterization, the mathematical model was developed in a Matlab code in order to perform the calculations. The code is able to calculate various engine configurations simply by varying each independent variable according to an established step. All the calculated results are filtered and a selection of acceptable results is condensated in a major matrix to be plotted.

The following diagram, Figure 57 resumes all the processes that were taken in the parameterization study.

Figure 57: Engine Evaluation Strategy Diagram

4.5 Parametric Results

In this section it will be shown the results from the Mathematical Model applied to all the four variables, comparing the situation with and without regeneration. By fixating one of the variables as a constant parameter, it is possible to study the behaviour of the remaining in a pre-established search range. It is also object of study, to assess a primary indication if the regeneration is a viable option.

From these results it will be possible to map the engine behaviour and acquire possible and viable ranges for each one of the considered variables for further studies.

4.5.1 Fs – *rpfan* 1.2

Following are the Fs results for a fixed *rpfan* of 1.2, varying the BPR from 10 to 20, TET from 1500K to 2100K and the *rpc* from 10 to 20. The graphics are in the Figure 58, Figure 59 and Figure 60.

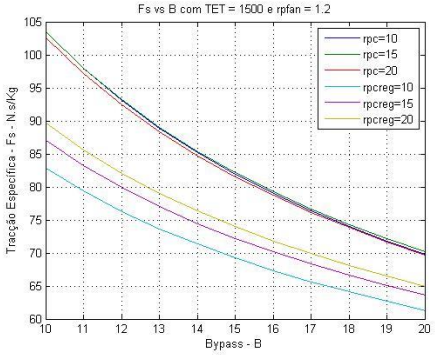

Figure 58: Fs vs BPR with and without regeneration (TET 1500K and *rpfan* 1.2).

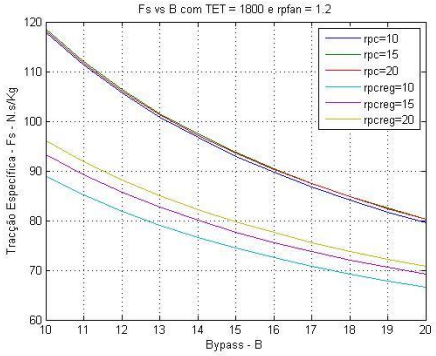

Figure 59: Fs vs BPR with and without regeneration (TET 1800K and *rpfan* 1.2).

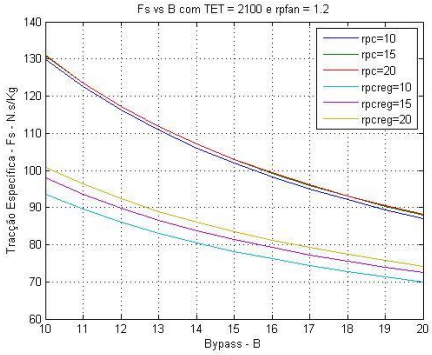

Figure 60: Fs vs BPR with and without regeneration (TET 2100K and *rpfan* 1.2).

It is possible to say that the values of Fs increase as TET rises, however the Fs decreases along with the BPR escalation. The range of Fs values are nearly from 70 N.s/kg (TET 1500K) until 130 N.s/kg(TET 2100K), being the major climbing from TET 1800K to TET 1800K. For the three values of *rpc*, the Fs curves are practically coincident. In TET 1500K, the *rpc* 15 shows the highest value of Fs and the lowest belongs to *rpc* 20. In the other set of temperatures the values of *rpc* 15 and 20 are similar.

Regarding the regeneration results, the trend of the Fs curves for each *rpcreg* along all the BPR is equal to the situation without regeneration. However for each *rpcreg*, there are distinctive values of Fs, contrary the situation without regeneration. The values of Fs with regeneration are lower than the Fs values with no regeneration. With a *rpcreg* of 10 are registered the lowest values of Fs and for a *rpcreg* of 20 the highest. The range of the regenerative Fs values goes from nearly 60 N.s/kg (TET 1500K) until 100 N.s/kg (TET 2100K).

4.5.2 Fs – *rpfan* 1.5

Following are the Fs results for a fixed *rpfan* of 1.5, varying the BPR from 10 to 20, TET from 1500K to 2100K and the *rpc* from 10 to 20. The graphics are in the Figure 61, Figure 62 and Figure 63.

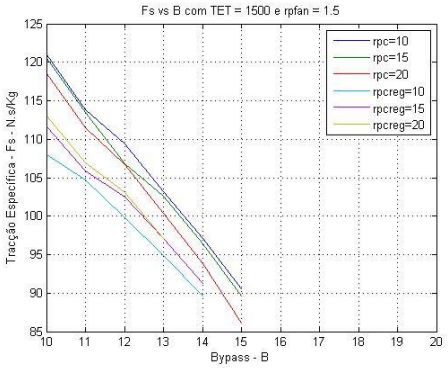

Figure 61: Fs vs BPR with and without regeneration (TET 1500K and *rpfan* 1.5).

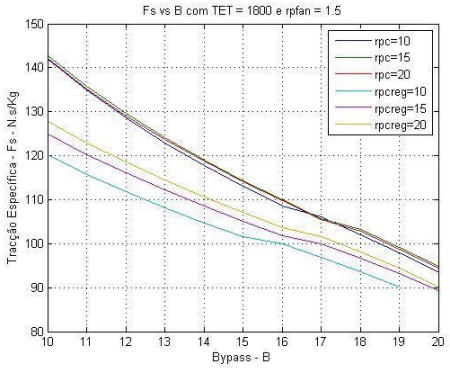

Figure 62: Fs vs BPR with and without regeneration (TET 1800K and *rpfan* 1.5).

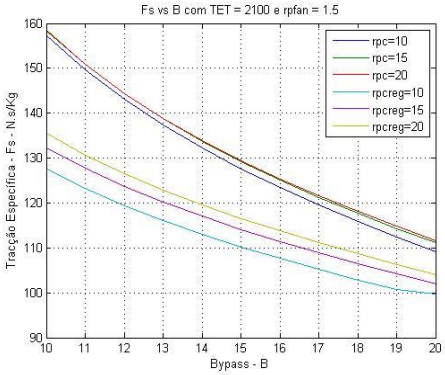

Figure 63: Fs vs BPR with and without regeneration (TET 2100K and *rpfan* 1.5).

Like the previous subsection, the behaviour of Fs regarding the BPR is equal. Also, the Fs values are superior when the regeneration is not present. For a TET of 1500K, without regeneration, the best values of Fs are achieved on *rpc* 10, on the contrary, the worse values are with a *rpc* of 20. With this turbine entry temperature it is only possible results until a BPR of 15. For a TET of 1800K and 2100K, a *rpc* of 15 and 20 mark the best values for all the BPRs. The range of Fs values goes from nearly 86 N.s/kg (TET 1500K), until 160 N.s/kg (TET 2100K).

In the regeneration results, for a TET of 1500K with a *rpcreg* of 20, it is registered the highest values of Fs until the BPR of 13. On the other hand, with a *rpcreg* of 10 and 15 the Fs is lower

but it is possible until a BPR of 14. For a TET of 1800K, the *rpcreg* of 20 still achieves the best Fs results for all the BPRs and the *rpcreg* of 10 scores the lowest results, being possible until a BPR of 19. For the last set of temperature, the 2100K, the behaviour is similar of the TET 800K and all the *rpcreg* are possible for all the BPRs. The regenerative Fs range values goes from nearly 90N.s/kg (TET 1500K) until 135 N.s/kg (TET 2100K).

4.5.3 Fs – *rpfan* 1.8

Following are the Fs results for a fixed *rpfan* of 1.8, varying the BPR from 10 to 20, TET from 1500K to 2100K and the *rpc* from 10 to 20. The graphics are in the Figure 64 and Figure 65.

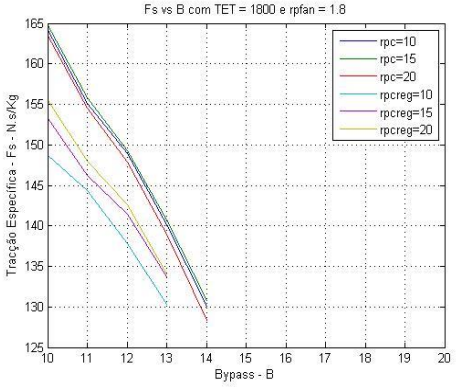

Figure 64: Fs vs BPR with and without regeneration (TET 1800K and *rpfan* 1.8).

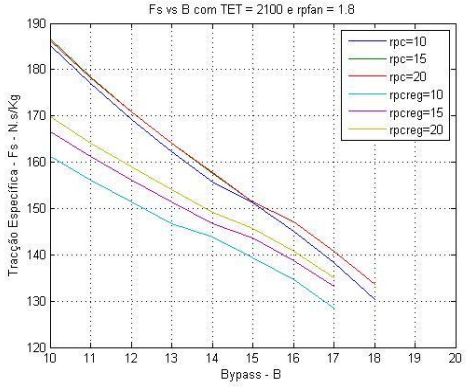

Figure 65: Fs vs BPR with and without regeneration (TET 2100K and *rpfan* 1.8).

For a *rpfan* of 1.8 with a turbine entry temperature of 1500K there are no possible values due to the reduced temperature regarding the fan pressure ratio that is imposed.

Similarly to the previous subsection of *rpfan* (1.2 and 1.5), the behaviour of the Fs regarding the increasing of BPR and TET is equal. Therefore, for a TET of 1800K and no regeneration, a *rpc* of 15 shows the highest values of Fs and these values are possible until a BPR of 14. However the lowest values of Fs are registered for a *rpc* of 20. For a TET of 2100K and still no regeneration, a *rpc* of 20 exhibits the highest values of Fs and there values are possible until a BPR of 20. The worst values are verified for a *rpc* of 10. The range values of Fs without regeneration, goes from nearly 128 N.s/kg (TET 1800k) until 185 N.s/kg (TET 2100K).

In the regeneration results, for a TET of 1800K, a *rpcreg* of 20 shows the best results of Fs, contrary to the *rpcreg* of 10. Both configurations are possible until a BPR of 13. For the TET of 2100K, the trends of the *rpcreg* with the BPR increase is the same but in a higher Fs output. The range values of Fs with regeneration, goes from nearly 131 N.s/kg (TET 1800K) until 170 N.s/kg (TET 2100K).

4.5.4 Fs – *rpc* 10

Following are the Fs results for a fixed *rpc* of 10, varying the BPR from 10 to 20, TET from 1500K to 2100K and the *rpfan* from 1.2 to 1.8. The graphics are in the Figure 66, Figure 67 and Figure 68.

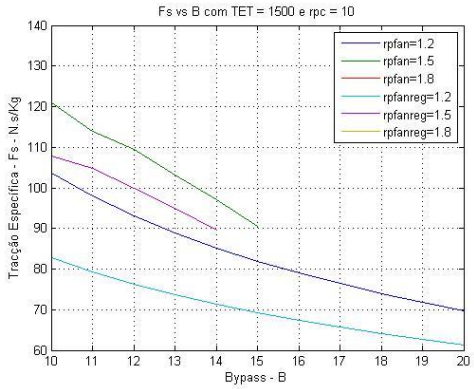

Figure 66: Fs vs BPR with and without regeneration (TET 1500K and *rpc* 10).

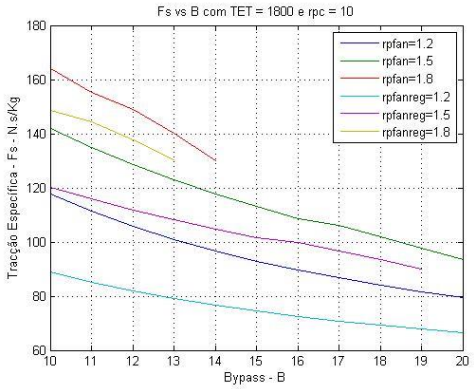

Figure 67: Fs vs BPR with and without regeneration (TET 1800K and *rpc* 10).

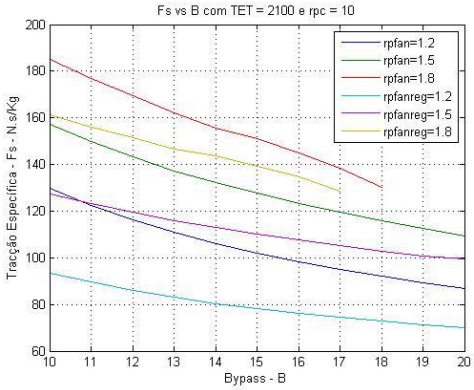

Figure 68: Fs vs BPR with and without regeneration (TET 2100K and *rpc* 10).

While the TET rises, it is verified an increase of the available Fs for both cases (with and without regeneration). Also, the possible range of the BPR grows for each TET, however, the bigger BPR less Fs will be available.

The results with no regeneration, show that for the TET of 1500K, a *rpfan* of 1.8 is not possible (previously demonstrated), leaving the *rpfan* of 1.5 with the best Fs results until a BPR of 15. In the situation of a TET of 1800K, the *rpfan* of 1.8 is already possible until BPR 14 exhibiting the best results. The lowest Fs belongs to the *rpfan* 1.2 with a range for all the BPRs. Finally, for a TET of 2100K, a *rpfan* of 1.8 still records the best Fs values with a maximum BPR of 18. While the *rpfan* of 1.2 and 1.5 score lower values bur are possible for all the BPRs. The Fs range values without regeneration goes from nearly 70 N.s/kg (TET 1500K) until 185 N.s/kg (TET 2100K).

When the regeneration is applied, for a TET of 1500K, a *rpfanreg* of 1.8 is also impossible, leaving the *rpfanreg* of 1.5 with the best values of Fs until a BPR of 15. With a TET of 1800K and a possible *rpfanreg* of 1.8, the best Fs results are achieved until a BPR of 13. The *rpfanreg* of 1.5 is the second option with a range until BPR 19 and at last the *rpfanreg* for all the BPRs. For the last TET, 2100K, the trend of the TET 1800K is maintained, only the Fs results are extended to higher values of BPR, with the *rpfanreg* 1.8 until BPR 17. The remaining *rpfanreg* are until 20 but with a fewer Fs. The range of Fs values with regeneration goes from nearly 60 N.s/kg (TET 1500K) until 160 N.s/kg (TET 2100).

4.5.5 Fs – *rpc* 15

Following are the Fs results for a fixed *rpc* of 15, varying the BPR from 10 to 20, TET from 1500K to 2100K and the *rpfan* from 1.2 to 1.8. The graphics are in the Figure 69, Figure 70 and Figure 71.

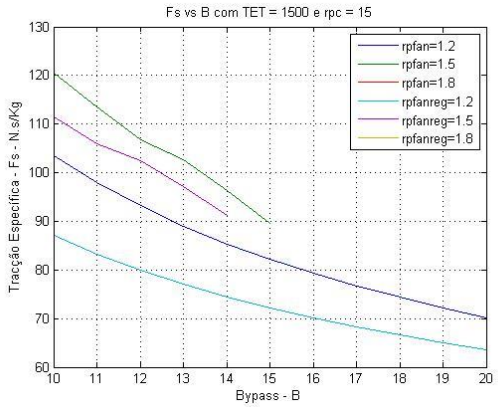

Figure 69: Fs vs BPR with and without regeneration (TET 1500K and *rpc* 15).

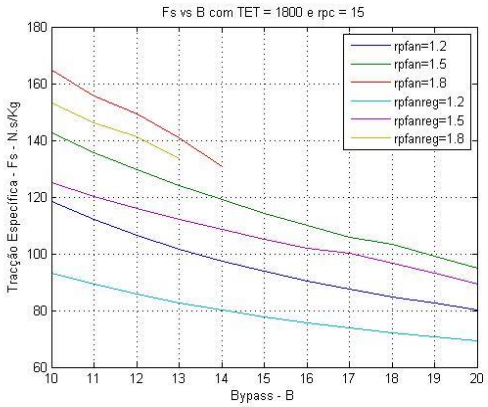

Figure 70: Fs vs BPR with and without regeneration (TET 1800K and *rpc* 15).

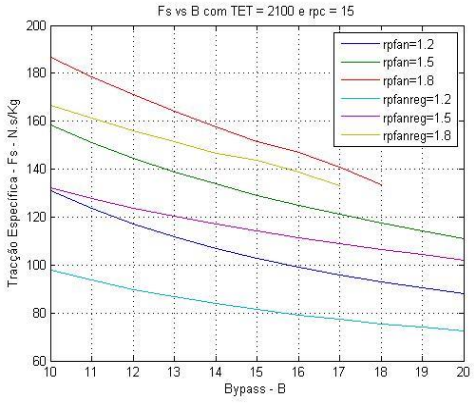

Figure 71: Fs vs BPR with and without regeneration (TET 2100K and *rpc* 15).

All the behaviour registered with this setup is equal to the previous subsection, registering only a slightly increase on the Fs values. For the TET of 1500K with the *rpfan* of 1.5 a small decline in the Fs is noticed.

4.5.6 Fs – *rpc* 20

Following are the Fs results for a fixed *rpc* of 20, varying the BPR from 10 to 20, TET from 1500K to 2100K and the *rpfan* from 1.2 to 1.8. The graphics are in the Figure 72, Figure 73 and Figure 74.

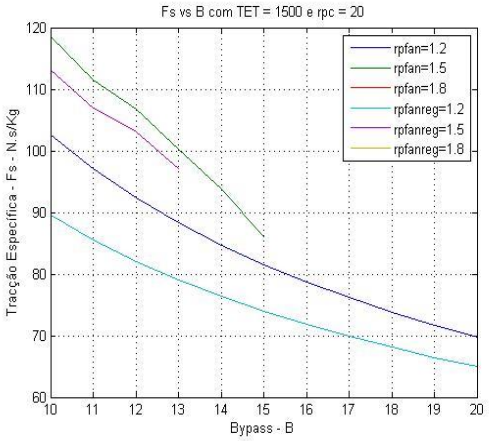

Figure 72: Fs vs BPR with and without regeneration (TET 1500K and *rpc* 20).

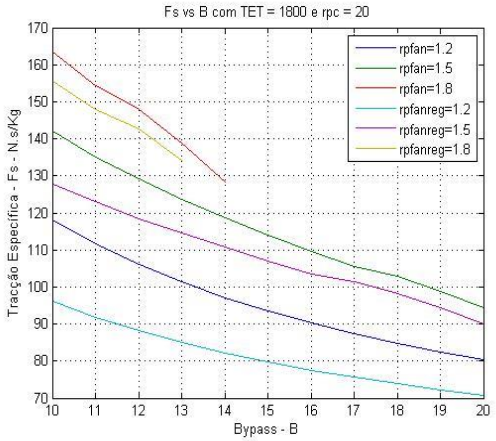

Figure 73: Fs vs BPR with and without regeneration (TET 1800K and *rpc* 20).

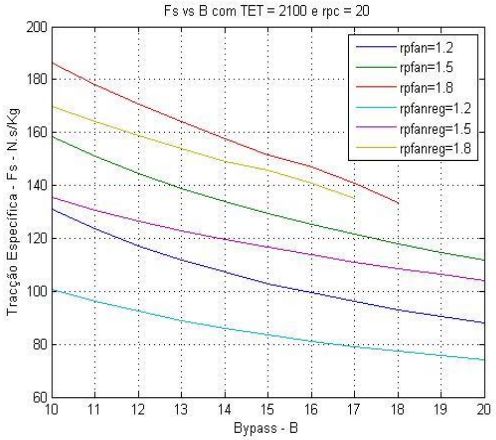

Figure 74: Fs vs BPR with and without regeneration (TET 2100K and *rpc* 20).

The same behaviour is also registered in this configuration comparatively to the last subsection. Still, it is possible to observe a slightly increase on the Fs values. For the TET of 1500K with the *rpfan* of 1.5 a small decline in the Fs is continued noticed.

4.5.7 TSFC – *rpfan* 1.2

Following are the TSFC results for a fixed *rpfan* of 1.2, varying the BPR from 10 to 20, TET from 1500K to 2100K and the *rpc* from 10 to 20. The graphics are in the Figure 75, Figure 76 and Figure 77.

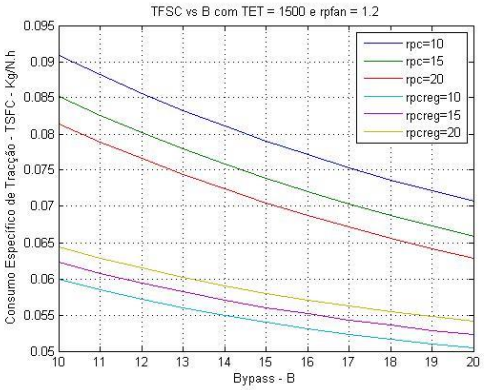

Figure 75: TSFC vs BPR with and without regeneration (TET 1500K and *rpfan* 1.2).

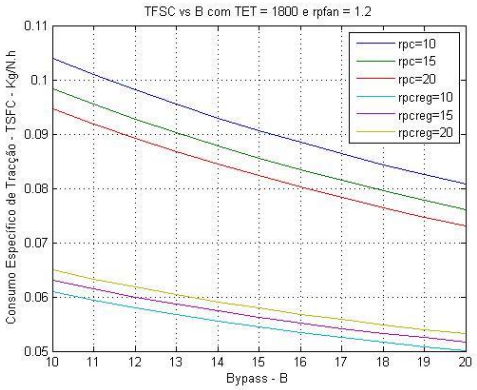

Figure 76: TSFC vs BPR with and without regeneration (TET 1800K and *rpfan* 1.2).

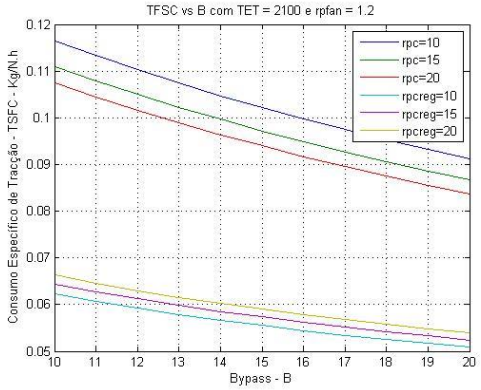

Figure 77: TSFC vs BPR with and without regeneration (TET 2100K and *rpfan* 1.2).

For the TSFC analysis, it can be observed that is reduced along with the BPR increase. It is increased when the *rpcreg* steps to higher values when regeneration is applied, as well as when the TET is raised. When the regeneration is off the cycle, the TSFC is lower for a higher *rpc* and also increases with the TET escalation. Therefore, the best values of TSFC without regeneration are when the *rpc* is 20 and with regeneration it will be 10, this is valid for all the BPRs. The range values of TSFC with no regeneration is nearly 0.00625 kg/N.h (TET 1500K) until 0.0118 kg/N.h (TET 2100K), for all the BPRs. Finally the range values of TSFC with regeneration is nearly 0.0500 kg/N.h (TET 1500K) until 0.0670 kg/N.h (TET 2100K), for all the BPRs.

4.5.8 TSFC – *rpfan* 1.5

Following are the TSFC results for a fixed *rpfan* of 1.5, varying the BPR from 10 to 20, TET from 1500K to 2100K and the *rpc* from 10 to 20. The graphics are in the Figure 78, Figure 79 and Figure 80.

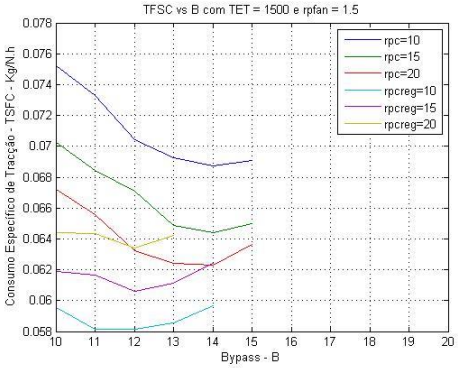

Figure 78: TSFC vs BPR with and without regeneration (TET 1500K and *rpfan* 1.5).

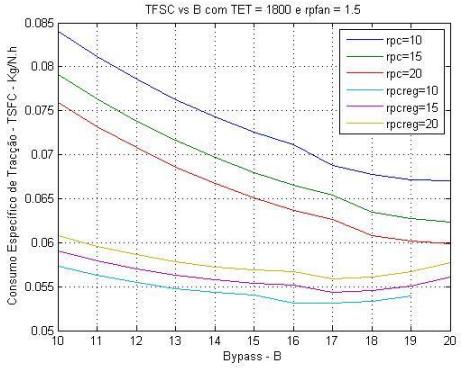

Figure 79: TSFC vs BPR with and without regeneration (TET 1800K and *rpfan* 1.5).

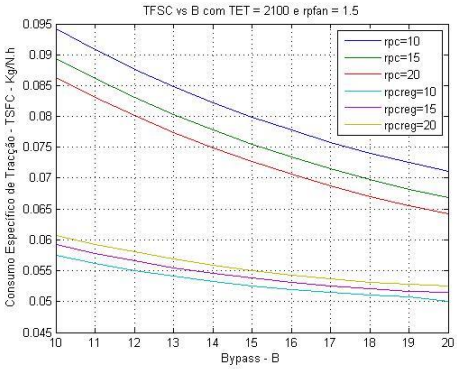

Figure 80: TSFC vs BPR with and without regeneration (TET 2100K and *rpfan* 1.5).

The trend of the TSFC curves in this setup is similar to the previous subsection; however there are some exceptions that are imperative to be mentioned.

For a TET of 1500K, in both configurations, the best values of *rpc* that register the lowest TSFC are a *rpc* of 20 and a *rpcreg* of 10 respectively. However without regeneration, these values are viable until a BPR of 15, where it is observed an inversion of the decrease of the TSFC. For the regeneration configuration this inversion is observed earlier and starts to be manifested around a BPR of 12. For a TET of 1800K, the best curve of TSFC is with a *rpc* of 20 for a conventional case and a *rpcreg* of 10 in the regenerated one, until a BPR of 19. In the highest TET (2100K), the trend of the previous TET is continued and all BPR are possible.

The range values of the conventional case for TSFC are nearly 0.0621 kg/N.h (TET 1500K) until a 0.095 kg/N. (TET 2100K). For the regeneration situation, are nearly 0.0581 kg/N.h (TET 1500K) until 0.061 kg/N.h (TET 2100K).

4.5.9 TSFC – *rpfan* 1.8

Following are the TSFC results for a fixed *rpfan* of 1.8, varying the BPR from 10 to 20, TET from 1500K to 2100K and the *rpc* from 10 to 20. The graphics are in the Figure 81 and Figure 82.

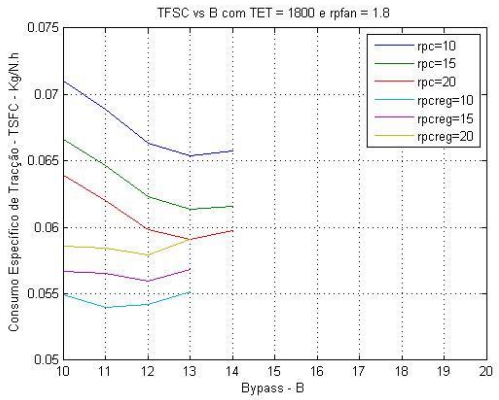

Figure 81: TSFC vs BPR with and without regeneration (TET 1800K and *rpfan* 1.8).

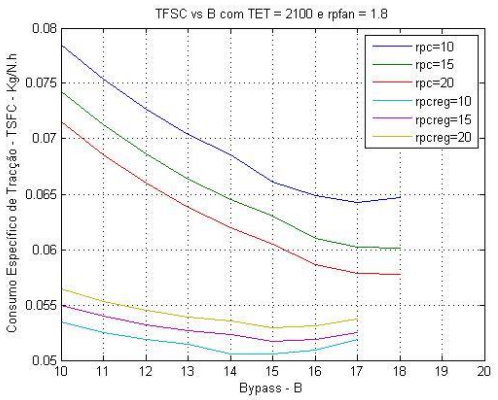

Figure 82: TSFC vs BPR with and without regeneration (TET 2100K and *rpfan* 1.8).

All the trends described previously are maintained but is important to note some limitations on higher BPRs.

With this choice of *rpfan,* in a TET of 1500K was not registered any values in the Fs analysis, so it was not possible to obtain any consumption readings. Although, for a TET of 1800K the best TSFC value was the *rpc* 20 curve on the BPR 13, increasing in the next BPR. For the TET of 2100K, the best consumption value was on the *rpc* 20 curve for BPR 18. Both results are with no regeneration.

In the regeneration setup, for the TET of 1800K, the best TSFC value is registered for a *rpcreg* of 10 in the BPR 11, following a slight increase until BPR 13. For the TET of 2100K the same *rpcreg* continues the trend of lowest TSFC values registering its minimum in the BPR 14/15, and then increasing until a BPR 17.

Therefore, the range values of TSFC with no regeneration go nearly from 0.0590 kg/N.h (TET 1800K) until 0.078 kg/N.h (TET 2100K). With regeneration, the range goes nearly from 0.0548 kg/N.h (TET 1800K), to 0.057 kg/N.h (TET 2100K).

4.5.10 TSFC – *rpc* 10

Following are the TSFC results for a fixed *rpc* of 10, varying the BPR from 10 to 20, TET from 1500K to 2100K and the *rpfan* from 1.2 to 1.8. The graphics are in the Figure 83, Figure 84 and Figure 85.

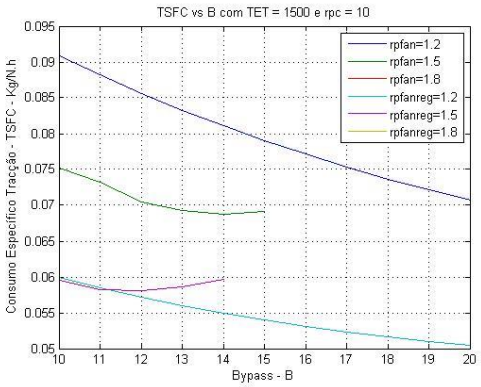

Figure 83: TSFC vs BPR with and without regeneration (TET 1500K and *rpc* 10).

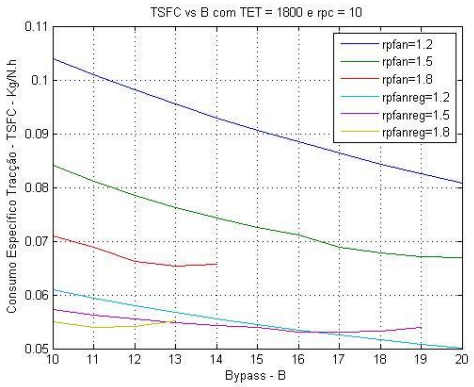

Figure 84: TSFC vs BPR with and without regeneration (TET 1800K and *rpc* 10).

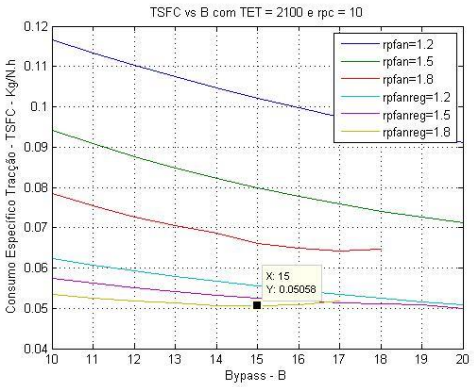

Figure 85: TSFC vs BPR with and without regeneration (TET 2100K and *rpc* 10).

While the TET increases, the TSFC values also increase, however they trend for lower values along the BPR increase. In general, raising the *rpfan* will contribute for a reduction of the TSFC. In the regeneration case, it is observed that all the *rpfanreg* curves tend for a single TSFC value on higher BPRs, and then separating from each other and reversing the trend that higher the *rpfan*, lower the TSFC.

Therefore, for a TET of 1500K a *rpfan* of 1.8 is not possible for already mentioned reasons. In a *rpfan* of 1.5 is registered a TSFC minimum in the BPR 14, increasing slightly afterwards until a BPR 15. In the TET of 1800K, the lowest value of TSFC is for a *rpfan* of 1.8 in the BPR 13, increasing slightly after that BPR. For the 2100K in the turbine entry temperature scenario, the lowest value of TSFC still belongs to the *rpfan* 1.8 in the BPR of 17, reaching a BPR of 18.

Regarding the regeneration results, initially, the *rpfanreg* of 1.5 until a BPR of 11, exhibits the lower TSFC, however that trend is inverted after that bypass. From there, is the *rpfanreg*

of 1.2 which reveals the lowest consumption on a TET of 1500K. When the TET is 1800K, the curves of *rpfanreg* 1.5/1.2 show the better results of TSFC until the BPR of 16, after that, the *rpfanreg* 1.5 reveals superior values of consumption for the remaining BPRs. The *rpfan* 1.2 curve has smooth behaviour, decreasing its values along all the BPRs. For the *rpfan* 1.8, its minimum is registered in the BPR 11. Finally, in the 2100K TET condition, the lowest values for the TSFC are scored with a *rpfanreg* of 1.8 in the BPR 15.

The range values of TSFC for a conventional configuration are nearly from 0.068 kg/N.h (TET 1500K) to 0.180 kg/N.h (TET 2100K). At last, the range values for the consumption in a regenerative scenario go from nearly 0.050 kg/N.h (TET 1500K) to 0.063 kg/N.h (TET 2100K).

4.5.11 TSFC – *rpc* 15

Following are the TSFC results for a fixed *rpc* of 15, varying the BPR from 10 to 20, TET from 1500K to 2100K and the *rpfan* from 1.2 to 1.8. The graphics are in the Figure 86, Figure 87 and Figure 88.

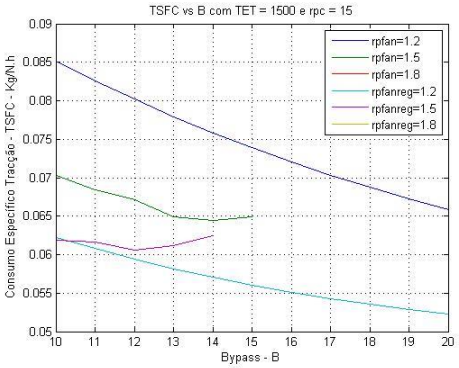

Figure 86: TSFC vs BPR with and without regeneration (TET 1500K and *rpc* 15).

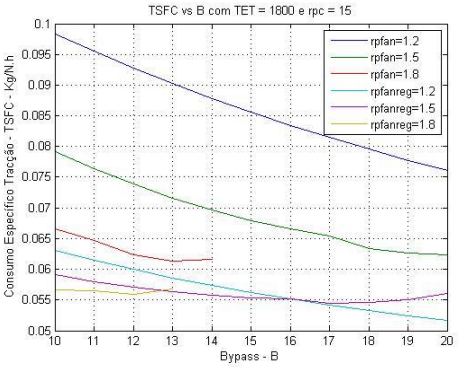

Figure 87: TSFC vs BPR with and without regeneration (TET 1800K and *rpc* 15).

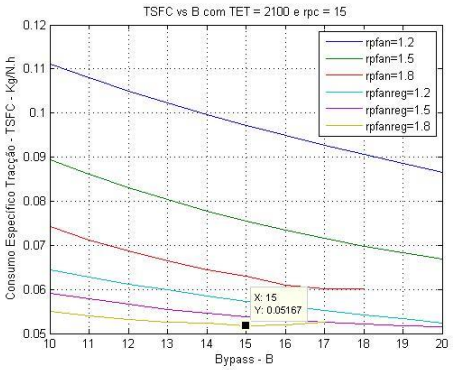

Figure 88: TSFC vs BPR with and without regeneration (TET 2100K and *rpc* 15).

Comparing with the previous subsection (*rpc* 10), the values of TSFC show a decreasing trend but increase with the TET escalation. In this case, the consumption also decreases along with

the BPRs. The consumption values with regeneration suffer a slightly increasing regarding the previous section and also show trend to increase with higher TET.

Therefore the results with the absence of regeneration, for a TET of 1500K, register the lowest TSFC value for the *rpfan* 1.5 curve in the BPR 14, increasing after that value until a BPR 15. In the TET 1800K setup, the best value is observed with a *rpfan* of 1.8 in a BPR of 13, increasing slightly until its limit (BPR 14). For the highest TET (2100K), the minimum belongs to the *rpfan* of 1.8 in the BPRs of 17/18.

The regeneration results show a *rpfanreg* of 1.2 with the best consumption value with a TET of 1500K until a BPR of 20. For the TET of 1800K, the best TSFC value is verified for the *rpfanreg* of 1.8 in the bypass 12, rising slightly until the BPR 13. Another minimum that can be observed is from the *rpfanreg* 1.5 curve, which registers a value even lower in the BPR 17, pairing with the *rpfanreg* 1.2. However, the *rpfanreg* 1.5 increases slightly from the lowest score. On the contrary, the *rpfanreg* 1.2, only decreases until the end of the graph. Finally for a TET of 2100K, the *rpfanreg* 1.8 marks the lowest TSFC in a BPR of 15 and increases slightly until a bypass of 17. With a *rpfanreg* of 1.2 and 1.5, the consumption will be higher, but they are possible in all the BPRs. It is important to notice that with a *rpfanreg* of 1.5, the TSFC values are equal of a *rpfanreg* of 1.8 in the BPRs 19 and 20.

The range values of TSFC for a conventional configuration are nearly from 0.063 kg/N.h (TET 1500K) to 0.112 kg/N.h (TET 2100K). At last, the range values for the consumption with a regenerative cycle go from nearly 0.054 kg/N.h (TET 1500K) to 0.064 kg/N.h (TET 2100K).

4.5.12 TSFC – *rpc* 20

Following are the TSFC results for a fixed *rpc* of 20, varying the BPR from 10 to 20, TET from 1500K to 2100K and the *rpfan* from 1.2 to 1.8. The graphics are in the Figure 89, Figure 90 and Figure 91.

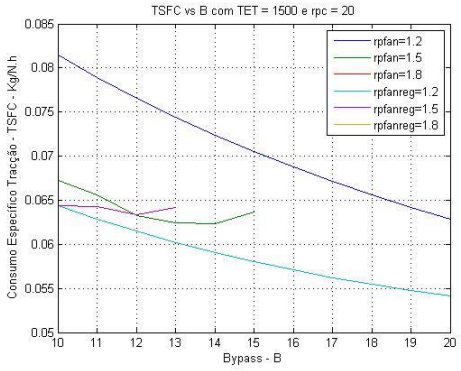

Figure 89: TSFC vs BPR with and without regeneration (TET 1500K and *rpc* 20).

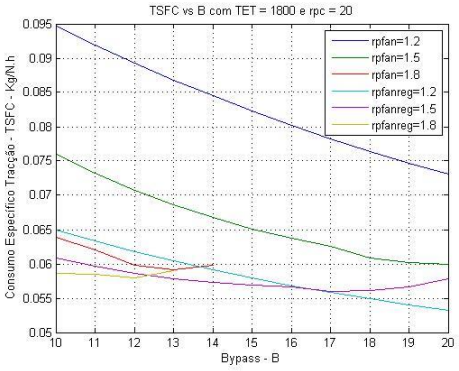

Figure 90: TSFC vs BPR with and without regeneration (TET 1800K and *rpc* 20).

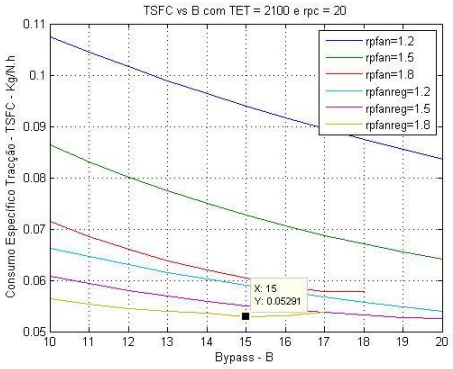

Figure 91: TSFC vs BPR with and without regeneration (TET 2100K and *rpc* 20).

The trend described previously for a *rpc* of 15 is still verified in this three setups. Therefore, with an increase of the *rpc* or *rpcreg* the consumption will decrease, while in a non-regenerative case it will increase with higher TETs. However, in a regenerative cycle the values of TSFC tend to be reduced with higher TET temperatures.

Analysing in a more separately way the conventional cycle, for a TET of 1500K and with a *rpfan* of 1.5 the lowest value of TSFC is in the BPR 14. While with a TET of 1800K, the lowest value of consumption will be with a *rpfan* of 1.8 in the BPR 13, increasing slightly after that BPR level. In the highest value of TET (2100K), the best value of consumption still will be the *rpfan* of 1.8, reaching its minimum in the BPR 17/18.

For the regenerative process, with a TET of 1500K and a *rpfanreg* of 1.2, the lowest TSFC value is registered in all the BPRs. While with a TET of 1800K, the results are equal of the previous subsection (rpc15). Finally, for the 2100K turbine entry temperature, the best consumption value is stationed in a BPR of 15, with a *rpfanreg* of 1.8. This value of TSFC will increase slightly after this BPR until the bypass 17.

The range values of TSFC for a conventional configuration are nearly from 0.0645 kg/N.h (TET 1500K) to 0.109 kg/N.h (TET 2100K). At last, the range values for the consumption with a regenerative cycle go from nearly 0.054 kg/N.h (TET 1500K) to 0.068 kg/N.h (TET 2100K).

5. Evolutionary Computation

It is necessary to expose some concepts before proceeding to the optimization of the engine in study. Since the optimization executed uses a genetic algorithm, the basic concepts of the evolutionary computation have to be explained. All the theory is developed and documented in (Engelbrecht 2007; The MathWorks 2013).

5.1 Concept

The evolution concept is an optimization process where the aim is to improve the ability of an organism or system to survive in dynamically changing and competitive environments. However, evolution may be interpreted differently. A usually analogy is made with the biological point of view to better understand the definition. While Darwin (1809-1882) is considered the founder of both theory of evolution and the principle of common descent, Lamarck (1744-1829) was possibly the first to theorize about biological evolution.

The main idea of Lamarck is that individuals adapt during their lifetimes, and transmit their traits to their offspring. In turn, the offspring continues the process and also adapts. The method of adaptation rests on the concept of use and disuse: over time, individuals lose characteristics not needed, and develop others that are useful.

Charles Darwin's theory of natural selection became the foundation of biological evolution. In a world with limited resources and stable populations, each individual competes with others for survival. The individuals with the "best" characteristics are more likely to survive and to reproduce; those characteristics will be passed on to their offspring. These characteristics will be manifested in the new generation and over time will become dominant among the population. Darwin also stats that, during the production of a child organism, random events generate random changes to the child organism's characteristics. If these new characteristics are a benefit to the organism, then the chances of survival for that organism are increased.

Summarizing, the evolutionary computation, refers to computed-based problem solving systems that use computational models of evolutionary processes already mentioned. Natural selection, survival of the fittest and reproduction, are the fundamental components of such computational systems.

5.2 Generic Evolutionary Algorithm

The concept of evolution in a natural selection, of a population of individuals can be thought of as a search through the space of possible chromosome values. In that sense, an evolutionary algorithm can be defined as a stochastic search for an optimal solution to a given problem. The evolutionary search process is influenced by the following main components:

- Encoding the solutions to the problem as a chromosome;

- A function to evaluate the fitness, or survival strength of the individuals;
- Initialization of the initial population;
- Selection operators;
- Reproduction operators;

The steps of an evolutionary algorithm are applied iteratively until some stopping condition is satisfied. Each iteration is interpreted as a generation.

Therefore, the different ways in which the EA components are applied results in different evolutionary computation paradigms:

- Genetic Algorithms (GAs), which model genetic evolution;
- Genetic Programming (GP), which is based on genetic algorithms, but the individuals are programs;
- Evolutionary programming (EP), which is derived from the simulation of adaptive behaviour in evolution;
- Evolution strategies (ESs), which are geared toward modelling the strategic parameters that control variation in evolution;
- Differential evolution (DE), which is similar to genetic algorithms, differing in the reproduction mechanism used;
- Cultural evolution (CE), which models the evolution of culture of a population and how the culture influences the genetic and phenotypic evolution of individuals;
- Co-evolution (CoE), where initially "dumb" individuals evolve through cooperation, or in competition with one another, acquiring the necessary characteristics to survive;

In the generic evolutionary algorithm it is applied both parts of Darwin's theory mentioned in the previous subsection.

5.3 The Chromosome

The characteristics that the organisms have, dictate their ability to survive and to reproduce. These characteristics are represented by strings of information contained in the chromosomes of the organism. Therefore, chromosomes are structures of compact intertwined molecules of DNA, found in the nucleus of organic cells. Each chromosome contains a large number of genes, where a gene is the unit of heredity. Genes determine many aspects of anatomy and physiology through control of protein production.

Transferring this concept to the EC, each individual represents a candidate solution to an optimization problem. The characteristics of an individual are represented by a chromosome, also referred to as a genome. These characteristics refer to the variables of the optimization problem, for which an optimal assignment is sought. Each variable that need to be optimized is referred to as a gene, the smallest unit of information.

The characteristics can be divided into two classes of evolutionary information: genotypes and phenotypes. A genotype describes the genetic composition of and individual, as inherited from its parents. On the contrary, a phenotype is the expressed behavioural traits of an individual in a specific environment; it defines what an individual looks like.

A crucial step in the design of an EA is to fan an appropriate representation of candidate solutions. The efficiency and complexity of the search algorithm greatly depends on the representation scheme Most EAs represent solutions as vectors of a specific data type.

5.4 Initial Population

As already mentioned, EAs are stochastic, population-based search algorithms. A population of candidate solutions is always present in an EA. To solve an EA, an optimization problem is to generate an initial population. This is accomplished by assigning a random value from the allowed domain to each of the genes of each chromosome. The goal of a random selection is to ensure that the initial population is a uniform representation of the entire search space.

However, it is important to note that the size of the initial population has consequences in terms of computational complexity and exploration abilities. Large numbers of individuals increase diversity improving the exploration abilities of the population but it will higher the computational complexity per generation. Not always a large population is synonymous of an acceptable solution; it may be the case that fewer generations are enough to locate the desired solution. On the contrary a small population will represent a small part of the search space, the time complexity per generation will be lower and the EA may need more generations to converge than for a large population. Before a small population the EA can be forced to explore more of the search space by increasing the rate of mutation.

5.5 Fitness Function

As already mentioned, individuals with the best characteristics have higher probabilities to survive and to reproduce. To assess the ability of survival of an individual, a mathematical function is used to quantify how good the solution represented by a chromosome is. The fitness function, f, maps a chromosome representation into a scalar value:

$$f: \Gamma^{n_x} \rightarrow \mathbb{R} \tag{35}$$

Where Γ is the data type of the elements of an n_x dimensional chromosome.

The fitness function can be interpreted as the objective function, Ψ, which describes the optimization problem. However, the chromosome representation cannot correspond to the representation expected by the objective function. In such cases, a more detailed description of the fitness function will be:

$$f: \mathcal{S}_C \xrightarrow{\Phi} \mathcal{S}_X \xrightarrow{\Psi} \mathbb{R} \xrightarrow{\Upsilon} \mathbb{R}_+ \tag{36}$$

Where $\mathcal{S}_C$ represents the search space of the objective function, and Φ, Ψ and Υ respectively represent the chromosome decoding function, the objective function and the scaling function.

Generally, the fitness function is able to give an absolute measure of fitness, which is the solution represented by a chromosome directly evaluated using the objective function. Also, it is possible to calculate a relative fitness value to quantify the performance of an individual in relation to other individuals in the population or a competing population.

The fitness function has different types of formulation according the type of optimization problem. The different types of optimization problems are:

- Unconstrained: where the fitness function is simply the objective function;
- Constrained: some EAs change the fitness function to contain two objectives: one is the original objective function, and other is a constraint penalty function;
- Multi-Objective: can be solved using a weighted aggregation approach, where the fitness function is a weighted sum of all the sub-objectives, or by using a Pareto-based optimization algorithm;
- Dynamic and noisy problems, where function values of solution change over time;

As a conclusion, the fitness function develops a crucial role in an EA. The evolutionary operators, selection, crossover, mutation and elitism, usually make use of the fitness evaluation of chromosomes. As an example, selection operators prefer the most-fit individuals when selection parents for crossover, while mutation leans towards the least fir individuals.

5.6 Selection

The selection of individuals is directly related to the concept of survival of the fittest. The main objective of selection operators is to emphasize better solutions, achieved by two steps in the EA:

- Selection of the new population: A new population of candidate solutions is selected at the end of each generation to serve as the population of the next generation. The

new population can be selected from only the offspring, or from both the parents and the offspring. The selection operator should ensure that good individuals do survive to next generations.

- Reproduction: Offspring are created applying crossover and/or mutation operators. In terms of crossover, “superior” individuals should have more opportunities to reproduce to ensure that offspring contain genetic material of the best individuals. In the case of mutation, selection mechanisms should focus on “weak” individuals. This is made with the intention of improving the weak individuals, thereby increasing their chances of survival.

Following is the most frequently used operators:

- Selective Pressure;
- Random Selection;
- Proportional Selection;
- Tournament Selection;
- Rank-Based Selection;
- Boltzmann Selection;
- $(\mu, ^{+}\lambda)$ Selection;
- Elitism;
- Hall of Fame;

5.7 Reproduction Operators

The reproduction process creates the new offspring from selected parents by applying crossover and/or mutation operators. Therefore:

- Crossover: is the process of creating one or more new individuals through the combination of genetic material randomly selected from two or more parents.
- Mutation: is the process of randomly changing the values of genes in a chromosome. The main objective is to introduce new genetic material into the population, thereby increasing genetic diversity. Mutation should be applied with care not to distort the good genetic material in highly fit individuals. For this reason, mutation is usually applied at low probability. It can be used to mutate the less fit individuals.

The reproduction can be applied with replacement, in which case newly generated individuals replace parent individuals only if the fitness of the new offspring is better than that of the corresponding parents.

5.8 Stopping Conditions

The evolutionary operators are iteratively applied in an EA until a stopping condition is satisfied. A convergence criterion is usually used to detect if the population has converged:

- Terminate when no improvement is observed over a number of consecutive generations;
- Terminate when there is no change in the population;
- Terminate when an acceptable solution has been found;
- Terminate when the objective function slope is approximately zero;

6. Genetic Algorithm

In this chapter all the concepts presented in the Evolutionary Computation chapter are to be taken in account, since the genetic algorithm is one of the evolutionary computation paradigms.

It is used to solve constrained and unconstrained optimization problems that are based on natural selection. The genetic algorithm repeatedly modifies a population of individual solutions. At each step, the genetic algorithm selects individuals at random from the current population to be parents and uses them to produce the children for the next generation. Over successive generations, the population reaches an optimal solution. It uses three main types of rules to create the next generation from the current population:

- Selection rules;
- Crossover rules;
- Mutation rules;

All of the rules used by the genetic algorithms were previously described in the Evolutionary Computation chapter.

The advantages of the genetic algorithms against the classical algorithms were already mentioned by (Ngatchou *et al.* 2005) in the Relevant Studies subsection.

The following steps summarize how the genetic algorithm works (The MathWorks 2013):

1. The algorithm begins by creating a random initial population;
2. The algorithm then creates a sequence of new populations. At each step, it uses the individuals in the current generation to create the next population. In order to create the new population, the algorithm performs the following steps:
    a. Scores each member of the current population by computing its fitness value.
    b. Scales the raw fitness scores to convert them into a more usable range of values.
    c. Selects members, called parents, based on their fitness.
    d. Some of the individuals in the current population that have lower fitness are chosen as elite. These elite individuals are passed to the next population.

e. Produces children from the parents. Children are produced either by making random changes to a single parent by mutation or by combining the vector entries of a pair of parents using crossover.

f. Finally the current population is replaced with the children to form the next generation.

3. The algorithm stops when the stopping criterion is met.

7. Multi-Objective Optimization

In this chapter a Multi-Objective Optimization of the parameterization results is performed. After an initial mapping the behaviour of engine using simple values for the independent variables, a better evaluation of the engine can be made by applying a multi optimization to the independent variables. The purpose of this method is to explore all the possible values and combinations of the engine components in order to obtain several optimized engine setups.

Several real-world problems need simultaneous optimization of a number of objective functions. However, some of the objectives may be in conflict with one another. For example, finding optimal routes in data communications networks, where the objective is to minimize congestion, and to maximize utilization of physical infrastructure. It is considered that an important trade-off between these two objectives exists. Minimization of congestion is achieved by reducing the utilization of links. A reduction in utilization, on the other hand, means that infrastructure, for which high installation and maintenance costs are incurred, is under-utilized.

7.1 Multi-Objective Problem

Following, is a brief description of the Multi-objective concepts applied in the MOO problem of this thesis using a genetic algorithm. The concepts are found in (Engelbrecht 2007; The MathWorks 2013).

Let $\mathcal{S} \subseteq \mathbb{R}^{n_x}$, where n_x is the dimensional search and decision space, and $\mathcal{F} \subseteq \mathcal{S}$ is the feasible space. Note that with no constrains, the feasible space is the same as the search space. Let $x = (x_1, x_2, \dots, x_{n_x}) \in \mathcal{S}$, referred to as a decision vector. A single objective function, $f_k(x)$, is defined as $f_k : \mathbb{R}^{n_x} \to \mathbb{R}$. Let $f(x) = \left(f_1(x),\ f_2(x), \dots, f_{n_k}(x)\right) \in \mathcal{O} \subseteq \mathbb{R}^{n_k}$ be an objective vector containing n_k objective function evaluations; $\mathcal{O}$ is assumed as the objective space. Therefore the multi-objective problem is defined as:

Minimize $f(x)$

Subject to $g_m(x) \leq 0,\ m = 1, \dots, n_g$ (37)

$$h_m(x) = 0, \qquad m = n_g + 1, \dots, n_g + n_h$$

Where $x \in [x_{min}, x_{max}]^{n_x}$

g_m and h_m are respectively the inequality and equality constraints while $\in [x_{min}, x_{max}]$ represents the boundary constraints.

Finding an optimum solution in a MOO does not represent the same as finding an optimum solution in a SO, where only one objective is optimized, a local optimum and global optimum is calculated. The main problem is the presence of conflicting objectives, where improvement in one objective may cause deterioration in another objective. As an example, the maximization of the structural stability of a mechanical structure may cause an increase in costs, working against the additional objective to minimize costs. The procedure is to find solutions that balance trade-offs between objectives. Such a balance is achieved when a solution cannot improve any objective without degrading one or more of the other objectives. These solutions are referred to as non-dominated solutions.

Therefore, the objective when solving a MOP is to create a set of good compromises, instead of a single solution. This set of solutions is referred to as the non-dominated set, or the Pareto-optimal set.

Genetic Algorithm approaches for solving MOPs can be grouped into three main categories:

- Weighted aggregation approaches where the objective is defined as a weighted sum of sub-objectives.
- Population-based non-Pareto approaches, which do not make use of the dominance relation.
- Pareto-based approaches, which apply the dominance relation to find and approximation of the Pareto front.

7.2 Pareto Optimality

In this subsection it will be resumed several definitions that are crucial to interpret a MOO. These definitions assume minimization.

7.2.1 Dominance Definition

A decision vector, x_1, dominates a decision vector, x_2, if and only if:

- x_1 is not worse than x_2 in all objectives, i.e. $f_k(x_1) \leq f_k(x_2), \forall k = 1, \dots, n_k$, and
- x_1 is strictly better than x_2 in at least one objective, i.e. $\exists k = 1, \dots, n_k : f_k(x_1) < f_k(x_2)$.

An objective vector, f_1, dominates another objective vector, f_2, if f_1 is not worse than f_2 in all objective values, and f_1 is better than f_2 in at least one of the objective values.

This concept is exhibited in the Figure 92, for a two-objective function. $f(x) = \big(f_1(x), f_2(x)\big)$. The striped area marks the objective vectors dominated by f.

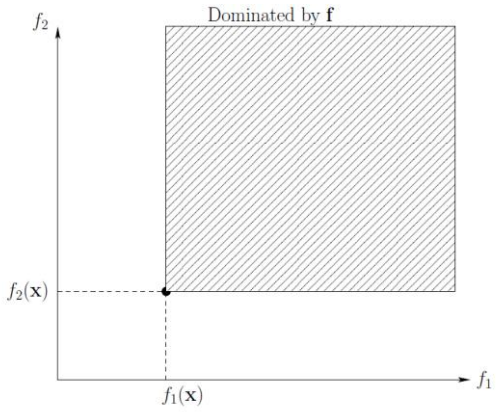

Figure 92: Dominance Example (Engelbrecht 2007)

7.2.2 Pareto-Optimal Definition

A decision vector, $x^* \in \mathcal{F}$ is Pareto-optimal if there does not exist a decision vector, $x \neq x^* \in \mathcal{F}$ that dominates it. This is, $\nexists k: f_k(x) < f_k(x^*)$. An objective vector, $f^*(x)$, is Pareto-optimal if x is Pareto-optimal.

7.2.3 Pareto-Optimal Set

The set of all Pareto-optimal decision vectors form the Pareto-optimal set, $\mathcal{P}^*$. Which is:

$$\mathcal{P}^* = \{x^* \in \mathcal{F} | \nexists x \in \mathcal{F}: x \prec x^*\} \tag{38}$$

It contains the set of solutions, or balanced trade-offs, for the MOP. The corresponding objective vectors are referred to as the Pareto-optimal front.

7.2.4 Pareto-Optimal Front:

Created by the objective vector, $f(x)$, and the Pareto-optimal solution set, $\mathcal{P}^*$, then the Pareto-optimal front, $\mathcal{P}^*\mathcal{F} \subseteq \mathcal{O}$, is defined as

$$\mathcal{P}^*\mathcal{F} = \left\{f = \left(f_1(x^*), f_2(x^*), \dots, f_k(x^*)\right) | x^* \in \mathcal{P}\right\} \tag{39}$$

Therefore, it contains all the objective vectors corresponding to decision vectors that are not dominated by any other decision vector. Following in Figure 93 is an example of Pareto Front.

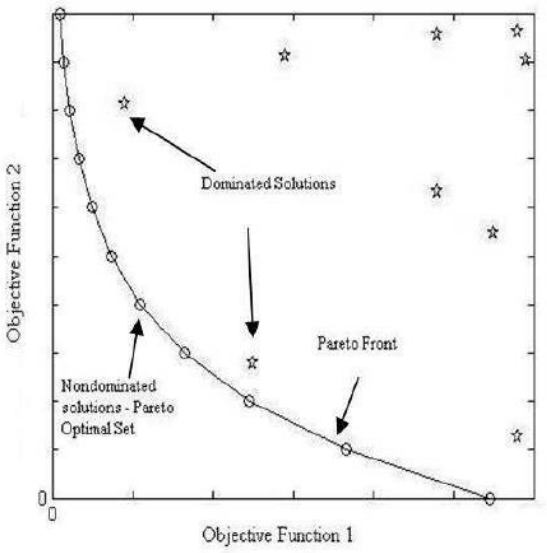

Figure 93: Pareto Front Example (Montoya & S. Mendoza 2011)

7.3 Multi-Objective Optimization Setup

In this subchapter it is presented the Multi-Optimization Setup performed in this thesis.

The multi-objective GA function applied, uses a controlled elitist genetic algorithm (a variant of NSGA-II). An elitist GA always favours individuals with better fitness value (rank) while a controlled elitist GA also favours individuals that can help to increase the diversity of the population even if they have a lower fitness value. One of the crucial points to assure convergence to an optimal Pareto front is to maintain the diversity. This multi-objective optimization was developed in a Matlab code, using and editing several built-in functions to assess the intended objectives.

This multi-optimization is applied with the intention of refining the parameterization results and to apply the optimization objectives to all possible engine setups. By not considering fixed values for each independent variable and perform an optimization of each one in a continuous range, it is possible to create several engine setups according to the optimization setups. It will be defined for this optimization, that a maximization of the specific thrust is one objective while the minimization of the TSFC is also important.

The optimization objectives are in the context of the requirements for the new generation of turbofan engines that will power the next airframes generations. Reducing pollutants (noise and consumption) saving the performance of the engines/aircraft are the two main drivers of engine and airframe manufacturers. Also, airlines and international community embrace this new objectives that force technology to react effectively. The new A320neo and the Boeing 737 Max will have power units that are the main drivers of this concept.

Therefore, the independent variables are the same used in the parameterization study but with an increase on the range values. This will provide to the GA a wider search space to

apply the fitness function. The fitness function is composed by the cycle equations used in the parameterization and the two objectives: minimize the TSFC and maximize the Fs.

The range of the independent variables is:

- BPR: from 10 to 20;
- The Fan Pressure Ratio (*rpfan*): from 1.1 to 2;
- The Compressor Pressure Ratio (*rpc*): from 3.8 to 20;
- The Turbine Entry Temperature (TET): 1500K to 2200K;

Following is the Table 15 of the Multi-Optimization Setup configurations:

Table 15: Multi-Optimization Setup for Conventional and Regenerated Cycles.

Parameter	Configuration/Value
Population Initial Range	[1.1 10 1500 3.8] to [2 20 2200 20]
Population Size	200
Crossover Fraction	0.6
Distance Measure Function	*@distancecrowding, 'phenotype'*
Pareto Fraction	0.4
Migration Direction	*'both'*
Migration Interval	10
Stall Generations Limit	10
Function Tolerance	$1e10^{-5}$
Generations	1000
Creation Function	Linear Feasible
Selection Function	Tournament
Crossover Function	Heuristic: 0.6
Mutation Function	Adaptive Feasible

- Crossover Fraction: is the percentage of individuals present in each population that are generated by the Crossover function;

- Distance Measure Function: helps to maintain the diversity on a Pareto front by favouring individuals that are relatively fay away on the front. The crowding distance measure function takes an optional argument to calculate distance either in function space (phenotype) or design space (genotype);

- Pareto Fraction: represents the percentage of individuals from the population that are present in the Pareto front.

- Migration Direction: is the movement of individuals between subpopulations, which the algorithm creates when a population size is set in a vector length greater than 1. The best individuals from one subpopulation replace the worst individuals in another population;

- Migration Interval: number of generations that migration is performed;

- Stall Generations Limit: if the weighted average change in the fitness function value of a defined number of generations is less than the Function Tolerance, the algorithm stops.

- Function Tolerance: if the weighted average change in the fitness function value of a defined number of generations is less than the Function Tolerance, the algorithm stops.

- Generations: is the maximum number of iterations that the GA performs;

- Creation Function: creates a random initial population the bounds and linear constraints;

- Selection Function: chooses parents for the next generation based on their scaled values from the fitness function. The Tournament type selects each parent by choosing two individuals randomly, and then choosing the best individual of that set to be a parent;

- Crossover Function: combines two individuals, or parents, to form a new individual, or child, for the next generation. The Heuristic type creates children that randomly lie on the line containing the two parents, a small distance away from the parent with the better fitness value, in the direction away from the parent with the worse fitness value;

- Mutation Function: the mutation function make small random changes in the individuals of each population, which provide genetic diversity and enable the GA to search a broader space. Choosing the Adaptive Feasible mode, it randomly generates directions that are adaptive with respect to the last successful or unsuccessful generation. A step length is chosen along with each direction so that linear constraint and bounds can be satisfied;

7.4 Results

In this section are presented the optimization results for the conventional cycle and with the addition of regeneration.

It is also possible through the Matlab code to determine if the hot and cold nozzles are chocked or unchoked. For a chocked nozzle the score will be 1. On the contrary for an unchoked nozzle the score will be 0.

The following tables and graphics will show the 80 solutions present in the Pareto front. Secondly it will be extracted from that results a zone, where it couples median trade-offs regarding the TSFC and Fs.

7.4.1 Conventional Cycle

Following, in Table 16, are the Pareto front results with the respective calculation of the nozzle status.

Table 16: Pareto front results and nozzle status for the conventional cycle.

rpfan	BPR	TET (K)	*rpc*	Fs (N.s/kg)	TSFC (kg/N.h)	Hot Nozzle	Cold Nozzle
2,00	10	2200	15,98	205,91	0,0706	1	1
2,00	10	2200	15,98	205,91	0,0706	1	1
1,99	10	2180	19,58	203,85	0,0684	1	1
1,99	10	2180	19,58	202,68	0,0680	1	1
1,99	10	2180	19,71	201,66	0,0676	1	1
1,99	10	2180	19,61	201,53	0,0676	1	1
2,00	10	2180	19,57	200,37	0,0671	1	1
2,00	10	2180	19,82	200,34	0,0669	1	1
2,00	11	2180	19,82	199,22	0,0666	1	1
2,00	11	2180	19,86	198,76	0,0664	1	1
2,00	11	2182	19,33	197,80	0,0664	1	1
2,00	11	2180	19,82	196,76	0,0658	1	1
2,00	11	2180	19,72	196,20	0,0657	1	1
2,00	11	2179	19,83	194,77	0,0652	1	1
2,00	11	2180	19,87	194,02	0,0650	1	1
2,00	11	2179	19,91	193,12	0,0647	1	1
2,00	11	2180	19,60	192,10	0,0646	1	1

2,00	11	2180	19,71	191,28	0,0643	1	1
2,00	11	2179	19,93	191,03	0,0640	1	1
2,00	12	2179	19,87	190,07	0,0639	1	1
2,00	12	2178	19,88	187,34	0,0631	1	1
2,00	12	2178	19,88	186,73	0,0630	1	1
2,00	12	2179	19,98	185,65	0,0627	1	1
2,00	12	2178	19,74	184,58	0,0625	1	1
2,00	12	2179	19,98	184,07	0,0623	1	1
1,99	12	2177	19,83	183,12	0,0622	1	1
2,00	12	2178	19,71	182,94	0,0621	1	1
1,99	13	2177	19,74	181,68	0,0620	1	1
2,00	13	2178	19,95	180,43	0,0615	1	1
1,99	13	2176	19,76	179,50	0,0614	1	1
2,00	13	2178	19,95	179,43	0,0612	1	1
1,99	13	2177	19,76	178,52	0,0612	1	1
2,00	13	2177	19,84	178,19	0,0610	1	1
2,00	13	2177	19,99	176,98	0,0607	1	1
1,99	13	2176	19,99	176,21	0,0607	1	1
1,99	13	2176	19,93	175,48	0,0605	1	1
2,00	14	2177	19,87	174,11	0,0603	1	1
2,00	14	2178	19,68	173,28	0,0602	1	1
1,99	14	2176	19,94	172,66	0,0590	0	1
1,99	14	2177	19,98	172,02	0,0589	0	1
1,99	14	2175	19,89	171,52	0,0589	0	1
1,99	14	2175	19,98	170,69	0,0588	0	1
1,99	14	2175	19,95	169,21	0,0586	0	1
1,99	14	2175	19,98	168,71	0,0585	0	1
1,99	15	2174	19,95	167,53	0,0584	0	1
1,99	15	2175	19,95	167,21	0,0583	0	1
1,99	15	2173	19,85	165,54	0,0582	0	1
1,99	15	2175	19,97	165,48	0,0581	0	1
1,98	15	2172	19,98	164,00	0,0581	0	1
1,99	15	2175	19,97	163,36	0,0580	0	1
1,97	15	2170	19,97	160,90	0,0579	0	1
1,99	15	2173	19,85	160,21	0,0579	0	1
1,96	16	2168	19,98	159,00	0,0578	0	1
1,99	16	2171	19,98	158,01	0,0578	0	1
1,96	16	2167	19,98	157,49	0,0578	0	1
1,96	16	2167	19,98	156,83	0,0578	0	1
1,95	16	2166	19,98	155,82	0,0577	0	1
1,94	16	2163	19,98	154,18	0,0577	0	1
1,93	16	2161	19,98	153,63	0,0577	0	1
1,93	16	2159	19,99	152,82	0,0577	0	1
1,93	16	2160	19,99	152,58	0,0577	0	1
1,92	16	2159	19,99	151,71	0,0577	0	1
1,92	16	2158	19,99	151,21	0,0577	0	1

1,91	16	2156	19,99	150,34	0,0577	0	1
1,89	17	2150	19,99	147,08	0,0576	0	1
1,88	17	2149	20,00	145,85	0,0576	0	1
1,87	17	2147	20,00	144,88	0,0576	0	1
1,38	16	1603	19,90	103,04	0,0575	1	0
1,38	17	1601	19,98	100,14	0,0565	1	0
1,38	17	1597	19,82	99,58	0,0564	1	0
1,38	17	1598	19,92	98,43	0,0560	1	0
1,38	17	1595	19,93	98,05	0,0547	0	0
1,38	18	1595	19,93	97,20	0,0544	0	0
1,38	18	1594	19,93	96,30	0,0542	0	0
1,38	18	1593	19,81	94,80	0,0538	0	0
1,38	19	1594	19,60	93,88	0,0537	0	0
1,38	19	1592	19,62	92,53	0,0534	0	0
1,38	19	1590	19,79	90,96	0,0531	0	0
1,38	20	1586	20,00	88,67	0,0527	0	0
1,38	20	1586	20,00	88,67	0,0527	0	0

The respective results are plotted in the Pareto front (Figure 94); a tendency curve is added to the results.

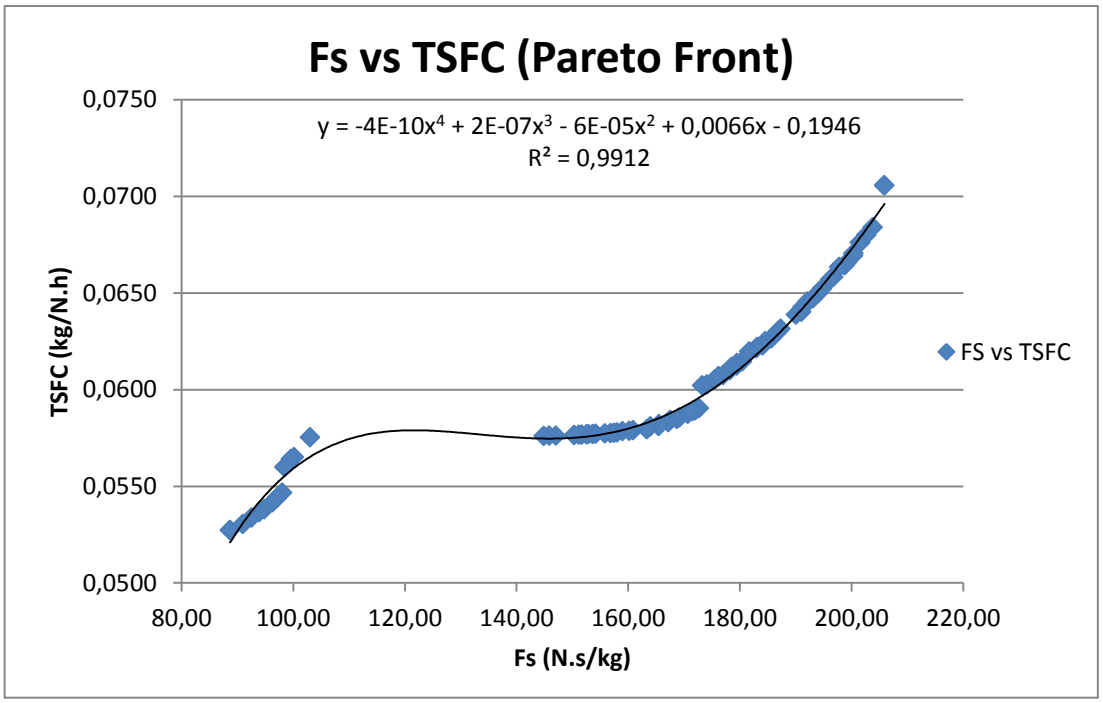

Figure 94: Fs vs TSFC Pareto front results.

Following (Table 17) is the median trade-off results, where the Fs and the TSFC are plotted with similar decision weights in Pareto front.

Table 17: Median trade-off results of the Pareto front for the conventional cycle.

rpfan	BPR	TET (K)	*rpc*	Fs (N.s/kg)	TSFC (kg/N.h)	Hot Nozzle	Cold Nozzle
1,99	14	2176	19,94	172,66	0,0590	0	1
1,99	14	2177	19,98	172,02	0,0589	0	1
1,99	14	2175	19,89	171,52	0,0589	0	1
1,99	14	2175	19,98	170,69	0,0588	0	1
1,99	14	2175	19,95	169,21	0,0586	0	1
1,99	14	2175	19,98	168,71	0,0585	0	1
1,99	15	2174	19,95	167,53	0,0584	0	1
1,99	15	2175	19,95	167,21	0,0583	0	1
1,99	15	2173	19,85	165,54	0,0582	0	1
1,99	15	2175	19,97	165,48	0,0581	0	1
1,98	15	2172	19,98	164,00	0,0581	0	1
1,99	15	2175	19,97	163,36	0,0580	0	1
1,97	15	2170	19,97	160,90	0,0579	0	1
1,99	15	2173	19,85	160,21	0,0579	0	1
1,96	16	2168	19,98	159,00	0,0578	0	1
1,99	16	2171	19,98	158,01	0,0578	0	1
1,96	16	2167	19,98	157,49	0,0578	0	1
1,96	16	2167	19,98	156,83	0,0578	0	1
1,95	16	2166	19,98	155,82	0,0577	0	1
1,94	16	2163	19,98	154,18	0,0577	0	1
1,93	16	2161	19,98	153,63	0,0577	0	1
1,93	16	2159	19,99	152,82	0,0577	0	1
1,93	16	2160	19,99	152,58	0,0577	0	1
1,92	16	2159	19,99	151,71	0,0577	0	1
1,92	16	2158	19,99	151,21	0,0577	0	1
1,91	16	2156	19,99	150,34	0,0577	0	1
1,89	17	2150	19,99	147,08	0,0576	0	1
1,88	17	2149	20,00	145,85	0,0576	0	1
1,87	17	2147	20,00	144,88	0,0576	0	1

The respective median trade-off results are plotted in Figure 95; a tendency curve is added to the results.

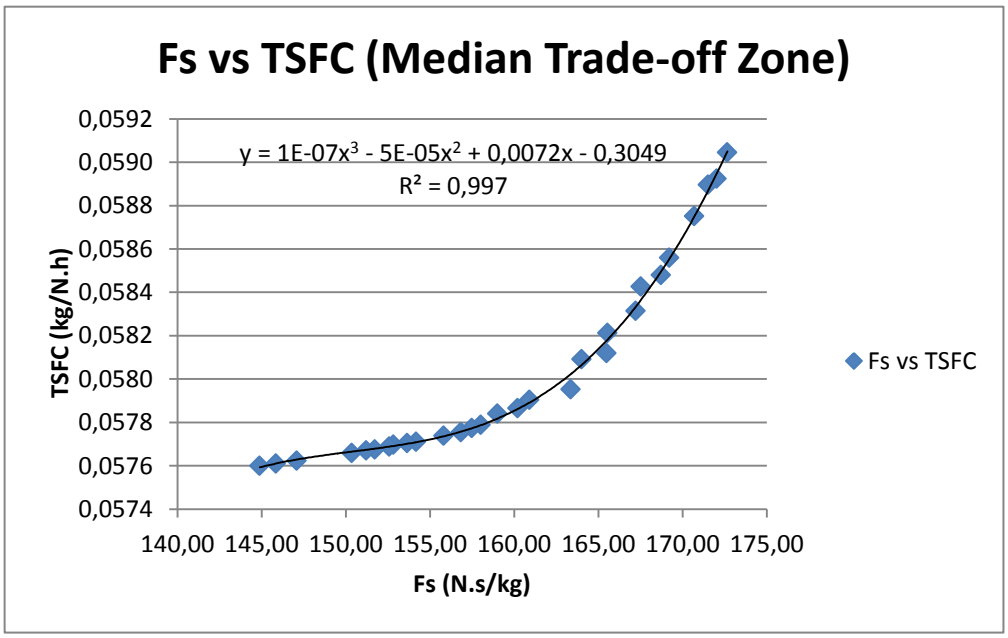

Figure 95: Median Trade-off results of the Pareto front for the conventional cycle.

7.4.2 Regenerated Cycle

Following, in the Table 18, are the Pareto front results with the respective calculation of the nozzle status.

Table 18: Pareto front results and nozzle status for the regenerated cycle.

rpfan	BPR	TET (K)	*rpc*	Fsreg (N.s/kg)	TSFCreg (kg/N.h)	Hot Nozzle	Cold Nozzle
2,00	10	2199	20,00	190,05	0,0555	1	1
2,00	10	2197	17,71	187,69	0,0548	1	1
2,00	10	2196	17,18	186,95	0,0546	1	1
2,00	10	2196	16,91	185,96	0,0544	1	1
2,00	10	2195	16,00	185,43	0,0542	1	1
2,00	10	2195	15,75	184,75	0,0540	1	1
2,00	11	2195	15,24	183,33	0,0538	1	1
2,00	10	2192	12,90	181,98	0,0532	1	1
2,00	11	2192	12,67	180,77	0,0530	1	1
1,99	10	2191	11,43	179,51	0,0527	1	1
2,00	11	2191	11,26	178,54	0,0526	1	1
2,00	11	2191	11,00	177,47	0,0524	1	1
2,00	11	2191	10,96	176,87	0,0524	1	1
1,99	11	2189	9,44	175,16	0,0520	1	1
1,99	11	2189	9,17	174,07	0,0519	1	1

2,00	11	2189	8,80	172,77	0,0517	1	1
2,00	11	2190	9,21	171,62	0,0517	1	1
2,00	11	2190	9,21	171,62	0,0517	1	1
1,99	11	2189	8,93	170,29	0,0516	1	1
1,97	11	2189	8,77	169,11	0,0515	1	1
1,98	12	2189	8,44	167,75	0,0514	1	1
1,96	12	2189	8,60	166,92	0,0514	1	1
1,99	12	2188	7,88	165,55	0,0506	0	1
1,97	12	2189	7,67	164,59	0,0505	0	1
1,97	12	2189	7,67	164,28	0,0505	0	1
1,96	12	2189	7,84	163,00	0,0504	0	1
1,95	13	2189	7,87	161,20	0,0503	0	1
1,93	13	2189	7,84	160,09	0,0503	0	1
1,95	13	2190	7,33	158,66	0,0502	0	1
1,91	13	2189	7,89	157,52	0,0502	0	1
1,92	13	2190	7,31	156,69	0,0501	0	1
1,90	13	2189	7,66	155,26	0,0501	0	1
1,89	13	2189	7,79	153,98	0,0500	0	1
1,88	13	2190	8,22	152,86	0,0500	0	1
1,89	13	2190	7,37	151,99	0,0499	0	1
1,87	14	2189	7,74	151,11	0,0499	0	1
1,87	14	2190	7,51	149,65	0,0498	0	1
1,86	14	2190	7,68	147,81	0,0498	0	1
1,83	14	2190	7,66	144,37	0,0496	0	1
1,83	15	2190	7,73	143,93	0,0496	0	1
1,82	15	2190	7,68	143,10	0,0496	0	1
1,80	15	2190	7,53	141,99	0,0495	0	1
1,81	15	2190	7,67	141,35	0,0495	0	1
1,78	15	2190	7,64	138,31	0,0494	0	1
1,78	15	2191	7,67	136,87	0,0494	0	1
1,77	16	2190	7,86	135,85	0,0494	0	1
1,76	16	2191	7,51	134,30	0,0493	0	1
1,76	16	2191	7,51	134,30	0,0493	0	1
1,74	16	2190	7,83	132,89	0,0493	0	1
1,74	16	2190	7,68	130,94	0,0492	0	1
1,71	16	2191	7,63	129,06	0,0492	0	1
1,71	16	2191	7,63	128,85	0,0492	0	1
1,71	17	2191	7,62	127,75	0,0491	0	1
1,70	17	2191	7,73	125,77	0,0491	0	1
1,70	17	2192	7,79	125,51	0,0491	0	1
1,69	17	2192	7,71	123,04	0,0491	0	1
1,68	17	2191	7,71	122,32	0,0490	0	1
1,67	18	2192	7,71	121,40	0,0490	0	1
1,67	18	2192	7,73	120,97	0,0490	0	1
1,66	18	2191	7,70	119,86	0,0490	0	1
1,65	18	2192	7,73	118,52	0,0490	0	1

1,64	18	2192	7,70	117,44	0,0489	0	1
1,63	19	2192	7,62	115,48	0,0489	0	1
1,62	19	2191	7,60	114,29	0,0489	0	1
1,62	19	2191	7,59	113,61	0,0489	0	1
1,38	15	2084	11,18	109,10	0,0488	1	0
1,38	15	2085	10,98	108,45	0,0487	1	0
1,38	16	2087	10,75	107,45	0,0482	1	0
1,38	16	2091	10,56	107,07	0,0481	1	0
1,38	16	2094	9,91	105,63	0,0475	1	0
1,38	17	2101	9,64	104,16	0,0470	1	0
1,38	18	2111	9,23	102,41	0,0463	1	0
1,38	18	2116	8,65	101,34	0,0459	1	0
1,38	18	2122	8,50	100,43	0,0457	1	0
1,38	19	2123	7,75	98,94	0,0452	1	0
1,38	20	2145	7,57	97,12	0,0445	1	0
1,38	20	2140	6,90	96,06	0,0445	1	0
1,38	20	2135	6,30	94,92	0,0444	1	0
1,38	20	2128	5,39	94,02	0,0438	0	0
1,38	20	2128	5,39	94,02	0,0438	0	0

The respective results are plotted in the Pareto front (Figure 96); a tendency curve is added to the results.

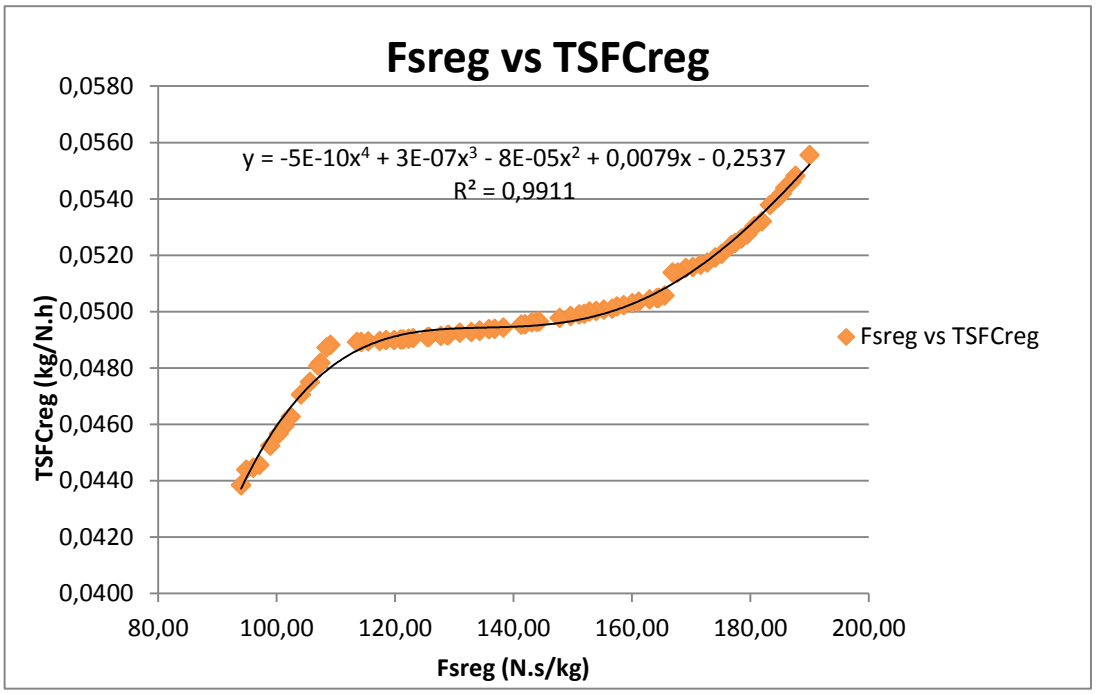

Figure 96: Fsreg vs TSFCreg Pareto front results.

Following (Table 19) is the median trade-off results, where the Fsreg and the TSFCreg are plotted with similar decision weights in Pareto front.

Table 19: Median trade-off results of the Pareto front for the regenerated cycle.

rpfan	BPR	TET (K)	*rpc*	Fsreg (N.s/kg)	TSFCreg (kg/N.h)	Hot Nozzle	Cold Nozzle
1,99	12	2188	7,88	165,55	0,0506	0	1
1,97	12	2189	7,67	164,59	0,0505	0	1
1,97	12	2189	7,67	164,28	0,0505	0	1
1,96	12	2189	7,84	163,00	0,0504	0	1
1,95	13	2189	7,87	161,20	0,0503	0	1
1,93	13	2189	7,84	160,09	0,0503	0	1
1,95	13	2190	7,33	158,66	0,0502	0	1
1,91	13	2189	7,89	157,52	0,0502	0	1
1,92	13	2190	7,31	156,69	0,0501	0	1
1,90	13	2189	7,66	155,26	0,0501	0	1
1,89	13	2189	7,79	153,98	0,0500	0	1
1,88	13	2190	8,22	152,86	0,0500	0	1
1,89	13	2190	7,37	151,99	0,0499	0	1
1,87	14	2189	7,74	151,11	0,0499	0	1
1,87	14	2190	7,51	149,65	0,0498	0	1
1,86	14	2190	7,68	147,81	0,0498	0	1
1,83	14	2190	7,66	144,37	0,0496	0	1
1,83	15	2190	7,73	143,93	0,0496	0	1
1,82	15	2190	7,68	143,10	0,0496	0	1
1,80	15	2190	7,53	141,99	0,0495	0	1
1,81	15	2190	7,67	141,35	0,0495	0	1
1,78	15	2190	7,64	138,31	0,0494	0	1
1,78	15	2191	7,67	136,87	0,0494	0	1
1,77	16	2190	7,86	135,85	0,0494	0	1
1,76	16	2191	7,51	134,30	0,0493	0	1
1,76	16	2191	7,51	134,30	0,0493	0	1
1,74	16	2190	7,83	132,89	0,0493	0	1
1,74	16	2190	7,68	130,94	0,0492	0	1
1,71	16	2191	7,63	129,06	0,0492	0	1
1,71	16	2191	7,63	128,85	0,0492	0	1
1,71	17	2191	7,62	127,75	0,0491	0	1
1,70	17	2191	7,73	125,77	0,0491	0	1
1,70	17	2192	7,79	125,51	0,0491	0	1
1,69	17	2192	7,71	123,04	0,0491	0	1
1,68	17	2191	7,71	122,32	0,0490	0	1
1,67	18	2192	7,71	121,40	0,0490	0	1
1,67	18	2192	7,73	120,97	0,0490	0	1
1,66	18	2191	7,70	119,86	0,0490	0	1
1,65	18	2192	7,73	118,52	0,0490	0	1
1,64	18	2192	7,70	117,44	0,0489	0	1
1,63	19	2192	7,62	115,48	0,0489	0	1
1,62	19	2191	7,60	114,29	0,0489	0	1
1,62	19	2191	7,59	113,61	0,0489	0	1

The respective median trade-off results are plotted in Figure 97; a tendency curve is added to the results.

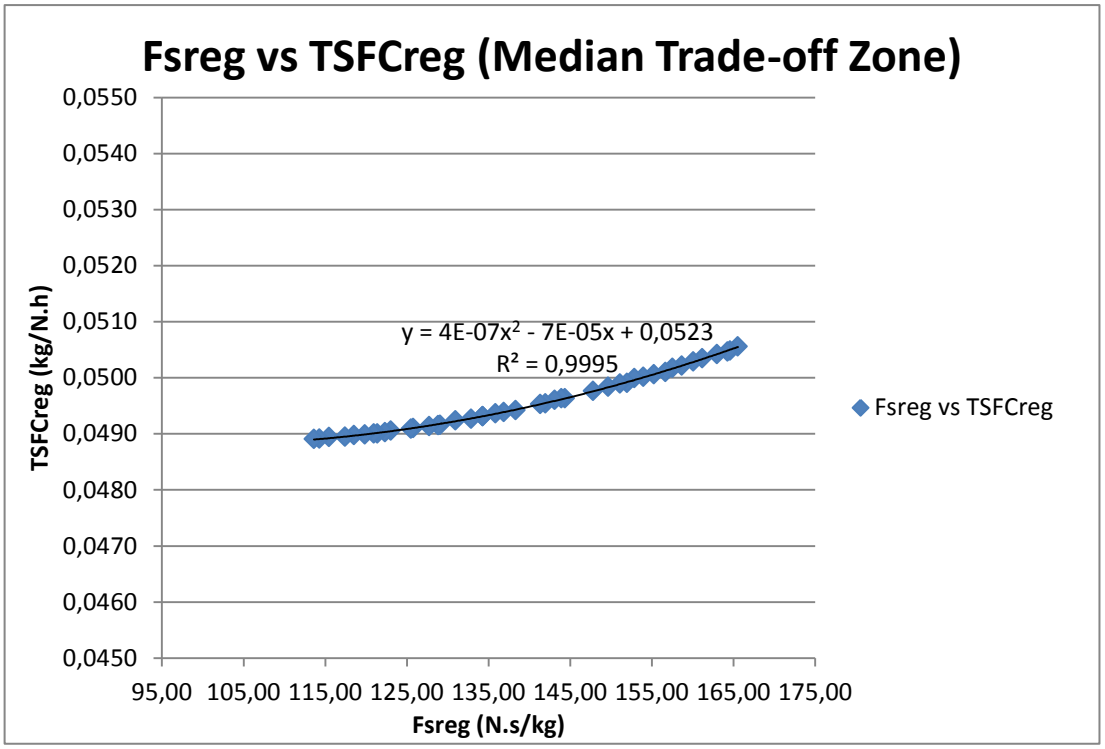

Figure 97: Median Trade-off results of the Pareto front for the regenerated cycle.

8. Conclusions and Future Work

8.1 Conclusions

In this work a performance study of a two spool turbofan engine in UHB conditions was performed. Accordingly to the trend of higher bypass ratio in the incoming engines for the Airbus A320neo and the Boeing 737Max, this study tries to envision some characteristics and behaviours of the new turbofan engines. For flight conditions, the cruise point was chosen where all the atmospheric and engine known/predicted conditions were taken in consideration. To evaluate these characteristics it was selected a group of independent variables: the BPR, the TET, fan pressure ratio (*rpfan*) and compressor pressure ratio (*rpc*). The results were translated in several performance readings of the engine, where the TSFC and the Fs were main references. It is good to notice that the study applies equations where several parameters are considered constant, therefore the results may not translate into real values but are still able to provide some viable conclusions. For more accurate results, the continuation of this study should be developed, where the addition of more variable parameters will be required.

In the first part of this thesis, a parameterization study was managed by fixating one of the independent variables (*rpfan* or *rpc*) and extracting results of the TSFC and Fs for three different sets of TET along the BPR window from 10 to 20. This initial evaluation not only served as a base for the next phase of the thesis, but also helped mapping the behaviour of the engine and evaluating the viability of a regenerated cycle regarding the considered outputs. The introduction of a regenerated cycle was to assess if it was possible to reduce the consumption in the new BPR range values.

From the results of the parameterization we can conclude that higher Fs values can be achieved by increasing the fan pressure ratio and the TET. The general behaviour with or without regeneration is the increase of TSFC with the increase of Fs. However, as the values of the *rpfan* increase, despite of higher Fs, the range of possible BPR is reduced. It is important to notice that for high values of *rpfan*, reduced TET lead to an impossible configuration of the engine, since the temperature of the turbine is not enough to supply the low pressure spool. Also, higher values of *rpc* produce higher specific thrust output; however, the values of Fs are similar for the majority of the *rpc* configurations in the conventional cycle. The same is not verified in the regenerated cycle, where the difference is more noticed for each *rpc* value. It is observed that the Fs values of the conventional cycle are superior when compared to the ones obtained from the regenerated cycle, as it would be expected.

Still in the parameterization, regarding the TSFC results, it is necessary to separate both cycles to perform a conclusion. For the conventional cycle it can be concluded that higher values of *rpfan* and lower TET produce a reduced consumption. Also, higher values of *rpc*

record lower TSFC values. On the other hand, for the regenerated cycle it can be concluded that the lower values of TSFC can be achieved with lower values of *rpc* at higher fan pressure ratios. The turbine entry temperature develops an important role in the regeneration process since the higher the temperature, more effective the regeneration process will be.

The second phase of this thesis consisted in a MOO problem where a genetic algorithm was successfully applied. With the results from the first phase of this study, the intention was to meet two objectives of actual interest of the airliners: reduce the TSFC while maximizing the specific thrust available. Therefore, each independent variable was optimized, generating a Pareto front. This provided not a unique set of optimized values, but instead several optimized sets were calculated with different weights regarding both objectives. This situation provides the decision maker the possibility of choosing a set of variables privileging one of the objectives or both. The Pareto fronts generated are well distributed, indicating a good diversity of results within the ranges considered. The disparities on each Pareto front are due to the changes of the BPR, which will influence the status of both cold and hot nozzle.

In the median trade-off zones, on both cases, the changing of the TSFC with the Fs values is less than in other explored zones (especially in the regenerated case). This allows the engine to work satisfactorily in a larger range of Fs without greater change in the TSFC. The optimal working point depends on the flight conditions or mission.

So a compromise of tradeoffs is necessary to choose a set of values to the independent variables, taking into account the proposed objectives in the optimization process. An example is suggested by (Breu *et al*. 2011) concerning the increasing of the BPR, where the addition of stages on the LPT is necessary as the BPR increases. Another consequence to consider is a wider fan. Both issues will add weight to the overall engine.

Accordingly to the performed study, there are positive indications for regenerated cycle on the new UHB turbofans, despite the use of the current equations where the specific heat and bleeds were considered constant. However, for a precise evaluation, further studies must be performed considering other aspects such as aerodynamic issues, weight, structural, mechanical and security points. With the current progress of technology, the use of a regenerated cycle may be closer than in the previous years due to the introduction of new materials, design concepts and engine modules that will provide the space and weight saving for the introduction of a regenerating system.

In the median trade-off zone in the regeneration case can be observed that the TSFC do not change significantly. Therefore, it can be concluded that there are several combinations of the independent variables (*rpfan*, *rpc*, BPR and TET) which use can increase the specific thrust without changing significantly the fuel consumption. In a cruise scenario, where

atmospheric conditions change continuously, applying regeneration, high fuel saving might be achieved with small changes of the independent parameters.

The trend of increasing the bypass ratio is certainly one of the chosen paths of engine manufacturers to reduce the TSFC. However, the components of the engine must keep up to meet the imposed objectives. One of the examples is the trend of using higher TET that is provided by more resistant materials. Values for other components are suggested in this study.

The introduction of a gearbox, gives the possibility for the low pressure spool to run at optimum velocities and also reducing the turbine stages. This concept is not new, however only now it was brought to a commercial level due to all the technology development that permitted to add an extra system to the engine, keeping or even increasing the performance compared to the DDTF. But, it is also important to notice that in some situations a geared configuration may not result in an increase of performance. Thus, it is necessary to evaluate the mission objective of the engine, in order to decide the best engine parameter values which can dictate whether to use a geared or a conventional configuration setup, as indicated by (Guynn *et al*. 2009).

8.2 Future Work

For future work, a more developed study is suggested by considering variable specific heat and bleed values and extending the research to other flight points, for example the take-off point.

Also, by adding other parameters like aerodynamic characteristics, weight and structural properties of the engine, as well as airframe factors, can provide a more realistic and complete performance evaluation. These additions can unveil new conclusions and search points. If none commercial propulsion software can be used, the developed Matlab code can be adapted by adding new calculation modules and the results can also be plotted for the conventional and regenerative configuration. Later, the work can be compared and verified by a commercial software like GasTurb.

In the optimization field, new algorithms or evolution strategies can be applied in order to explore several optimization possibilities. Also, an option of work is to edit the optimization functions to improve the efficiency of the algorithm and create a more robust optimization tool to gas turbine engines, especially turbofans.

9. Bibliography

A. Çengel, Y. & A. Boles, M., 2006. *Thermodynamics: an Engineering Approach* Fifth Edit. I. The McGraw-Hill Companies, ed.,

Aiken, D. et al., 2009. *Aerohead Aeronautics: AA SB-01 - Response to 2008/2009 AIAA Foundation Undergraduate Team Aircraft Design Competion*, Virginia.

Airbus, 2012. NEW "SHARKLETS" AND A320NEO. Available at: http://www.airbus.com/aircraftfamilies/passengeraircraft/a320family/technology-and-innovation/.

Analytics, F., 2013. *Special Report - Commercial Engines 2013*,

Andriani, R. & Ghezzi, U., 2006. Main Characteristics of Regenerated and Intercooled Propulsion Systems. , p.7.

Banda, S., 2014. Pratt & Whitney's PurePower® PW1000G Engine Family is not just a concept or a promise for the future—it is reality. *United Technologies Corporation - Pratt & Whitney Division*. Available at: http://www.pw.utc.com/PurePowerPW1000G_Engine.

Becker, R., Schaefer, M. & Reitenbach, S., 2013. Assessment of the efficiency gains introduced by novel aero engine concepts. , pp.1–10. Available at: http://core.kmi.open.ac.uk/download/pdf/11156209.pdf [Accessed June 15, 2014].

Boggia, S. & Rüd, K., 2004. INTERCOOLED RECUPERATED AERO ENGINE Advanced Project Design , MTU Aero Engines. , pp.1–10.

Borguet, S., Kelner, V. & Leonard, O., 2007. Cycle optimization of a turbine engine: an approach based on genetic algorithms. *power*. Available at: http://www2.ulg.ac.be/turbo/research/paper/NCTAM2006.pdf [Accessed June 15, 2014].

Breu, F., Guggenbichler, S. & Wollmann, J., 2011. Mission Optimization of the Geared Turbofan Engine. *Vasa*, pp.1–7. Available at: http://medcontent.metapress.com/index/A65RM03P4874243N.pdf [Accessed June 15, 2014].

Canada, P., 2014. PurePower Engine Family Specs Chart. *United Technologies Corporation - Pratt & Whitney Division*. Available at: http://www.pw.utc.com/Content/PurePowerPW1000G_Engine/pdf/B-1-1_PurePowerEngineFamily_SpecsChart.pdf.

CFM, 2013. CFM Leap - The Power for the Future. Available at: http://www.cfmaeroengines.com/files/brochures/LEAP-Brochure-2013.pdf.

Corchero, G. et al., 2008. An insight into some innovative cycles for aircraft propulsion. *Proceedings of the Institution of Mechanical Engineers, Part G: Journal of Aerospace Engineering*, 222(6), pp.731–747. Available at: http://pig.sagepub.com/lookup/doi/10.1243/09544100JAERO346 [Accessed May 19, 2014].

Cumpsty, N., 2003. *Jet Propulsion: A simple guide to the aerodynamic and thermodynamic design and performance of jet engines*, Available at: http://books.google.com/books?hl=en&lr=&id=yy2YoIKDC3gC&oi=fnd&pg=PR7&dq=JET+PROPULSION+A+Simple+Guide+to+the+Aerodynamic+and+Thermodynamic+Design+and+Per

formance+of+Jet+Engines&ots=GtiofF8Q7w&sig=qZv9HzG9AN0PeLBq0JHU4F3yTJ8 [Accessed September 3, 2014].

El-Sayed, A.F., 2008. *Aircraft Propulsion and Gas Turbine Engines*, CRC Press.

Engelbrecht, A.P., 2007. *Computacional Intelligence , An Introduction* Second Edi., West Sussex: John Wiley & Sons, Ltd.

Guynn, M. et al., 2009. Analysis of Turbofan Design Options for an Advanced Single-Aisle Transport Aircraft. *AIAA Paper*. Available at: http://arc.aiaa.org/doi/pdf/10.2514/6.2009-6942 [Accessed July 7, 2014].

Houghton, E.L. & Carpenter, P.W., 2003. *Aerodynamics for Engineering Students* Fifth Edit. B. Heinemann, ed.,

Humhauser, W., 2005. ISABE-2005-1266 ATFI-HDV : Design of a new 7 stage innovative compressor for 10 – 18 klbf thrust. , pp.1–9.

Kyprianidis, K.G. et al., 2008. EVA: A Tool for EnVironmental Assessment of Novel Propulsion Cycles. *Volume 2: Controls, Diagnostics and Instrumentation; Cycle Innovations; Electric Power*, pp.547–556. Available at: http://proceedings.asmedigitalcollection.asme.org/proceeding.aspx?articleid=1623629.

Larsson, L., Grönstedt, T. & Fan, U., 2011. GT2011-46451 CONCEPTUAL DESIGN AND MISSION ANALYSIS FOR A GEARED TURBOFAN. , pp.1–12.

Lebre, J. & Brójo, F., 2010. Effects of Intercooling and Regeneration in the Performance of a Turbofan Engine. *International Review of Aerospace Engineering*, xx(April). Available at: http://scholar.google.com/scholar?hl=en&btnG=Search&q=intitle:Effects+of+Intercooling+and+Regeneration+in+the+Performance+of+a+Turbofan+Engine#0 [Accessed June 15, 2014].

Mattingly, J., 2002. Aircraft Engine Design. Available at: http://scholar.google.com/scholar?hl=en&btnG=Search&q=intitle:Aircraft+Engine+Design#0 [Accessed September 14, 2014].

Montoya, C.A.G. & S. Mendoza, T., 2011. Implementation of an evolutionary algorithm in planning investment in a power distribution system. *Ingeniería e Investigación*, 31. Available at: http://revistas.unal.edu.co/ojs/index.php/ingeinv/rt/printerFriendly/25222/33726.

Ngatchou, P., Zarei, a. & El-Sharkawi, a., 2005. Pareto Multi Objective Optimization. *Proceedings of the 13th International Conference on, Intelligent Systems Application to Power Systems*, pp.84–91. Available at: http://ieeexplore.ieee.org/lpdocs/epic03/wrapper.htm?arnumber=1599245.

Pasini, S. et al., 2000. Heat Recovery From Aircraft Engines. *AIAA Paper*.

Riegler, C. & Bichlmaier, C., 2007. The Geared Turbofan Technology–Opportunities, Challenges and Readiness Status. *Proceedings of the 1st CEAS European …*. Available at: http://mtu-epool.com/en/technologies/engineering_news/others/Riegler_Geared_turbofan_technology.pdf [Accessed June 15, 2014].

S. Arvai, E., 2011. Comparing the new technology Narrow-body engines: GTF vs LEAP maintenance costs. *Air Insight: A comercial aviation consultancy*. Available at: http://airinsight.com/2011/11/09/comparing-the-new-technology-narrow-body-engines-gtf-vs-leap-maintenance-costs/#.VA86ivldWaJ.

The MathWorks, I., 2013. Matlab Help.

Wulff, a. & Hourmouziadis, J., 1997. Technology review of aeroengine pollutant emissions. *Aerospace Science and Technology*, 1(8), pp.557–572. Available at: http://linkinghub.elsevier.com/retrieve/pii/S1270963897900043.

Appendix A Proposed Articles